Modelling and Mapping of Above-ground Biomass and Carbon Sequestration in the Cool Temperate Forest of North-east China

Ram Kumar Deo

March, 2008

Modelling and Mapping of Above-ground Biomass and Carbon Sequestration in the Cool Temperate Forest of North-east China

by

Ram Kumar Deo

Thesis submitted to the International Institute for Geo-information Science and Earth Observation in partial fulfilment of the requirements for the degree of Master of Science in Geo-information Science and Earth Observation, Specialisation: Forestry for Sustainable Development

Thesis Assessment Board

Dr. Yousif Hussin
Chairman, Degree Assessment Board, NRM Department, ITC, The Netherlands
Prof. Dr. Ir. Robert de Wulf
External Examiner, University of Gent, Belgium
Dr. Iris van Duren
Internal Examiner, NRM Department, ITC, The Netherlands
Prof. Dr. Ir. Alfred de Gier
First Supervisor, NRM Department, ITC, The Netherlands
Dr. Martin Schlerf
Second Supervisor, NRM Department, ITC, The Netherlands

INTERNATIONAL INSTITUTE FOR GEO-INFORMATION SCIENCE AND EARTH OBSERVATION
ENSCHEDE, THE NETHERLANDS

Disclaimer

Abstract

Accurate assessment of above-ground woody biomass is important for sustainable forest management and to understand the role of forest as source or sink of carbon. The best way of improving assessment accuracy is to develop predictive equations based on locally collected data. The use of remote sensing (RS) techniques with limited field data, have got popularity in forest resource assessment over large area in a cost effective manner. The absence of local biomass equations and the uncertainty of estimates when using existing regional or global equations motivated this study towards developing equations for biomass and carbon sequestration on tree basis for the cool temperate forest in Wangqing, north-east China. A 'tree sub-sampling method' was employed for the estimation of biomass of 60 sample trees harvested in the field that served as the basis for the development of equations. The method was found to be reliable and non-sensitive to branching pattern of the trees and species. Three forms of biomass equations namely polynomial, power and combined variable were developed. A weighted third-degree polynomial equation was found to be the best alternative while considering the small error margins and the problem in tree height measurements. Comparing the polynomial-based plot biomass estimates with the estimates from existing Chinese and IPCC equations revealed that the three estimates differed significantly. Field data from the growth ring and bark-thickness measurements of sample trees, combined with the first derivate of the polynomial dry biomass equation permitted the calculation of annual carbon sequestration. The estimated average dry biomass density of the forest using the Polynomial, Chinese and IPCC equations were respectively 81.88±5.63, 97.11±6.43 and 112.12±7.48 tons/ha (at 95% confidence level). The average carbon sequestration rate in the forest was estimated to be 1.88±0.12 ton/ha.yr. For RS-based assessment, an empirical relationship of forest plot biomass and annual carbon sequestration was sought with the Landsat TM spectral data. Although poor, a significant linear relationship was observed with corrected-NDVI for both the forest parameters thereby implying that the existing level of biomass did not show a saturation effect of the VI. The average forest biomass and annual carbon sequestration estimated using the RS data were 65.36 ton/ha and 1.52 ton/ha respectively. The equations developed in this study are area-specific, hence, should be applied at other locations only after verification. Accurate assessments of biomass/ carbon from RS data require further research incorporating advanced techniques.

Keywords: above-ground biomass, biomass equations, carbon sequestration, remote sensing, vegetation indices

Acknowledgements

I am very grateful to the Dutch government and ITC Directorate for providing me the scholarship and the big educational opportunity.

I wish to express my sincere gratitude to my supervisor Prof. Dr. Ir. Alfred de Gier for his continuous support, encouragement and helpful comments from the designing of research proposal till the completion of thesis work. Thank you Prof. I enjoyed your guidance very much.

I am thankful to Dr. Martin Schlerf, my second supervisor, for his effective guidance in image processing and ideas about remote sensing based biomass modelling. Thanks to Dr. Yousif Hussain, who gave me the first impression about the use of remote sensing for biomass mapping. My sincere gratitude also to Dr. Michael Weir, Program Director, NRM, for his cooperation throughout the M.Sc. Course. Special thanks to Prof. Dr. Ir. Robert de Wulf, external examiner, for his comments and suggestions during the mid-term presentation.

I would like to thank Ms Yanqiu Xing, Ph.D. student at ITC, for her keen guidance and supervision during the field work in Wangqing, China. I am highly indebted to Wangqing Forest Bureau that gave me the permission to harvest sample trees. I express my sincere appreciations to all the crew members whose active involvement made the field work possible in the limited time. Thanks to my Chinese friend Huadong, who translated Chinese language for me and did laboratory work with the wood samples. Thanks to the North-East Forestry University of China for providing the laboratory facilities and relevant secondary information. Thanks a lot to my colleagues David, Junjie and Ashenafi for sharing the hard time together with me during the field work in China.

My sincere thankfulness to all student colleagues of NRM Program (2006) for making the student life at ITC memorable forever. My heartfelt appreciation to the students of FSD specialization and especially my cluster mates Rubeta, Sonia, Chris, Mutuma and Daniel for creating a homely environment. Thanks to all Nepalese friends at ITC and outside who contributed in my study by providing moral and material support. Special thanks to Raju, Kamal and Sardu for their continuous support.

Last but not least, I would like to thank the entire ITC family who directly or indirectly contributed in this work. Worth mentioning are my course supervisor Dr. Iris van Duren for sustained support, Mr. Willem Nieuwenhuizen for technical help with iPAQ operation and Mr. Benno Masselink and Mr. Job Duim for providing field equipments.

I am proud of my family members for their patience to keep me away so long.

Table of contents

List of figures

List of tables

1. Introduction

1.1. Background

1.1.1. Assessment of above-ground biomass and carbon in forests

The subject of biomass assessment has received considerable attention for quite sometime, especially after pulpwood demand in 1960s and oil crisis in 1970s (de Gier, 2003). Estimation of biomass of forests is a usual practice to quantify fuel and wood stock and allocate harvestable amount (Dias *et al.*, 2006). Forest biomass assessment is important for national development planning as well as for scientific studies of ecosystem productivity, carbon budgets, etc (Hall *et al.*, 2006; Parresol, 1999; Zheng *et al.*, 2004; Zianis and Mencuccini, 2004). Biomass is an important element in the carbon cycle, specifically carbon sequestration; it is used to help quantify pools and fluxes of Green House Gases (GHG) from the terrestrial biosphere to the atmosphere associated with land-use and land cover changes (Cairns *et al.*, 2003). The concentration of atmospheric carbon dioxide (CO_2) which is the major constituent of GHG, has increased from 278 ppm in the pre-industrial era (1970) to 379 ppm in 2005 at an average of 1.9 ppm per year (IPCC, 2007; UNEP, 2007). With the increasing concern for rising CO_2 concentrations, the role of forests, as a long-term carbon pool, for assimilation of atmospheric CO_2 is being increasingly realized; hence studies are currently afoot for assessing the use of forest biomass sinks to sequester carbon as part of a global mitigation effort. The amount of carbon stored in the biomass has gained special attention as a result of the United Nations Framework Convention on Climate Change (UNFCCC) and its Kyoto Protocol. Under these agreements, countries are required to estimate and report CO_2 emissions and removals by forests. The developing global carbon markets, particularly because of the incorporation of a Clean Development Mechanism (CDM[1]) in the Kyoto protocol, require accurate and reliable methods to quantify the sources and sinks of carbon in forest.

Forests play a major role in the global carbon budget because they dominate the dynamics of the terrestrial carbon cycle. Forest biomass constitutes the largest terrestrial carbon sink and accounts for approximately 90% of all living terrestrial biomass (Tan *et al.*, 2007; Zhao and Zhou, 2005). Many studies suggest that about 1-2 gigatons (Gt) ($1Gt=10^9$ kg) carbon are sequestered annually in pools on land in temperate and boreal regions (Dong *et al.*, 2003). Plant biomass constitutes a significant carbon stock and is the main conduit for CO_2 removal from the atmosphere primarily through photosynthesis. For this reason, the UNFCC and its Kyoto Protocol has recognized the role of forests

[1] CDM is a provision in the Kyoto protocol under which industrialized countries and economies under transition (Annex B countries) can earn certified emission reduction (CER) credits for funding projects that reduce greenhouse gas emissions in developing countries and contribute to sustainable development. Countries with a commitment to reduce their greenhouse gas emissions by around 5% below 1990 levels (in terms of CO_2 equivalent) by 2008-2012, buy CERs to cover a portion of their emission reduction commitments under the treaty.

in carbon sequestration. However, forest biomass can act as either a source or sink for GHG. The growth in forest biomass results in net atmospheric carbon sequestration in the terrestrial biosphere whereas the loss causes emissions to the atmosphere. The amount of carbon sequestered by a forest can be inferred from the biomass accumulation since approximately 50% of forest dry biomass is carbon (Cairns *et al.*, 2003; de Gier, 2003). Change in forest biomass (or carbon fluxes) are influenced by natural succession, anthropogenic actions such as deforestation, harvesting, plantation, silviculture, and natural disturbances by pests, fire and climate change (Brown, 1997; IPCC, 2006; Schroeder *et al.*, 1997). Thus biomass assessment is important to understand changes in forest structure.

FAO (2005) has defined biomass as "the organic material both above and below the ground, and both living and dead, e.g., trees, crops, grasses, tree litter, roots, etc." Above-ground biomass, below-ground biomass, dead wood, litter, and soil organic matter are the main carbon pools in any forest ecosystem (FAO, 2005; IPCC, 2003; IPCC, 2006). Above-ground biomass (AGB) includes all living biomass above the soil, while Below-ground biomass (BGB) includes all biomass of live roots excluding fine roots (< 2 mm diameter). Forest biomass is measured either in terms of fresh weight or dry weight. For the purpose of carbon estimation dry weight is preferred as dry biomass roughly contains 50 % carbon (Brown, 1997; IPCC, 2003). Majority of biomass assessments are done for AGB of trees because these generally account for the greatest fraction of total living biomass in a forest and do not pose too many logistical problems in the field measurements (Brown, 1997). AGB in this study is defined as the total amount of above-ground organic matter in living trees greater than 10 cm diameter at breast height (dbh) and taller than 1.3 m excluding foliage and branches less than 2.5 cm, expressed as oven-dry weight. The AGB, thus defined, often make the field work more practical and reduces the risks of measurement errors (e.g. double counting or omitting of trees in sample plots), especially in dense forests. Excluding the foliage biomass is justifiable as such biomass store carbon only temporarily.

Accurate estimation and mapping the distribution of forest biomass is a prerequisite in answering a long-standing debate on the role of forest vegetation in the regional and global carbon cycle (Lu, 2006). Selection of appropriate biomass estimation method and use of reliable forest inventory data are two key factors for this purpose (Zhao and Zhou, 2005). This study, implemented in the north-eastern cool temperate forest of China, has focused on biomass and carbon sequestration estimation at landscape level in Wangqing forest. North-east China maintains a large area of forests and has been experiencing the largest increase in temperature over the past several decades in the country; over the past two decades, the average temperature in the region has increased at the rate of 0.066 ^{0}C/year (Tan *et al.*, 2007). Since China occupies a pivotal position globally as a principal emitter of CO_2 and at the same time also as host to some of the world's largest reforestation efforts, and as a key player in international negotiations aimed at reducing global GHG emissions (Chen *et al.*, 2007), therefore, studying its forest biomass stock is important for sustainable use of the resources and understanding the forest carbon budget. This study is in line with the recently held 13th meeting of the Conference of Parties (COP) in Bali where parties realized the need for further methodological work on assessment of the amount of reduction or increase in GHG emission (UNFCCC, 2007).

1.1.2. Methods for assessment of forest biomass and carbon sequestration

Application of appropriate biomass estimation methods and transparent and consistent reporting of forest carbon inventories are needed in both scientific literature and the GHG inventory measures (Somogyi *et al.*, 2006). Different approaches, based on field measurements, remote sensing and GIS have been applied for AGB estimation (Lu, 2006). The traditional techniques based on field measurements only are the most accurate but have also proven to be very costly and time consuming (de Gier, 2003). The use of remote sensing (RS) techniques has been investigated, but as yet this approach has met with little success for multi-age, multi-species forests and only with limited success in forests with few species and age classes representing a broad range of biomass distributions (Schroeder *et al.*, 1997). Nevertheless, even where RS data are useful for estimating forest biomass/ carbon, ground data is still necessary to develop the biomass predictive model (i.e. calibration) and its validation (Zianis *et al.*, 2005); because remote sensing does not measure biomass, but rather it measures some other forest characteristics (e.g. spectral reflectance from the canopy). A sufficient number of field measurements are a prerequisite for developing AGB estimation models and for evaluating the AGB estimation results. GIS-based methods require ancillary data such as on land-cover, site quality and forest age to establish an indirect relationship for biomass in an area (Lu, 2006). Such methods are difficult to implement because of problems in obtaining good quality ancillary data and the comprehensive impacts of environmental conditions on biomass accumulation (Brown, 2002; Lu, 2006).

Biomass assessments on an area basis are usually carried out by using a multi-phase sampling design (de Gier, 2003) as illustrated in Figure 1.1. It can be simplified into three phases when we also consider the integration of RS data into the field data. The first phase of the design may use pixels from optical satellite imagery as sampling units from where spectral signatures can be extracted easily. In the second phase, sample plots corresponding to the pixels of first phase are established in the field and all the trees inside it are measured for dbh, among other things (these trees are not measured for their biomass). In the third phase, a relatively small but representative sample of trees are selected and they are measured for biomass in addition to dbh, height, etc (Cunia, 1986a). These sample trees are used to develop biomass equation based on tree variables like dbh and height. This relationship is then applied to calculate biomass of each tree in the sample plots of the second phase; the sum of which gives the total tree biomass in the plot. To obtain a good regression equation, one should randomly select an equal number of sample trees from each diameter class so that the entire range of the diameters are covered (de Gier, 2003). When previously developed biomass equations exist, the third phase is no longer required; however, a critical assumption in such a case would be that the population for which the equations exist and the population being inventoried are similar (Cunia, 1986a). This is a big assumption, since biomass equations from one location can not simply be used in another location, even when they are ecologically comparable (Cunia, 1986a; de Gier, 1999). Before applying any equation directly in the field, its suitability should be explored in terms of the range of dbh, cover-type, geographic location and the management system and also it should be validated by felling a sufficient number of trees. The application of existing equations without validation is prone to a bias of unknown magnitude (de Gier, 2003).

If validation of existing equation is to be carried out, felling of a sufficient number (>25) of representative trees is indispensable (de Gier, 2003). Such felled trees, however, might be better used

to derive new biomass equations for the area concerned, since these equations are always better than the validated ones (de Gier, 2003; IPCC, 2003).

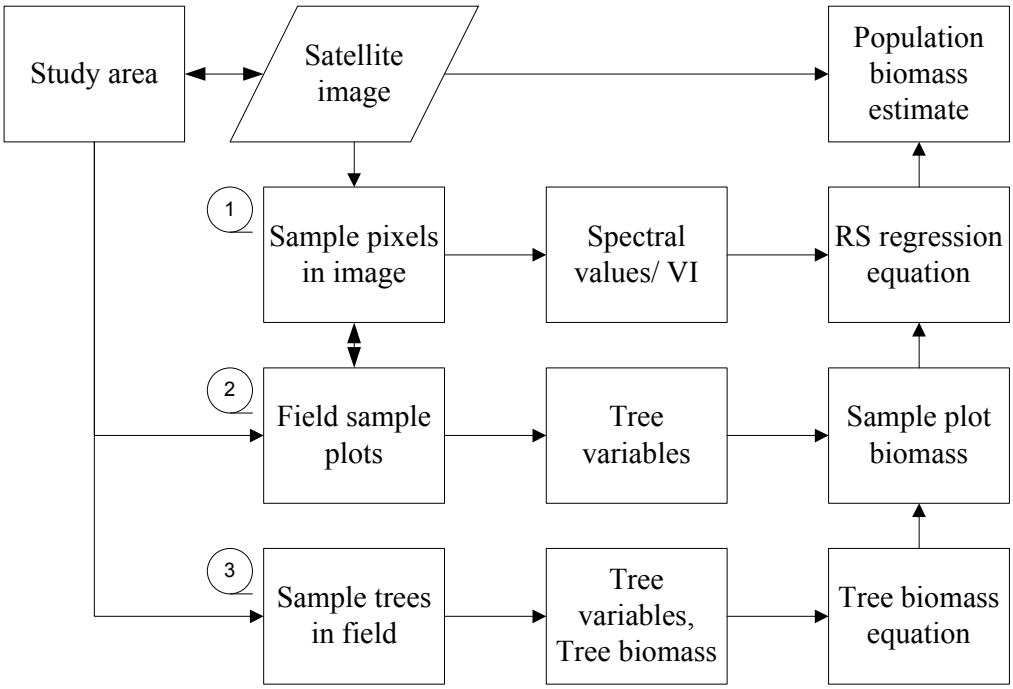

Figure 1.1 Multiphase sampling design for biomass assessment; 1, 2 and 3 indicate first, second and third phases; (adopted from de Gier, 2003).

If existing equations are lacking, measurements of sample tree biomass and its variables in the field is necessary. While measuring the sample tree variables is easy and straight forward, measuring the sample tree biomass is difficult. The existing methods of sample tree biomass measurement can be categorized into non-destructive and destructive. The non-destructive methods do not require tree felling. Tree measurements are made either by climbing the tree or taking photographs. These methods, however, can give only the volume of trees non-destructively. To estimate the tree biomass one has to rely on density values (which is already a product of destructive process) of tree components from literature. The calculated biomass by these procedures can not be validated unless the sample trees are still felled and weighted. So in effect purely non-destructive biomass sampling does not exist. The conventional destructive method is felling down the sample trees and weighing it totally with a scale. Total weighing can only be done for small trees as bigger trees can not fit onto a scale. In such cases, sectioning of bigger trees into parts/ components becomes obligatory. Such measurements confine themselves initially with fresh or green weight estimates, with or without a minimum diameter limit (de Gier, 2003). While the green biomass of the entire tree can be measured without any appreciable error, the oven-dry biomass of a given tree component is usually estimated based on haphazardly selected sub-samples that are first measured in the field for the fresh biomass and then oven-dry biomass determined in laboratory is used to estimate the total biomass using ratio estimator (Cunia, 1986b). Dry weight estimation of sample trees based on such sub-samples of the sections are, therefore, subjected to bias (de Gier, 2003). Field measurements are very demanding for accurate biomass assessment, although requires considerable amount of labour and cost.

Sub-sampling method

In view of the lack of cost effective and unbiased biomass estimation methods, de Gier (1989) adopted a sub-sampling method as suggested by Valentine *et al.*, (1984). Although destructive, this method is found to be cost effective and overcomes many of the constraints identified in biomass measurements. It also produces unbiased estimates of tree volume, fresh weight and dry weight (de Gier, 1999; de Gier, 2003; Mabowe, 2006). The method uses the principles of randomized branch sampling (path selection) and importance sampling (de Gier, 2003). In the first step a 'path' is selected through the tree (see section 2.3.2), starting from the butt and ending at a predetermined minimum branch diameter. At every node of branching a decision is has to be made about the continuation of the path. The path continues towards the branch (segment) with higher probability that is proportional to the size (base diameter, d_i). The path selection terminates at the point where a minimum diameter is reached. The minimum diameter is fixed to reduce the amount of work. The unconditional probability of a segment (see formula in section 2.3.2) is the result of multiplication of the probabilities of all the segments in the path from the butt end till the segment concerned. Thus the last segment has lowest probability. The second step of the method is importance sampling where by one randomly located disk from the path is removed. At this stage, the path of the tree is considered to consist of an infinite number of infinitely thin disks, of which one is selected with a probability proportional to its diameter squared (de Gier, 2003).

For volume calculation by the method, points are located along the path where change in taper occurs. The diameters and corresponding distances from the butt are measured at each of these points. The inflated areas at the points are calculated by dividing diameter squared by its unconditional probability. The calculated inflated areas of two subsequent points and the distance between them are used to calculate the inflated volume of the segment using the Smalian formula (see section 2.3.2). Adding all such volumes, of all sections, results in an unbiased estimate of the total tree woody volume (de Gier, 2003).

For the weight estimation, a disk (about 10 cm thick) is removed from a random point along the path. This point is determined by multiplying the estimated total tree volume with a random number. The segment in the path at which this volume is reached is identified and the exact point within the segment where the disk is to be removed is determined by interpolation. The weight per unit thickness of the disk is determined and is divided by the unconditional probability of the segment from where it was removed. Multiplying this value with the estimated total tree woody volume and dividing it by the square of the disk diameter gives the total woody fresh biomass. The oven dry weight of the disk can be used to calculate the total tree dry biomass in the same way as with fresh weight (de Gier, 2003). If the disk is large, it can be split into wedges and one wedge is selected with a probability proportional to weight. The weight of the selected wedge when divided by its selection probability results in the estimate of the disk weight.

The method has the strength to give on the spot estimates of volume and fresh weight. After oven-drying the disks or wedges, tree dry weight is calculated. The path selection reduces much of the work as the branches that are not included in the selected path, do not require measurements. Further there is no need to weigh the whole tree, a small sample disk/ wedge is enough. Hence it is time efficient and cost effective. The equipments required in the method are mostly light-weight; the heaviest piece is a power saw but that can also be carried by hand. Field work can be efficiently carried out by two

people (de Gier, 2003). However, the procedure uses considerable amount of computations that makes use of a hand-held computer necessary. De Gier (2003) tackled this problem by developing a 'biomass assessment' program adapted for use with an iPAQ PDA.

Biomass equations

Most of the existing equations relate above ground dry biomass of trees to its biophysical variables such as dbh, height, etc (Zianis *et al.*, 2005). Using more variables in an equation requires measurement of sufficient number of trees to cover the full range of the variables. This calls for equations that use as few as possible variables, because necessary tree felling will be reduced (de Gier, 2003). Incorporating more variables in the equation does not necessarily improve the accuracy of the estimate significantly; De Gier (1989), Schroeder (1997) and Wang (2006) found that incorporating the height did not significantly improve the models based on dbh alone. Further, measurements of some of the variables (e.g. total tree height) in the field are more difficult, time consuming and less accurate than measuring dbh (Gower *et al.*, 1999). Hence, dbh is the most common predictor in biomass equations (Jenkins *et al.*, 2003; Wang, 2006; Zheng *et al.*, 2004; Zianis and Mencuccini, 2004). The method of least squares regression is quite common in the development of biomass equations (Furnival, 1961; Parresol, 1999). When biomass regressions are calculated by statistical least squares methods, the random part of sub-sampling error is automatically taken into account (Cunia, 1986a). Unweighted least squares estimates are fully efficient only when homoscedasticity exists or, in other words, only when the standard error of the residuals is constant for all classes of the dependent variables (Furnival, 1961). In reality, the standard error of the residuals tend to vary with the size of trees; larger trees deviate more from the regression curve than do small trees. So weighting of the regression coefficients is important (Parresol, 1999); theoretically weights should be employed that are inversely proportional to the variance of the residuals (Furnival, 1961).

Large number of biomass models exists in literatures; and it is really difficult to decide which model form is most appropriate for a particular set of data. However, the usual index of fit, the root mean square error (RMSE), can be used to compare models that have the same dependent variable (Furnival, 1961). Prediction errors, logical behaviour of the models, coefficient of determination (R^2) and simplicity of the models are some other criteria for choosing appropriate model (Schroeder *et al.*, 1997). The commonly used mathematical models for biomass studies take the form of the power function (Fehrmann and Kleinn, 2006; Green *et al.*, 2005; Hall *et al.*, 2006; Meng *et al.*, 2007; Samalca, 2007; Ter-Mikaelian and Korzukhin, 1997; West *et al.*, 1997; Zianis and Mencuccini, 2004; Zianis *et al.*, 2005); polynomial function (Cunia, 1986a; de Gier, 2003; Parresol, 1999; Zianis *et al.*, 2005) or combined variable models (de Gier, 2003; Gregoire and Williams, 1992; Parresol, 1999; Zianis *et al.*, 2005), as given below.

Power function,	$M = aD^b$	(1)
Combined variable model,	$M = a_0 + a_1D^2H$	(2)
Polynomial model	$M = a_0 + a_1D + a_2D^2 + a_3D^3 + \ldots\ldots\ldots\ldots$	(3)

Where, M = biomass (kg); D = diameter at breast height (dbh); H = tree height and a_i = regression coefficients that are reported to vary by species, stand age, site quality, climate and stand density (Fehrmann and Kleinn, 2006; Zianis and Mencuccini, 2004).

The equation (1) is simple to use as it contains only one variable, dbh. It is solved by taking logarithms on both sides and employing simple linear regression techniques. But the problem with this model is that the calculated coefficient 'a' from the log transformed model is biased and the relationship between biomass and dbh can not be established because the correlation coefficient and the coefficient of determination refer to the log transformed equation, not to the power function (de Gier, 2003; Parresol, 1999; Zianis *et al.*, 2005). The equation (2) can be solved by simple linear regression technique. This model requires two variables, dbh and height. The polynomial equation (3) also requires only one variable, dbh and it can be solved by multiple linear regression techniques. Models (2) and (3) allow a correct calculation of its precision, although usually require weighting (de Gier, 2003). The problem of heteroscedasticity with biomass data is solved by weighing.

Biomass equations are preferred if one has access to a representative sample of tree-wise data from the target population (Somogyi *et al.*, 2006). The biomass estimates from local site specific equations are considered accurate in forestry applications. The Good Practice Guidance (IPCC, 2003) and the guidelines for national greenhouse gas inventories (IPCC, 2006) by the Intergovernmental Panel on Climate Change (IPCC) prefer the selection and use of species-specific or similar-species allometric equations in the priority order of local to national to global scale. So, development of a local biomass equation can be helpful in the evaluation of the precision of biomass estimates while using alternative models. Only the above mentioned three models are evaluated in this study because of their simplicity and wide application.

Annual wood increment and carbon sequestration

Estimating the annual biomass or carbon increments in a live tree is an important component towards understanding the carbon balance of forested ecosystems. The measurements of annual growth rings (if exists) in trees in conjunction with biomass equations is an established method for determining above-ground woody biomass increment in live trees (Heath, 2000). Bouriaud *et al.*, (2005) found very strong relationships between basal-area increment and annual wood accumulation in trees. The growth rings of a tree can be measured either by removing a disk or taking out a core from the trunk. In the latter case, an instrument called increment borer is drilled into the tree trunk and a cylindrical core of wood is extracted. In areas having a distinct growing season, most species have equally well defined annual rings. In a tree, the cambium (the cells that will become wood or bark) grows in a light layer during late spring/early summer changing to a dark layer in later summer/early fall. The light layer is early wood, formed when the tree is growing rapidly. The dark layer is late wood and is grown more slowly. The growth occurs at the outside of the trunk, just under the bark, so that a light and dark ring pair represents one year. The procedure for using increment core data for the assessment of annual biomass increment is explained by de Gier (1989). Loetsch *et al.*, (1973), as cited by de Gier (1989), derived a relation for annual tree volume increment based on tree volume equation and annual over-bark diameter increment. The annual over-bark diameter increment is the sum of the annual increments in under-bark diameter and bark-thickness. The under-bark diameter increment and the increment in bark-thickness can respectively be estimated from the measurements of growth rings and bark-thickness at the breast heights in sample trees (see the procedure in section 2.3.2). In a similar way as for volume increment, a relation for annual increment of tree biomass (both fresh and dry) can be obtained (de Gier, 1989). The tree biomass increment equation can be used to estimate the plot

biomass increment based on available plot diameter data. From that annual carbon sequestration can be estimated since roughly 50 % of the dry biomass is carbon.

Lack of location specific biomass equations and unknown precision of estimates from existing regional and global equations has inspired this study for a reliable estimation of biomass, annual biomass accumulation and carbon sequestration at a landscape level in Wangqing forest in Jilin Province, Northeast China. This study has focused on developing good quality local biomass equations based on easily measurable tree variable such as dbh. The use of sub-sampling method for the estimation of sample tree biomass and validation of its accuracy is also sought by undertaking total weighing of some sample trees. The area-based estimates from the newly developed equations can then serve as a reference to assess the accuracy of similar estimates while using existing regional or global equations. As North east China has distinct winter and summer seasons and most of the tree species bear annual growth rings, an attempt is made to use tree growth rings and barks thickness data to develop a relation for carbon sequestration estimation.

Once the equations for tree biomass, annual wood accumulation and carbon sequestration are derived, sample plot estimates can be obtained by applying the equations to the sampled plot tree diameter data. These plot estimates can then be taken as independent variables and related to satellite data such as vegetation indices, for large scale mapping.

1.1.3. Remote sensing for mapping of biomass and carbon

The traditional approach of biomass assessment relying heavily on field measurements is often time consuming, labour intensive and difficult to implement, especially in remote areas. While for small scale biomass assessment the conventional method is good, they cannot provide the spatial distribution of biomass over large areas. The challenging issues of carbon sequestration require biomass estimation over large area. Remote sensing techniques has been extensively used for vegetation mapping and monitoring (Boyd *et al.*, 2002; Brown *et al.*, 2000; Ingram, 2005; Lu *et al.*, 2004; Maynard *et al.*, 2007). Use of remote sensing data has been employed in many studies on biomass assessment (Dong *et al.*, 2003; Foody *et al.*, 2003; Foody *et al.*, 2001; Heiskanen, 2006; Lu *et al.*, 2004; Maynard *et al.*, 2007; Muukkonen and Heiskanen, 2005; Steininger, 2000; Zheng *et al.*, 2004). Remote sensing may be the only feasible way to acquire forest stand parameter information at a reasonable cost, with acceptable accuracy, and feasible effort because of its data advantages which include repeated data collection, multi-spectral and multi-temporal images, synoptic view, fast digital processing of large quantities of data, and compatibility with geographic information systems (GIS) (Lu, 2006). Remote sensing also allows independent monitoring of resources (de Gier, 2003). These advantages of remotely sensed data, and observed high correlations between spectral data and vegetation parameters in many cases make it the primary source for large scale AGB mapping. In general, the AGB can be estimated using remotely sensed data with different approaches, such as multiple regression analysis, K-nearest-neighbour, and neural network (Lu, 2006).

The most frequently used RS data continue to be from the optical moderate resolution sensors like Landsat Thematic Mapper (TM) (Hall *et al.*, 2006; Heiskanen, 2006; Ingram, 2005; Lu, 2006; Lu *et al.*, 2004). Estimation of forest biomass over large areas from the analysis of such satellite data would enable many additional questions about the ecological functioning of natural or human modified

landscapes to be addressed (Steininger, 2000). Studies have shown that TM data provide comparable and in some cases, stronger predictions of certain forest structural features when compared to radar satellite systems or other optical sensors of similar spectral and spatial resolution (Ingram, 2005). Biomass can not be directly measured from space, but, remotely sensed spectral signatures can be used to estimate biomass (Dong *et al.,* 2003). The biomass measurements from sample plots can then be integrated into the RS techniques to get cost effective and large spatial information on AGB distribution.

The possibility of estimating biomass by satellite RS has been investigated in several studies at various spatial scales and environments (Heiskanen, 2006). Biomass estimation using RS has remained a challenging task, especially in areas with complex forest stand structures and environmental conditions (Lu, 2006). A good understanding of relationships between forest biomass and remote-sensing spectral data is a prerequisite for developing appropriate biomass estimation models (Steininger, 2000). Identifying the spectral wavelengths or wavelength combinations that are most suitable to use to acquire information about a specific biophysical parameter in a given study area is difficult (Lu *et al.*, 2004). Vegetation indices (VIs) and band ratio based models are most commonly used to produce estimates of biomass (Foody *et al.*, 2003; Hurcom and Harrison, 1998; Schlerf *et al.*, 2005; Zheng *et al*., 2004). A variety of VIs have been developed, with the most popular ones using red and near infrared wavelengths to emphasize the difference between the strong absorption of red electromagnetic radiation and the strong scatter of near infrared radiation. VIs are used to remove the variability caused by canopy geometry, soil background, sun view angles, and atmospheric conditions when measuring biophysical properties (Lu, 2006). Nonetheless, VIs are also sensitive to internal (such as canopy geometry, terrain factors, species composition) and external factors (sun elevation angle, zenith view angle, atmospheric conditions) that affect vegetation reflectance (Lu *et al.*, 2004). There is wide disagreement in literature as regards the biomass- VIs relationship. Many studies report a significantly positive relationship between the values of the VIs and the biomass at least up to the reflectance asymptote of the canopy (Boyd *et al.*, 1999; Heiskanen, 2006; Hurcom and Harrison, 1998; Maynard *et al.*, 2007; Steininger, 2000; Zheng *et al.*, 2004); however, some results have shown poor relationship (Foody *et al.*, 2003; Schlerf *et al.*, 2005).

The normalized difference vegetation index (NDVI) (see formula in section 2.5) is one of the most commonly used VIs in many applications relevant to analysis of biophysical parameters of forest. The strength of NDVI is in its ratioing concept, which reduces many forms of multiplicative noise (illumination differences, cloud shadows, atmospheric attenuation, certain topographic variations) present in multiple bands (Huete *et al.*, 2002). However, conclusions about its value vary, depending on the use of specific biophysical parameters and the characteristics of the study area. Foody *et al.*, (2003) tested several VIs and found that NDVI was never among the top 10 indices defined in terms of the strength of correlation with biomass of sample plots. Although in some cases NDVI have shown good correlation with leaf-area index (LAI), it did not appear to be a good predictor of stand structure variables such as height, basal area or total biomass in uneven age and mixed broadleaf forests (Lu *et al.*, 2004). Zheng *et al.,* (2004) used five VIs and found best result with corrected NDVI (NDVIc) in predicting AGB. NDVIc is calculated from Red, near-infrared (NIR), and middle infrared (MIR). NDVIc can help account for understory effects and is useful in secondary forests (Zheng *et al.*, 2004). Simple ratio, SR (ratio of NIR and Red) is another commonly used VI for the study of forest

biophysical variables (Schlerf *et al.*, 2005). Heiskanen (2006) and Lu *et al*., (2004) found SR to be significantly correlated with AGB.

Vegetation has a high near-infrared reflectance, due to scattering by leaf mesophyll cells and a low red reflectance, due to absorption by chlorophyll pigments. The value of the NDVI for vegetation will hence tend to one. By contrast, clouds, water and snow have a larger red reflectance than near-infrared reflectance and these features thus yield negative NDVI values. Rock and bare soil areas have similar reflectances in the two bands and result in values of NDVI near zero.

Previous studies have shown that middle-infrared reflectance (TM band 5) have strongly negative relationships with biomass (Boyd *et al.*, 1999; Lu, 2006; Steininger, 2000). Schlerf *et al.*, (2005) observed better relation between middle-infrared VI (MVI: ratio of NIR and MIR) and tree crown volume than SR and NDVI and concluded that the MIR band in combination with the NIR band contain more information relevant to the characterization of forest canopies than the combination of Red and NIR bands.

Shortwave infrared (SWIR) modification to simple ratio called Reduce Simple Ratio (RSR) (see formula in section 2.5) can also be used to study the relationship with biomass as it has been found be sensitive to change in LAI; reduces the effect of back ground reflectance; negates the effect of higher NIR reflectance in deciduous canopies and unifies deciduous and coniferous species in LAI retrieval from RS data (Brown *et al.*, 2000). The Enhanced Vegetation Index (EVI) was developed to optimize the vegetation signal with improved sensitivity in high biomass regions and improved vegetation monitoring through a de-coupling of the canopy background signal and a reduction in atmospheric influences (Huete *et al.*, 2002).

A number of soil adjusted vegetation indices also exists to reduce the effect of the soil background reflectance. However, in the forested environment the bare soil is rarely visible and the definition of soil line is difficult and the line is discontinuous (Heiskanen, 2006). Hence application of soil adjusted vegetation indices becomes futile.

Saturation issue

The saturation of the relationship between biomass and the NDVI is a well-known problem (Mutanga, 2004). The most logical explanation is that as canopy cover increases, the amount of red light that can be absorbed by leaves reaches a peak while NIR reflectance increases because of multiple scattering with leaves (Tenkabail *et al.*, 2000). Further, NIR reflectance also saturates with increasing leaf area index (LAI) ≥ 3 and so does NDVI (Schlerf *et al.*, 2005). The imbalance between a slight decrease in the red and high NIR reflection results in a slight change in the NDVI ratio, hence yields a poor relationship with biomass (Mutanga, 2004). Rauste (2005) reports that saturation level may depend on the tree species and forest types as well as the ground surface type (because, Imhoff (1995) found saturation level at 40 tons/ha of dry biomass in temperate forests in USA; Luckman *et al.*, (1998) observed saturation level at 60 tons/ha in a tropical forest in Brazil; Fransson and Israelsson (1999) observed the saturation at 143 m^3/ha in a boreal forest in Sweden) [Note: as an approximation, forest stem volume (m^3/ha) in boreal forests can be converted into dry biomass (tons/ha) by multiplying the stem volume estimate by 0.6, as cited by Rauste (2005)]. Steininger (2000) found that the canopy

reflectance saturated when AGB approached about 15 kg/m^2 i.e. 150 tons/ ha in a tropical secondary forest in Manaus, Brazil.

This study will try to identify the most likely VIs or band ratio that best correlate with AGB of Wanqing forest. The saturation issue of VIs will be investigated for the existing level of biomass stock in Wangqing forest.

1.2. Problem statement

There is considerable interest today in estimating the biomass of forests for both practical forestry issues and scientific purposes (Parresol, 1999; Tan *et al.*, 2007; Wang, 2006). However, the quantification of biomass or carbon pools of a forest suffers from a number of methodological problems. Accurate biomass estimation requires locally applicable tree biomass equations. Unfortunately, all forests do not have such equations. Although a large number of biomass equations exist in literature, their applicability to any forest is questionable. Very often it is unknown how many trees of what kinds were used and how they were selected for the development of biomass equation (de Gier, 2003; Zianis *et al.*, 2005). The unclear description of the existing equations regarding the range of dbh, cover-type, geographic location and the management systems for which they are applicable makes the use and estimate uncertain. Biomass equations may vary by forest/ cover type, age, site conditions, stand density and climate (de Gier, 2003; Fang *et al.*, 2001; Zianis *et al.*, 2005). So before applying any secondary equation, they need to be validated by felling a sufficiently large number of trees (> 25) (de Gier, 1999). But instead of felling trees for verification, they can better be used for the development of local equation. The 'Good Practice Guidance (GPG) for Land Use, Land Use Change and Forestry' (IPCC, 2003) has shown a lot of flexibilities in terms of the use of existing equations. The GPG has given priority for the use of allometric equations in the order of local to nation to global scales in biomass calculation. However, the effect on precision of biomass estimates at the area concerned while using an equation developed at different geographic location, needs to be tested.

Developing a biomass equation requires harvesting and measurement of sample trees for their biomass. True biomass of the sample trees can only be obtained by total weighing using a scale. But this method is very laborious and expensive. One choice is tree sub-sampling which is time-efficient and cost effective. Although the sub-sampling method of biomass assessment is designed to substitute the time consuming field measurement techniques or biased methods, the sub-sampling estimates still needs to be tested for its accuracy. As this method was never tested in cool temperate forest such as in north-east China; its reliability can not be established without verifying by felling some trees and subsequently measuring biomass by both sub-sampling and total weighing. The existing equations (national or global) can also be tested for the level of precision by comparing field measurements on sample trees with the estimates from the equation.

The study area, Wangqing forest in Jilin Province, north-east China, maintains abundant forests characteristic of cool temperate zone. Wang (2006) has mentioned that only few biomass equations exist for the tree species in Chinese temperate forests. The local forest management authorities do not have information on the available and harvestable stock of AGB in the area. At a time when the issue of reducing GHG emissions is seriously growing, the carbon sequestration potential of the forest is

still unknown. The temperate region biomass equations suggested by GPG (IPCC, 2003), hereafter called IPCC equations, have originated from the forest trees of eastern USA. Similarly, one existing local Chinese equation evaluated in this study is based on temperate forest in another province in north-east China. This study is also meant to see the precisions of the biomass estimates while using the regional (local Chinese) and global (IPCC) equations.

Measurements of growth rings can be applied for the estimation of annual wood accumulation and carbon sequestration (de Gier, 1989). But this potential has not been explored in the Wangqing forest. Whether the relationship between diameter increment and annual wood increment exists for the Chinese tree species; whether the relationship can be combined for all the trees species together; whether it is feasible and accurate are some of the issues that can be attempted from annual growth ring measurements. If the method be established by developing equations for annual wood accumulation and carbon sequestration then it would greatly benefit the concerned stakeholders.

In RS based biomass assessment, biomass equation is still vital to estimate plot biomass which is correlated with spectral data for large scale mapping. Tree based biomass estimate is calculated by applying the biomass equation to the individual trees of randomly selected plots. The biomass estimate of all trees in each plot is then aggregated to obtain the plot biomass estimate. Tan *et al.*, (2007) has mentioned that no studies have been done to estimate the forest biomass for northeast China by using remote sensing data. The general lack of spatial forest biomass data has been considered one of the persistent problems at policy level for sustainable management planning. This study is directed at the integrated use of RS and field inventory data to map the spatially explicit patterns of AGB distribution. Models derived from RS and verified with ground data can be used appropriately to predict AGB for a given landscape. Also the problem such as saturation effect of VI with RS data in mapping the distribution of AGB needs to be explored; saturation effect of VI with vegetation abundance is unknown for the study area that can be explored. This study is intended to look into the accuracy levels of different biomass assessment methods with scientific eye.

1.3. Research questions

1. How accurate is the estimate of tree biomass by sub-sampling method?
2. Which model out of polynomial, power and combined variable forms is appropriate for the estimation of above-ground biomass at a landscape scale while considering the accuracy and problems in tree variables measurement?
3. How do the estimates from the existing Chinese and IPCC equations compare (with respect to precision) with the sub-sampling estimates and what would be their impact on assessing carbon reservoirs and sinks?
4. How reliable is the estimate of carbon sequestration obtained from growth ring measurement?
5. Which vegetation index or spectral bands best relate to above-ground biomass? And what is the biomass estimate of Wangqing forest?
6. Is there a saturation problem of VI in the study area? If yes, at what level of biomass does VI start to saturate?

1.4. Objectives

1. To assess the accuracy of sub-sampling method for reliable, unbiased and cost effective-biomass estimation
2. To develop biomass equations based on field measurements of sample trees for landscape level biomass estimation
3. To compare the effect of area based above-ground biomass estimates using local Chinese equations and IPCC equations in respect of precision with the field measurements
4. To estimate the carbon sequestration of the forest using growth ring measurements and compare with secondary information
5. To map the spatial distribution of forest biomass using the best combination of remote sensing and ground truth data
6. To evaluate the saturation issue of VIs

1.5. Hypotheses

1. The estimates of biomass by the sub-sampling method and total weighing do not differ significantly
2. Locally developed biomass equations give better estimates of above-ground biomass compared to the existing regional or global equations
3. Carbon sequestration estimates obtained from growth ring measurements is comparable to secondary information
4. Linear relationship of spectral VIs and plot biomass can be used to map the distribution of above-ground biomass and carbon sequestration

1.6. Research Approach

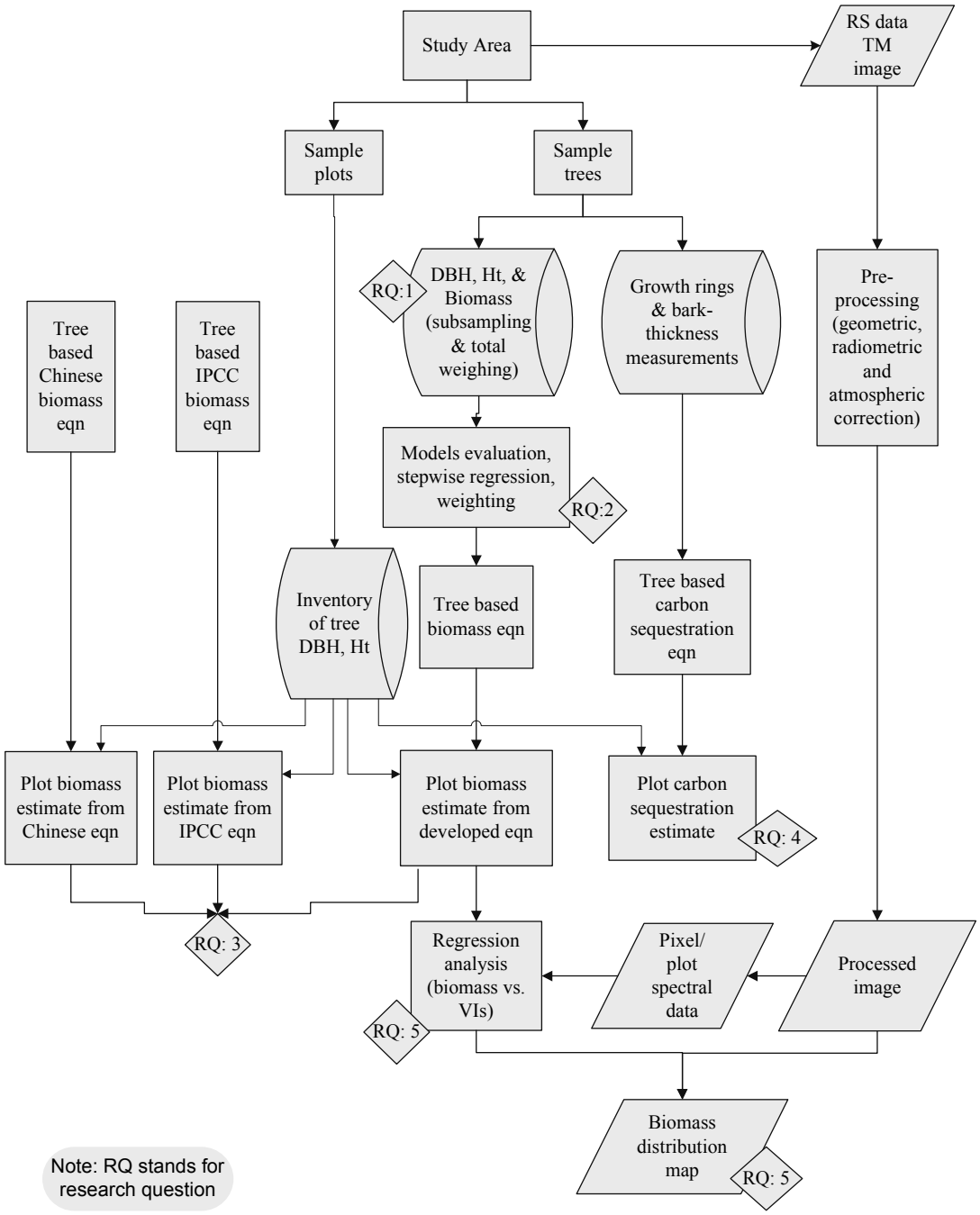

Figure 1.2 Flow diagram of the research approach

2. Methods and Materials

2.1. Study area

The study was implemented in Wangqing forest in Jilin Province, Northeast China (see Figure 2.1). The criteria for the selection of the study area were: cutting of trees for the research purpose should be permissible; area should be accessible by foot or vehicle; support staff and local labours should be available during field measurement; satellite imagery and maps should be available; and the area should represent typical cool temperate region experiencing severe influence of global warming. Since the area is also research site for some other ITC students and the local forest authority have collaboration with ITC and required data and resources for the study were available, the site was selected for the study.

The study area (43°05′-43°40′N and 129°56′-131°04′E) covers approximately 85×60 km^2 cool temperate forest and is located along the border between China and North Korea. The Wangqing forest area belongs to Changbai mountain system which is one of the most valuable Chinese forest reserves because of its rich floral diversity. The climate is continental monsoon with windy spring, a warm and humid summer, cool autumn and dry cold winter (Wang, 2006). Mean annual temperature is 3.9 ^{o}C. The mean annual precipitation is 438 mm, about 80% of which takes place between May and September. The elevation of the Wangqing forest ranges from 360 to 1,477 m above sea level and the steep slopes of the terrain even exceed 75%. September is the end of growing season of vegetation in Wangqing.

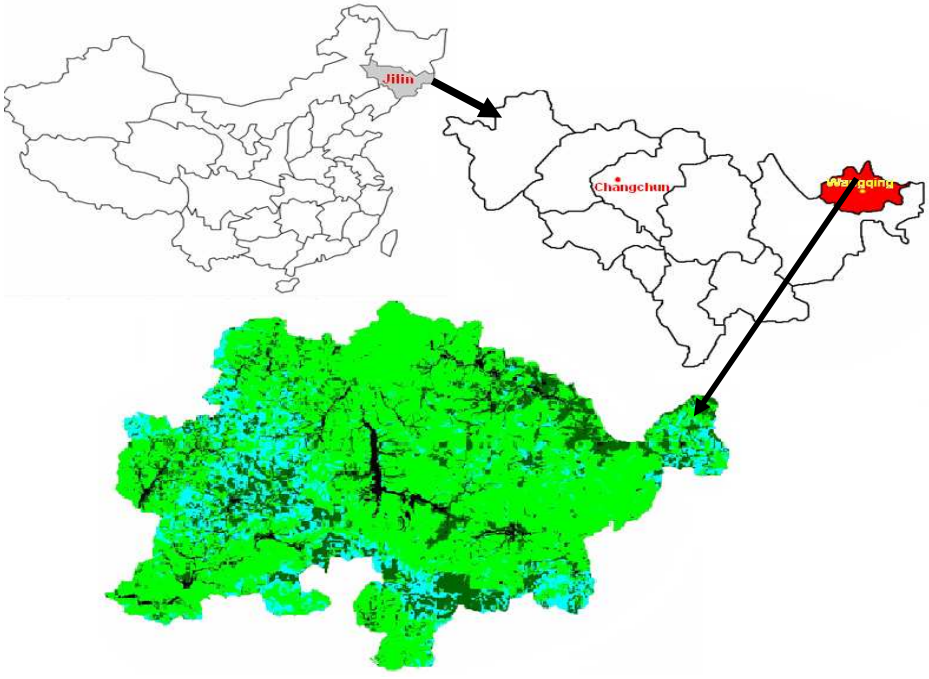

Figure 2.1 The study area, Wangqing forest in Jilin Province, North-east China

The area broadly covers 3 forest types by structure: needle-leaved, broad-leaved and mixed forests (Xing, 2007b). The main needle-leaved forest tree species are *Picea jezoensis, Larix olgensis, Abies holophylla* and *Pinus koraiensis* while the deciduous broadleaf forests are characterized *Betula platyphylla, Quercus mongolica, Betula castata, Populus ussuriensis, Fraxinus mandshurica and Ulmus pumila*. The mixed forest tree species are *Pinus koraiensis, Picea jezoensis, Pinus sylvestris var. mongolica, Larix olgensis, Abies holophylla, Tilia amurensis, Ulmus pumila, Betula platyphylla, Betula castata* and *Acer mono* (Xing, 2007b). The forests in the study area are essentially even-aged secondary forests which are the result of large scale industrial logging by Russian and Japanese invaders and the Chinese government since the turn of the 20th century (Wang, 2006). In many places the primary forests have been replaced by large scale plantations of pine and larch. The Mongolian oak (*Quercus mongolica*) forests are distributed at arid infertile steep slopes, mixed deciduous forests are distributed over well drained fertile mid-slopes and hardwood forest at moist fertile gentle toe slopes (Wang, 2006).

2.2. Research Approach

A multiphase (three-step) sampling approach as described in Chapter 1 (section 1.1.2; Figure 1.1) was used for the estimation of biomass and carbon sequestration. The first phase involved analysis of satellite image while the second and third phases respectively comprised the enumeration of sample plots and measurements of sample trees. Inside the sample plots all the trees were measured for dbh only while the sample trees, selected randomly and independently outside the sample plots, were measured for biomass besides dbh and height. Biomass of all the sample trees was estimated by a sub-sampling method. In addition, total weighing of a number of randomly selected sample trees was also done to validate the estimation by sub-sampling. After validation, biomass data obtained from the measurements of sample trees through sub-sampling were used in a regression analysis, together with tree variables dbh and height. The developed biomass equations (dry weight, fresh weight and volume) were then used to estimate biomass of each tree in the sample plots, the aggregate of which gave the plot biomass. The plot biomass values thus calculated were then related by regression analysis to the spectral values (vegetation index/ band ratios) of corresponding pixels in the TM image of the study area. The resulting regression model, using spectral data as explanatory variable and plot biomass as response variable, was then used to estimate total biomass in the Wangqing forest and also to make a biomass distribution map.

In order to develop annual wood accumulation and carbon sequestration equation (explained in section 2.3.2), growth ring and bark-thickness measurements were made on disks removed at breast height from the same trees as used for sub-sampling.

2.3. Data collection

2.3.1. Secondary data collection

A local (regional) tree biomass equation for north-east Chinese temperate forests was collected from literature (Wang, 2006). The IPCC equations for temperate forest trees species are given in Annex 4A.2 of the Good Practice Guidelines by IPCC (2003) and Schroeder *et al.*, (1997). Topographic and vegetation information of the study area were obtained from Xing, Y. (2007) through personal communication who also helped in the processing of satellite data. Scientific names of tree species were validated by literature analysis.

2.3.2. Primary data collection

Field data are necessary for both conventional and remote sensing based biomass assessment (FAO, 1981). The primary field data collection basically involved two phases. One phase was the enumeration of randomly located sample plots and the other was harvesting and measurements of sample trees. In addition, for the purpose of assessing annual wood accumulation and carbon sequestration in trees, annual growth rings of some randomly selected sample trees were measured. The descriptions of the measurement process are as follows:

2.3.2.1. Sample plot measurements

Sample plot measurements were necessary to estimate the above-ground biomass (AGB) and annual carbon sequestration on per hectare basis and also for the whole study area. A general idea on the distribution of forest in the study area was obtained from an unsupervised classification of TM imagery (of September, 2006) of the area. 138 circular plots of 500 m^2 (radius 12.62 m on flat terrain), randomly established throughout the study area, were enumerated in September, 2007. Random selection of the sample plots was first made on the false color composite of the geometrically corrected TM image and was positioned in the field with the aid of a GPS. A Garmin GPS set in the UTM projection system was used to locate the plot centres in the field. Next, slope, aspect and altitude of each plot were recorded. The slope was recorded after cross verification by taking measurements up and down the slope by two persons standing roughly at 25 m distance on the plot diameter along the slope. A slope correction table was used to obtain plot radius in order to get a horizontal plot area of 500 m^2. Circular plots were preferred because they were easy and quick to layout in the field, and determination of trees inside the plot was less problematic than in square plots. A bigger plot size was not used to avoid the risk of double counting or omission of trees in the dense forest during enumeration. The size of the circular plot is comparable to the spatial resolution of TM image (30×30m). Species and dbh (at 1.3 m above the ground) of each standing tree above a minimum dbh of 10 cm were recorded in each plot (Brown, 1997; FAO, 2004; Foody *et al.*, 2003; Schroeder *et al.*, 1997). Over-bark dbh of each tree in the plots was measured with a caliper to the nearest mm in two perpendicular directions. To avoid bias in dbh measurement, the direction of the first measurement was always with the caliper oriented towards the plot centre and the second one perpendicular to it (de Gier, 1989). Smaller trees <10 cm dbh were not considered since they contribute a relatively small quantity of biomass (Brown, 1997; Schroeder *et al.*, 1997). An additional set of 34 plot inventory data, collected by the same technique (Xing, 2007b) in September 2006, was also used in this study. Thus a total of 172 plot data sets were used for the assessment of biomass and carbon sequestration.

2.3.2.2. Sample trees, sub-sampling and total weighing

Sixty sample trees, representing the existing diameter range and forest types, were harvested and measured in the second week of September, 2007. The existing data set of 102 plots inventoried in 2006 (Xing, 2007b) was used as reference to select the sample trees. A similar number of sample trees were randomly selected from each 5 cm class intervals of the existing dbh range so that each class had a nearly even tree distribution. The sample trees belonged to the nine most abundant botanical genera. The species selected, the dbh range and the number of trees by species are given in the Table 2.1. The dbh range of the sample trees was 7.2-36.5 cm which constitutes the predominant diameter range of the nearly even-aged secondary forest of Wangqing. A number of sample trees smaller than 10 cm dbh

were also included to fine tune the trend line at smaller dbh values. All trees were sampled from fully stocked stands. Only healthy trees were selected in the sample.

Table 2.1 Number of sample trees by species and diameter range

S.N.	Species	DBH range (cm)	Number of trees
1.	*Betula platyphylla*	8.5-35.3	10
2.	*Quercus mongolica*	7.2-31.6	7
3.	*Ulmus pumila*	8.9-36.5	7
4.	*Tilia amurensis*	13.1-24.3	3
5.	*Populus ussuriensis*	14.4-18.9	2
6.	*Fraxinus mandshurica*	17.1	1
7.	*Larix olgensis*	7.7-33.5	11
8.	*Picea jezoensis*	8.4-26.5	9
9.	*Abies holophylla*	8.5-30.4	10

Each sample tree was assigned an identity code, its local name and location were noted and dbh was measured before felling while the total height was measured by a tape after felling. The scientific names of the tree species were identified from literature by Wang (2006), Wang *et al*.,(2006) and Xing (2007b). The stems were cut as close to the ground as possible. All 60 sample trees were measured by sub-sampling method- a computer based biomass assessment program.

Sub-sampling method: An iPAQ (a portable hand-held computer, PDA) based 'biomass assessment' program developed by de Gier (2003) was used for the biomass estimation of the sample trees. The program guides the user through all the necessary steps to estimate woody biomass and volume. The method is called sub-sampling because the total woody biomass of a tree is estimated based on a small wood sample (disk or wedge) selected from a random location of the tree so that the sample has a selection probability proportional to size. The common terms used in the method are branch, path and segment. Branch is the complete stem system that develops from a single bud; the path is a series of connected branch segments or internodes. A segment is a part of a branch between two consecutive nodes. Each segment in a path has associated selection probability proportional to size. The butt is the first node (see the level L1 in Figure 2.2) and has selection probability $q_1=1$. The second node occurs at the point of tree limbs (level L2 in Figure 2.2). The program incorporates two main procedures namely path selection and importance sampling (also see section 1.1.2) to estimate tree biomass and volume.

Step 1: Path selection

After felling a tree, a path was selected through it, starting from the butt and ending at the specified minimum branch diameter of 2.5 cm. The path selection involved the measurement of base diameter of each branch (above 2.5 cm) at each node staring from the butt end to the minimum of 2.5 cm. At each node a path was selected by the computer along a branch based on probability proportional to its size. The 'size' is meant here to the proportional measure of biomass in a branch and can be approximated by 'd^2l' where 'd' is the base diameter of the branch and 'l' is the length of the branch part (segment) between two successive nodes. De Gier (1989, 2003) has found 'd^2l' to be proportional to '$d^{2.5}$', so biomass of a branch is simply proportional to '$d^{2.5}$'. The principle of path selection can be

understood from an example. As shown in the Figure 2.2, suppose three branches namely 3-1, 3-2 and 3-3 are emanating from a node (level L5-L6); so there are three different path continuations possible. Assume that the base diameter of the three branches are $d_{3\text{-}1}$=15, $d_{3\text{-}2}$=12 and $d_{3\text{-}3}$=10 cm respectively. The associated proportional measures of biomass are then 871.4 (=$15^{2.5}$), 498.8 and 316.2 for 3-1, 3-2 and 3-3 respectively. The cumulative totals are 871.4, 1370.2 and 1686.4. If a random number is drawn, say 0.457, then the result of multiplying this by 1686.4 is 770.7. Since 770.7 <871.4, the first branch (3-1) is selected.

In general the selection probability of the k_{th} branch (or segment) out of m branches at a node is: $q_k = d_k^{2.5} \Big/ \sum_{i=1}^{m} d_i^{2.5}$. In the above example $q_{3\text{-}1}$ = 871.4/1686.4 = 0.52 i.e. the first branch had 52 % probability of being selected.

The path then continued in the selected branch to the next node and the procedure was repeated till the minimum diameter limit (2.5 cm) was reached (the coloured branch in the Figure 2.2 represent a path). Following the above procedure, the program calculated a probability value for each segment emanating from the nodes along the selected path. Unconditional probability of selection of a particular segment is obtained by multiplying the probabilities of all the segments in the path from the butt end till the segment concerned.

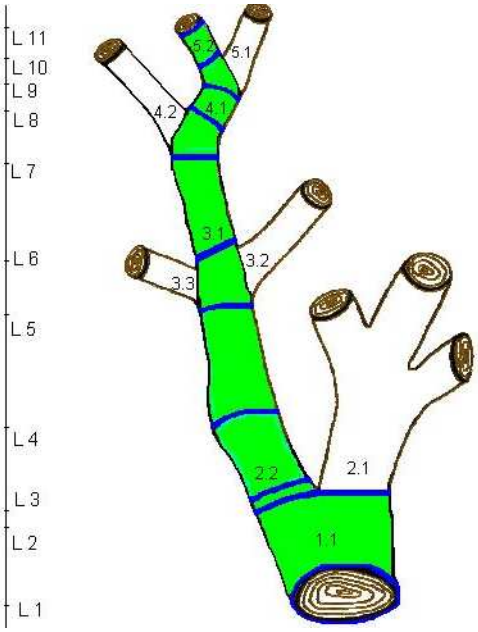

Figure 2.2. Principle of sub-sampling path selection (adopted from de Gier, 2003)

Unconditional probability of the K_{th} segment: $Q_k = \prod_{i=1}^{k} q_k$

From the unconditional probability (Q_k) and the weight (B_k) of a selected segment in the path, the program estimates the total tree weight (B_{est}) by the following formula:

$B_{est} = \sum_{k=1}^{n} \left(B_k / Q_k \right)$, where n is the number of segments in the path.

Step 2: Importance sampling

This step was basically to select a randomly located disk in the selected path, for the actual biomass estimation. In this case, the path is considered to consist of an infinite number of thin disks, one of which is selected with a probability proportional to its diameter squared. The process involved marking the points along the selected path where change in taper occurred (notably at the butt and just before and after nodes) and measurement of diameters at each of these points along with their corresponding distances from the butt end. These measurements alone already allow volume estimation of the tree. For volume estimation, the program calculates a so called inflated area at each point of diameter measurements. Inflated area at a point is the ratio of diameter squared to unconditional probability of the point. Since the distance between two successive points are

measured, the inflated volume of the corresponding section is obtained using Smalian formula as below.

Smalian formula: $V = L \times (A_1 + A_2)/2$ where A_1 and A_2 are the end cross-sections of a segment, L is the length and V is the estimated volume.

The sum of all such volume sections results in an unbiased estimate of the total tree woody volume.

A random location of a point from where disk had to be removed, in order to estimate fresh and dry weights of the tree, was obtained from the above measurements. The program calculates the position of the point by multiplying the total tree volume estimate with a random number. The segment of the path in which this volume is reached, say K_{th} segment, is identified and the exact position of the point where the disk has to be removed is determined using an interpolation function based on trapezoidal rule. The position of the point is obtained from the following formula:

$L_{KX} = L_{K0} + \{(-b + \sqrt{(b^2 - 4ac)})/2a\}$; Where

$a = (V_{K1} - V_{K0})/(L_{K1} - L_{K0})$;

$b = 2V_{K0}$;

$c = -2(uV_t - V_{K0})$;

Where L_{KX} is the distance of the point from the butt end along the path in K_{th} segment where disk is to be cut; L_{K0} is the distance of the beginning of K_{th} segment from the butt end. V_{K0} and V_{K1} are the sum of volumes of all segments in the path respectively till the beginning and end of K_{th} segment; u is a random number and V_t is the total tree volume.

Then a disk about 10cm thick was removed by making cuts 5 cm above and 5 cm below the point. Approximately 10 cm thick disk was cut considering the limited weighing capacity of the digital scale (1 gram precision) used. For the biomass estimation, the program calculates the weight (kg) per unit thickness (m) of the disk and divides the value by the unconditional probability of the segment from which it is removed. The result when multiplied by the estimated total tree volume (m^3) and divided by the square of the disk diameter (m^2), gives the estimate of the tree woody biomass. It should be noted that if the weight of the disk is fresh weight, the result will be estimated fresh biomass of the tree; and if the weight of the disk is oven-dry, the result will be estimated dry biomass of the tree.

When the disk was too big for the weighing scale, it was further divided into a number of radially cut wedges and their fresh weights were measured at the site with a precision of 1 gram. After entering the data for the individual fresh weights of the wedges, one was selected with a probability proportional to the fresh weight. It should be noted that the fresh weight of the selected wedge divided by its selection probability results in the estimate of the fresh weight of the disk (similarly for dry weight). When the measurements on the fresh weight of the selected wedge and its average thickness were entered into the iPAQ, total fresh woody biomass of the sample tree was obtained. The randomly selected wedge was then marked with an identity code and brought to laboratory for oven drying. The program also gives the value of a factor, called k-factor, for each of the selected wedge which when multiplied by the oven dry weight of that wedge gives the estimate of the total dry woody biomass of

the sample tree. The wedges were oven-dried at a temperature of 105^0C till a final constant weight in the laboratory at North-East Forestry University in Harbin, China.

Total weighing of sample trees: To test the accuracy of sub-sampling estimates, fresh biomass of 34 sample trees, randomly selected from the 60 trees, was also measured by direct weighing in the field in the conventional way using a balance. Total weighing was done by cutting the trees into sections of convenient lengths (0.5-2 m) and using a scale of 25 kg capacity; the foliage and branch parts less than 2.5 cm in diameter were not included because biomass in this study is defined as the AGB of trees to a minimum of 2.5 cm branch diameter.

To further aid in assessing the accuracy of sub-sampling, biomass estimation of another 15 sample trees (among the 60) was made by combining the 'customary method' of volume and biomass measurement. This involved separating the trees into stem and branch components above 10 cm diameter and between 10 to 2.5 cm in diameters. Larger branches and main stem above 10 cm diameter were cut into sections (taking account of the taper, length varied from 0.5 to 2 m), end cross-sections were measured and volumes were calculated using the Smalian formula. The volume, when multiplied by the value of fresh biomass per unit volume gave fresh weight of the component. To obtain the value of fresh biomass per unit volume, a disk (about 10 cm thick) of wood was removed from breast height of the sample tree. The fresh weight of the disk was taken in the field and volume was calculated as cross sectional area times thickness. The biomass of branch parts, 2.5 to 10 cm in diameter, was determined by direct weighing on a scale. The total fresh weight of trees was obtained from the sum of weights of the components above 10 cm and between 2.5 -10 cm in diameters.

2.3.2.3. Annual growth ring measurement

In the north-east Chinese cool temperate environment where there is a defined growing season (winter temperatures drop to minus 30^0C and lower), most species have well defined annual rings. The information contained in the annual rings in trees can be used to predict the annual wood increment (Bouriaud *et al.*, 2005; de Gier, 1989; Husch *et al.*, 1982). Increment measurements are preferably made in permanent sample plots (de Gier, 1989). Unfortunately, such permanent plot increment data were not available for the study area. It was, therefore, decided to obtain tree increment data from the measurement of annual growth rings on the disks removed from the sample trees from breast height (1.3m above the ground). As the sample trees had an even distribution across the diameter classes, the growth ring measurements on them were expected to give the increments of the existing size classes. Among the 60 sample trees felled for sub-sampling measurements, 48 trees were found to have conspicuous annual growth rings. Species namely *Populus ussuriensis* and *Betula platyphylla* did not show distinct rings. After completing the sub-sampling measurements, a disk was removed at breast height from each of the 48 trees belonging to the remaining 7 species. The cross sections of the disks were then smoothened by using a chisel-plane. The annual growth rings of the last five years and bark thickness were measured as follows:

i. On each disk, four points were marked at the ends of two perpendicular diameters (rings were measured in four directions to correct for wood compression or tension effects in the rings, if present).
ii. Using an 8x magnifying lens and a vernier-caliper, the total width of the rings of the last five full years was measured to a precision of 0.1mm at each of the four points. Care was taken to make measurement perpendicular to the tangents of the rings. The four width measurements

were added; then divided by 5, and then again divided by 2 to obtain average under-bark diameter increment.

iii. At the same four points, bark thickness was also measured to the nearest mm. Using a steel ruler, bark thickness was measured from the sapwood to the position where a caliper would have touched the bark. The four measurements were added and divided by 2 to obtain double bark thickness.

From the above measurements, a relationship between over-bark dbh and annual wood accumulation (or carbon sequestration) in trees was developed as shown in the section 2.4.3.

2.4. Data analysis

2.4.1. Validation of sub-sampling method

Accuracy assessment of the sub-sampling biomass estimates was done by taking total fresh weight of 34, among the total 60, sample trees and comparing these with the sub-sampled biomass data. The measured fresh biomass by total weighing and the estimated fresh biomass by sub-sampling method were compared by undertaking a *t*-test (paired two sample for means). A customary method of fresh biomass estimation of another 15 sample trees (among the 60) was also used to check the consistency with the fresh biomass estimates by sub-sampling. The sub-sampling method was the only way to get unbiased estimates of dry biomass of the sample trees. Following validation, the biomass estimates of the sample trees obtained by sub-sampling were related to dbh (D) and height (H) to develop the biomass equations.

2.4.2. Comparison of biomass models

Biomass equations are most commonly expressed in polynomial, power and combined variable model forms (Brown, 1997; de Gier, 2003; Parresol, 1999; Samalca, 2007; Zianis *et al.*, 2005) (see section 1.1.2). Only these types of model were evaluated to determine the one that best describes the relationship between tree biomass and its variables namely dbh and height. The polynomial and power models are based on dbh only as independent variable while the combined variable model are based on dbh and total tree height as independent variables. Complicated models, involving more variables, were not considered in this study since additional variables do not necessarily improve the fit of the model significantly, but can create problem with multi-collinearity and can hence reduce the applicability of the biomass equation (Chojnacky, 2003; Samalca, 2007; Zianis *et al.*, 2005). The sample tree biomass data were plotted against D (i.e. dbh) and D^2H. From the scatter plot of D verses biomass, polynomial and power models were derived while from the plotting of D^2H and biomass, the combined variable model was determined. The biomass data were analyzed first by putting all species together and then by broad-leaved and needle-leaved category. The coefficients of the polynomial and combined variable models were estimated by weighted linear regression technique in SPSS; backward stepwise elimination method was used in case of polynomial to remove the non-significant coefficients. The weighing was necessary to remove heteroscedasticity in biomass data and to develop biomass regression model of higher precision. Theoretically, weight should be inversely proportional to the variance of the residuals (Furnival, 1961). So variances of residuals were calculated by dbh class in case of polynomial model and D^2H class in case of combined variable model. The class variances were then plotted against mid-values of dbh classes for the polynomial model and the mid-value of D^2H classes for combined model. A trend line in power form was then fitted to each plotting to determine the weights for the two models (Brown *et al.*, 1989; Leeds, 2007).

The coefficients of power model were obtained directly from the scatter plot of biomass versus dbh. However, the coefficients thus obtained are biased (Brown *et al.*, 1989; de Gier, 2003; Parresol, 1999) as it is calculated after linearizing the power model by undertaking log transformation and doing linear regression. Although log transformation removes heteroscedasticity (Parresol, 1999), obtaining unbiased untransformed biomass estimates from the log transformed model is not direct because antilogarithm of log(biomass) yields geometric mean of the skewed arithmetic distribution rather than the mean. The common goodness-of fit statistics of power model relate to the transformed equation only (Parresol, 1999).

A number of statistics have been mentioned by Parresol (1999) for evaluating goodness-of-fit and for use in comparing alternative biomass models. Among them the common ones are coefficient of determination (R^2), standard error of estimate (Se) (standard deviation of residuals), root mean square error (RMSE), coefficient of variation (CV), mean percent standard error (S%) and Furnival Index (FI). Although the statistics like R^2 computed for the three functions can not be compared directly, FI has the characteristic to be able to also compare models that have either biomass or some function of biomass as dependent variables (Furnival, 1961). FI reduces to the usual estimate of standard error about the curve when the dependent variable is biomass i.e. for polynomial and combined variable models the FI is equal to RMSE. FI is based on maximum likelihood approach; it also reflects the magnitudes of residuals and possible departures from assumptions of normality and homogeneity of variance (Furnival, 1961). Large value of FI represents a poor fit and vice versa. The goodness-of-fit statistics calculated for the tree models to identify the best fitting model are given in the Table 2.2 below:

Table 2.2 Statistics used to compare the models

Statistics	Formula	Remarks
R^2	$1-\frac{RSS}{TSS}$	RSS= $\sum_{i=1}^{n}\left(Y_i-\hat{Y}_i\right)^2$ and TSS = $\sum_{i=1}^{n}\left(Y_i-\bar{Y}\right)^2$ are residual sum and total sum of squares respectively
S_e	$\sqrt{RSS/(n-p)}$	n= number of sample observations p=number of model coefficients
RMSE	$\sqrt{\sum_{i=1}^{n}\left(Y_i-\hat{Y}_i\right)^2\Big/n}$	Y_i is observed value of biomass; $\hat{Y}_i$ is estimated value of biomass by the models
CV	$\left(S_e/\bar{Y}\right)\times 100$	$\bar{Y}$ is the arithmetic mean of observed biomass values
S%	$\left(\sum_{i=1}^{n}\left\|Y_i-\hat{Y}_i\right\|/\hat{Y}_i\right)\times\frac{100}{n}$	
FI	$[f'(Y)]^{-1}\times RMSE$	$f'(Y)$ is the first derivative of the dependent variable w.r.t. biomass; the brackets signify geometric mean

Besides the prediction errors, the logical behaviour and simplicity of the models were also considered while evaluating them.

2.4.3. Calculations for annual wood accumulation and carbon sequestration

The under-bark diameter increment (i_{dub}) and double-bark thickness (T_{db}) calculated for the sample trees as explained in the section 2.3.2, were separately related to their over-bark dbh (D_{ob}) to obtain the relations for annual wood accumulation and carbon sequestration as follows.

Suppose a linear relationship was obtained from the regression analysis between the variables D_{ob} and i_{dub}. The evidence of linear relationship among these variables has been mentioned by de Gier (1989). As the forest in the study area is almost even-aged secondary forest, linear relationship can be expected. Let it be

$$i_{dub} = a_0 + a_1.D_{ob} \quad \text{……...…….. (1)}$$

A linear relationship can also be expected in regression analysis between the variables D_{ob} vs. T_{db}. Let it be

$$T_{db} = b_0 + b_1.D_{ob} \quad \text{……..... (2)}$$

After taking the first derivative of equation (2) with respect to (w.r.t.) D_{ob}, annual increment in bark thickness (i_{tb}) can be obtained as follows:

$$dT_{db}/dD_{ob} = b_1 = i_{tb}/i_{Dob}$$

Or, $i_{tb} = b_1.i_{Dob}$ ……..... (3)

We know that the increment in over-bark dbh (i_{Dob}=dD_{ob}) is the sum of the increments in under-bark dbh (i_{dub}) and double-bark-thickness (i_{tb}), i.e.

$$i_{Dob} = i_{dub} + i_{tb} \quad \text{……} \quad (4)$$

When we use the relations (3) and (1) in (4), we get a relation for increment in over-bark dbh as function of over-bark dbh as below:

$$i_{Dob} = i_{dub} + i_{tb} = i_{dub} + b_1.i_{Dob}$$

Or, $i_{Dob} = i_{dub}/(1-b_1) = (a_0 + a_1.D_{ob})/(1-b_1)$ ……...…….. (5)

If we have a polynomial function (or any function dependent on dbh only) as a biomass equation, then from its first derivative we can estimate the annual wood accumulation in a tree using the relation (5) as follows. Suppose the polynomial function for dry weight[♣] (DW) is

$DW = l.D_{ob}^3 + m.D_{ob}^2 + n.D_{ob} + k$, then its first derivative w.r.t. D_{ob} is

$$dDW/dD_{ob} = 3.l.D_{ob}^2 + 2.m.D_{ob} + n$$

Or, $dDW = (3.l.D_{ob}^2 + 2.m.D_{ob} + n).dD_{ob}$

Or, $dDW = (3.l.D_{ob}^2 + 2.m.D_{ob} + n).(a_0 + a_1.D_{ob})/(1-b_1)$ …… (6)

Where dDW represents the annual wood increment in a tree of over-bark dhh, D_{ob}. The equation (6) follows from de Gier (1989). Since nearly 50% of the dry weight of a tree is carbon, from the relation (6) we can also estimate the annual carbon sequestration by a tree in the AGB. The annual wood

[♣] The terms biomass and weight have been used interchangeably in this study, although biomass is the total content of matter (kg) in a body while weight is the force (Newton) exerted by gravity on mass of a body.

increment and carbon sequestration thus calculated can be related to the remote sensing data. Various vegetation indices (VIs) were tried (see section 2.5) to relate the increments with the Landsat TM data of the study area for large scale estimation and mapping.

Measurements of growth rings in a sufficiently large number of trees (at least 30 trees per species) are necessary to know the differences in increments by species (de Gier, 1989). This study attempted to estimate the average increment by tree size (rather than species) based on the growth ring increment data of all species put together.

2.4.4. Evaluation of existing equations

The biomass estimates based on the most suitable equation developed in this study was compared with the estimates from existing equations for similar forest types. The existing equations considered were local one for north-east Chinese temperate forest developed by Wang (2006) and also global suggested by IPCC (2003) and developed by Schroeder *et al.* (1997) for temperate forest tree species of eastern U.S.A. The local Chinese equation is general (i.e. not species specific) applicable to both broad-leaved and needle-leaved species while there are two IPCC equations one for broad-leaved and the other for needle-leaved. The equations and their characteristics are mentioned in the Table 2.3 below

Table 2.3 The secondary biomass equations used in the study

Name of the equation	Equation[1]	Valid dbh range (cm)	R^2	No. of sample trees used in the eq^n
Local Chinese	$DW = 88.10489 D_{ob}^{2.467}$	2.4-57.1	0.96	98
IPCC broad-leaved	$DW = 0.5 + \frac{25000.D_{ob}^{2.5}}{D_{ob}^{2.5} + 246872}$	1.3-85.1	0.99	454
IPCC needle-leaved	$DW = 0.5 + \frac{15000.D_{ob}^{2.7}}{D_{ob}^{2.7} + 364946}$	2.5-71.6	0.98	83

[1] D_{ob} is overbark dbh; *DW* is oven-dry above-ground biomass that includes stem, stump, branch, twig, bark and foliage. Unit of *DW* for the Chinese equation is gram while for the IPCC equations are kg. Note that the above R^2 values are biased since they are based on log-transformed data.
Source: (IPCC, 2003; Schroeder *et al.*, 1997; Wang, 2006).

Using the 172 plot inventory data for dbh, biomass of each tree was calculated using the above three equations besides the most suitable equation developed in this study. To get plot biomass, biomass of individual trees was added together. Thus, three sets of plot biomass estimates, one each corresponding to the Chinese equation, IPCC equation and the equation of this study, were obtained. The three sets of plot biomass data for the three levels of equations were then compared to see the effect of location specific equations in area based biomass assessment. The comparison was made by making box plots and undertaking ANOVA test.

2.5. RS based assessment and mapping of biomass and carbon

Landsat TM image covering the whole study site was obtained for 22 September 2006. The image was exactly one year ahead of the field work and was cloud free. Projection of the image was defined to WGS_1984_UTM_Zone_52N which is the standard projection system for north China. The acquired image was subjected to geometric, atmospheric and topographic corrections. Geometric correction of the image was done in ERDAS IMAGINE 9.1 using 11 ground control points (GCPs) from the digital topographic map of the study area. First order polynomial transformation was used for the geometric correction and re-sampling was done to the pixel size 30×30m using nearest neighbour method. This approach has the advantage of being simple, efficient and preserving the original values (Foody *et al.*, 2003). The RMSE was 0.54 pixels. Radiometric correction was done in ERDAS IMAGINE 9.1 using ATCOR 3 that integrates DEM data (via generating slope, aspect, shadow and sky view images) of the image area as an input to remove the atmospheric and topographic effects. ATCOR 3 has the advantage that it minimizes the effects of topography (e.g. shadow in mountainous terrain) and haze and automatically converts the raw digital numbers (DN) values into surface reflectance using the calibration file for TM, DEM, solar zenith angle, azimuth, and some atmospheric parameters.

The shape file of the total 172 sample plots was overlaid on the corrected image to see the matching of plot positions with the ground. It was found that a few of the plots that should have actually been inside the forest were coming to non-forest land-use such as grass-land, agricultural field and road. This problem was observed with few plots at fringes of the forest i.e. close to non-forest. It may be due to the error in coordinates recoded from GPS because of poor satellite signal or because of the error in geometric correction of the image. A higher accuracy in the geometric correction of the image could not be achieved because the ground control points (GCP) for the forested area were not conspicuous on the image. So while relating the remote sensing data with plot biomass or carbon, only the plots lying well inside the forests were considered. Thus out of the 172 sample plots, 142 plots were used for remote sensing based assessment. Spectral signatures of all seven TM bands were extracted from the pixels corresponding to the 142 plots in ENVI 4.2 using the shape file of the plots. Different VIs mentioned in Table 2.4 were calculated considering their advantages for forested environment and good relations with biomass in previous studies (see chapter 1, section 1.1.3). Mainly bands 3, 4 and 5 were used to calculate VIs and band ratios because these bands have been used successfully in previous studies to predict forest structural features (Ingram, 2005). Band 5 (MIR) is less studied than the bands 3 (red) and 4 (NIR), but has been found to be the most useful TM band for estimating forest biomass (Ingram, 2005; Steininger, 2000). Some complex band ratio suggested by Foody *et al.*, (2003) was also calculated to investigate the relationship. Soil adjusted VIs were not used because bare soil background was not prominent in the forest environment of the study area. Ordinary least square regression analysis was done to study the relationship between plot biomass/ carbon sequestration as dependent and different VIs or band ratios as independent variables. Both linear and non-linear models were examined for the relationship between forest variable and reflectance data; although very often the relationships are either linear or exponential, depending on the presence of saturation effect (Schlerf *et al.*, 2005; Steininger, 2000). The plot biomass and carbon sequestration values were estimated respectively using the most appropriate biomass equation and carbon sequestration equation developed in the study. The relationship of VI with plot biomass was also analyzed to investigate the saturation issue of VIs. The best fitting RS-based model was determined based on the goodness of fit statistics such as RMSE and R^2. After determining the best

model, separately for the predictions of biomass and carbon sequestration, maps were prepared in ArcGIS 9.1.

Table 2.4 Vegetation indices and band ratios used to study the relation with biomass

Vegetation Indices	Formula	Source
NDVI	$(\rho_{TM4}- \rho_{TM3})/ (\rho_{TM4+} \rho_{TM3})$	Lu *et al.*, 2004; Heiskanen, 2006
ND5,4	$(\rho_{TM4}- \rho_{TM5})/ (\rho_{TM4+} \rho_{TM5})$	Foody *et al.*, (2003)
MVI	ρ_{TM4}/ρ_{TM5}	Fassnacht *et al.*, 1997; Schlerf *et al.*, 2005
SR	ρ_{TM4}/ρ_{TM3}	Lu, 2004; Schlerf *et al.*, 2005; Heiskanen, 2006
RSR	$SR[1-(\rho_{TM5}- \rho_{TM5min})/(\rho_{TM5max}- \rho_{TM5min})]$	Brown *et al.*, (2000); Heiskanen, 2006
EVI	$2.5(\rho_{TM4}- \rho_{TM3})/(\rho_{TM4}+6\rho_{TM3}-7.5\rho_{TM1}+1)$	Huete *et al.*, 2002)
Complex Ratio (4,5,2)	$(\rho_{TM4}-(\rho_{TM\,5}+ \rho_{TM\,2}))/ (\rho_{TM\,4}+ \rho_{TM\,5}+ \rho_{TM\,2})$	Foody *et al.*, (2003)
Complex Ratio (4,3,5)	$(\rho_{TM\,4}-(\rho_{TM\,3}+ \rho_{TM\,5}))/ (\rho_{TM\,4}+ \rho_{TM\,3}+ \rho_{TM\,5})$	Foody *et al.*, (2003)
NDVIcorrected	$NDVI[1-(\rho_{TM5}- \rho_{TM5min})/(\rho_{TM5max}- \rho_{TM5min})]$	Heiskanen, 2006; Zheng *et al.*, 2004
ND45corrected	$ND45[1-(\rho_{TM5}- \rho_{TM5min})/(\rho_{TM5max}- \rho_{TM5min})]$	Foody *et al.*, (2003)

3. Results

3.1. DBH distribution of trees in sample plots and sample trees

A total of 172 randomly selected sample plots, each of 500 m^2, were used in this study. *Quercus mongolica*, *Betula platyphylla*, *Larix olgensis*, *Abies holophylla*, *Populus ussuriensis*, *Picea jezoensis*, *Tilia amurensis* and *Acer mono* were the major tree species observed in the plots (see Fig 3.1). *Betula* was the most dominant genus while *Acer* was the least abundant genus observed as can be seen in the Figure 3.1. A total of 6097 trees, ≥10 cm dbh, were measured in the sample plots. The number of trees from unidentified species shared only 9% of the total while nine genera constituted 91%. The majority of the trees in the plots belonged to the dbh range of 10 to 35 cm; more than 97 % of the trees were below 35 cm dbh (see Figure 3.2). The inverted J-distribution of trees' dbh size is expected in any natural forest. The high share of small trees in natural forests can be attributed to their high mortality and the role to replace the bigger ones.

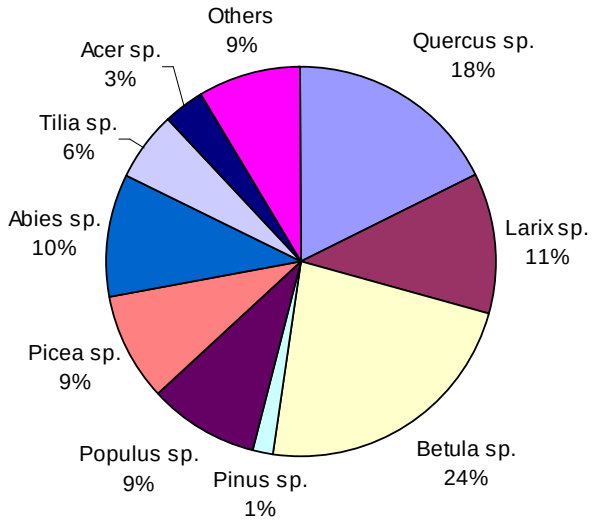

Figure 3.1 Distribution of trees by genus in the sample plots

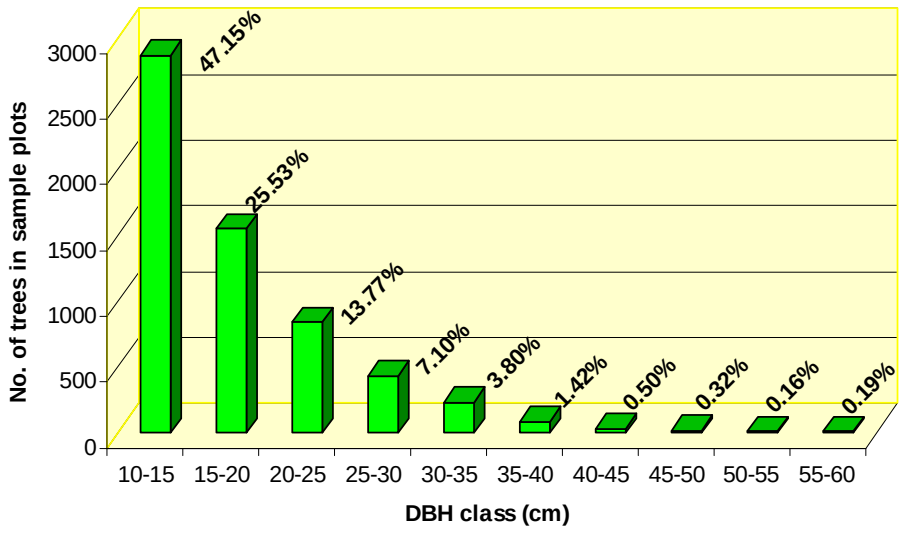

Figure 3.2 Distributions of trees by dbh class in the sample plots (all species)

A total of 60 sample trees ranging in dbh from 7.2 to 36.5 cm and belonging to nine species were harvested and measured for above-ground biomass (see Appendix 1). The distribution of the sample trees based on dbh class interval of 5 cm is shown in the Figure 3.3. Relatively large numbers of sample trees were taken from the smaller diameter classes, compared to the bigger classes, since finding representative trees from the bigger classes was difficult because of their low abundance and also due to the difficult mountainous terrain.

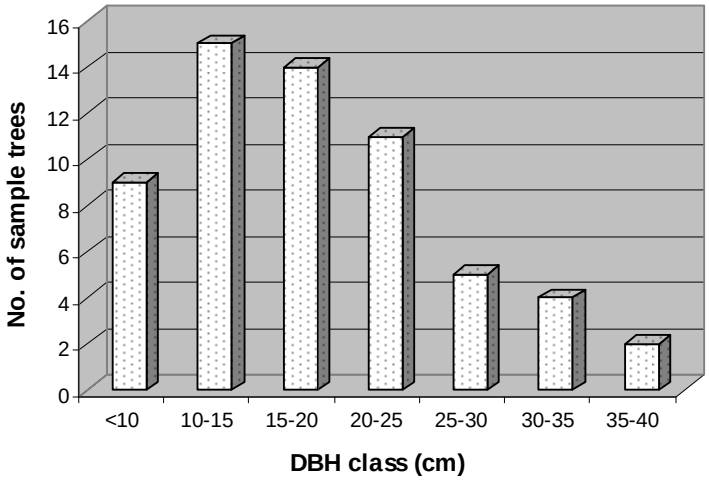

Figure 3.3 Distribution of sample trees by dbh class

3.2. Reliability assessment of sub-sampling

The sub-sampling biomass estimates were validated by comparing these with the weights obtained from total weighing of fresh biomass of 34 sample trees and indirect fresh weight estimation (by the customary method explained in section 2.3.2) of another 15 trees. The fresh-weight biomass estimates by sub-sampling explained more than 96 % of variation in the total fresh weights of the 34 sample trees (see Figure 3.4, left). When the biomass data of sample trees measured by total weighting and the indirect approach (customary method) were combined (i.e. 49 trees) and compared with the sub-sampling estimates, it still explained more than 95% of variability (Figure 3.4, right). The root mean square error (RMSE) of sub-sampling estimates against total weighing (for 34 trees) was 12.26 kg (dry weight) which is 13.19 % of the average sample tree biomass.

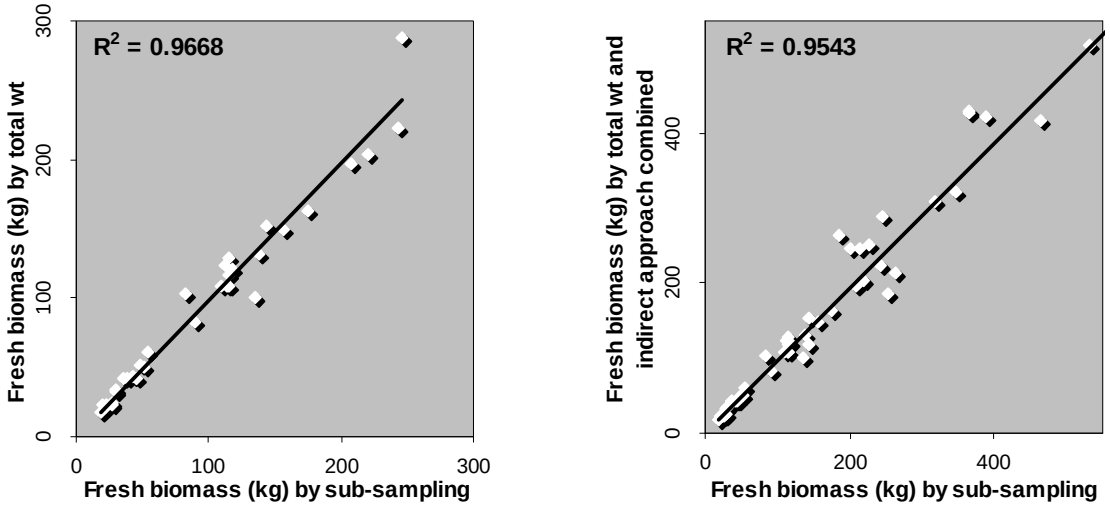

Figure 3.4 Comparisons of sub-sampling biomass estimates with total weighing (left) and total weighing combined with indirect weight estimation (right)

The statistical 'paired sample *t*-test' approved the null hypotheses that the sub-sampling biomass estimates do not differ significantly from the total weighing or the combination of total weighing and indirect approach (see Table 3.1 below). The calculated *t*-statistics for the two pairs are respectively 0.137 and 0.120 while the two-tailed critical values from table of *t*-distribution for 33 and 48 degrees of freedom at 5 % level of significance are 2.03 and 2.01; this implies the validity of null hypothesis.

Table 3.1 Paired sample *t*-test for the comparison of biomass estimates by sub-sampling, total weighing and combination of total weighing and indirect approach

	Paired Differences						
		Std. Error	95% Confidence Interval				
	Mean	Mean	Lower	Upper	t	df	Sig.
Pair-1	.293	2.134	-4.049	4.635	.137	33	.892
Pair-2	.553	4.628	-8.752	9.858	.120	48	.905

Pair-1: Fresh biomass estimates by sub-sampling vs. total fresh weights$^{\Psi}$ of the 34 sample trees

Pair-2: Fresh biomass estimates by sub-sampling vs. combined fresh weights by total weighing and indirect approach (49 trees)

When linear regression was performed in SPSS with sub-sampling estimate of fresh biomass as explanatory variable (X) and measured total fresh biomass as response variable (Y), the table of estimated coefficients (see Table 3.2 below) revealed that the intercept term was non-significant and only the independent variable explained the model significantly at $p<0.001$. So when we neglect the non-significant constant term, the model becomes $Y=0.977X$ or Y nearly equals X. The relation, however, gives an indication that the sub-sampling method slightly overestimates the biomass values.

Table 3.2 Parameters of the linear relation between sub-sampling and total biomass

Model predictors	Un-standardized Coefficients		Standardized Coefficients	t	Sig.
	B	Std. Error	Beta		
Constant	1.819	3.671		.495	.624
FW_SS	.977	.032	.983	30.633	<0.001

Dependent variable: fresh biomass by total weighing;

Independent variable: fresh weight estimates by sub-sampling (FW_SS)

Some further analysis was done with the fresh biomass data of the 34 sample trees that were also measured for the total weight. To test whether the sub-sampling estimates of biomass are influenced by the branching pattern of trees, the difference in sub-sampling biomass estimate and the total weight of the trees were plotted against the number of branching nodes in the path. The graph demonstrated that the sub-sampling estimates are not affected ($R^2 = 0.0874$) by increasing number of branches in the trees (see Figure 3.5). Since the graph is for all the species combined together, the sub-sampling estimates are also insensitive to species.

$^{\Psi}$ Note: the terms biomass and weight have been used interchangeably in the study

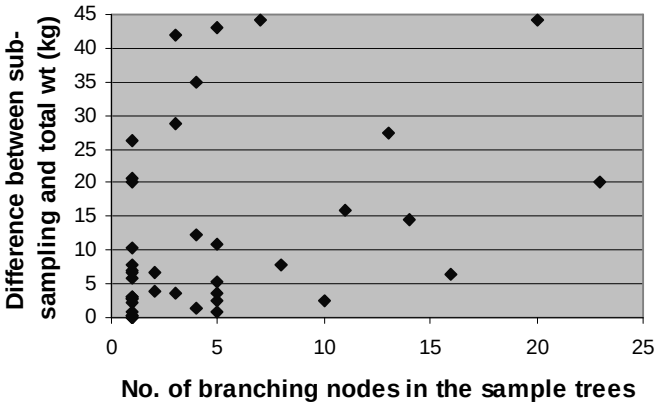

Figure 3.5 Difference in sub-sampling estimate of biomass and total sample tree weight against the number of branching nodes in the sample trees

3.3. Biomass equations based on estimates of sub-sampling method

Since the sub-sampling method had a very high correlation with the true weights of the sample trees and it has also an advantage of giving unbiased dry biomass estimates of the sample trees, the sub-sampling estimates were used for the purpose of developing biomass equations. While exploring the sub-sampling dry biomass data (of all sample trees) by fitting the three common models namely, polynomial (third degree), power and combined variable, first check for presence of outliers was made. For this, residuals were calculated for each model and converted to z-scores (standardized residuals) which are the residuals divided by an estimate of their standard deviation. None of the z-score value was beyond -3 to +3 range (see Table 3.3). From statistics, we know that in a normally distributed sample 99.9% of z-scores should lie between -3.29 and +3.29. So there was no obvious outlier.

Table 3.3 z-score range of the three models fitted to dry biomass data of the sample trees

Model	z-score (minimum)	z-score (maximum)
Combined ($M = a_0 + a_1.D^2H$)	-2.47	2.83
Power ($M = a.D^b$)	-2.65	2.30
Polynomial ($M = a_0 + a_1.D + a_2.D^2 + a_3.D^3$)	-2.68	2.30

Next it was determined whether species-specific biomass equations were necessary or whether a general combined species equation would be enough. Figure 3.6 below represents the scatter plot of sub-sampling dry biomass data of the 60 sample trees plotted against their dbh by species or similar species-group. Only one tree of *Fraxinus mandshurica* and 3 trees of *Tilia amurensis* could be harvested in the field because of their low abundance; since the two species by their physiognomic characteristics look similar to *Ulmus pumila* (also local people reported their wood strength to be similar), they were grouped into one species group. Similarly, as only two trees of *Populus ussuriensis* were measured and they looked similar to *Betula platyphylla*, the two were combined into another species group. Although the number of sample trees per species or species-group was not enough, the plotting (Figure 3.6) revealed that separate biomass equation for individual species was not necessary as the points of individual tree species or species-group are mixed randomly among other species or group. The decision is also supported by Figure 3.7 showing three third degree polynomial curves one each for broadleaved species, needle-leaved species and all species together. The three polynomial equations when used to estimate the dry biomass of trees in dbh range of 10-40 cm at 2 cm class

intervals and subjected to ANOVA test (Appendix 2) showed that the estimates by the three equations do not differ significantly at 5% level of significance. Further paired sample *t*-test made to compare the means of the three estimates in pair showed that they do not differ significantly at 5% level of significance (see Appendix 2). Thus, there was no need for separate equations by species. The advantage of combined species equation for its applicability over a large number of tree species made the large area (landscape scale) biomass assessment and mapping easy in the Wangqing forest.

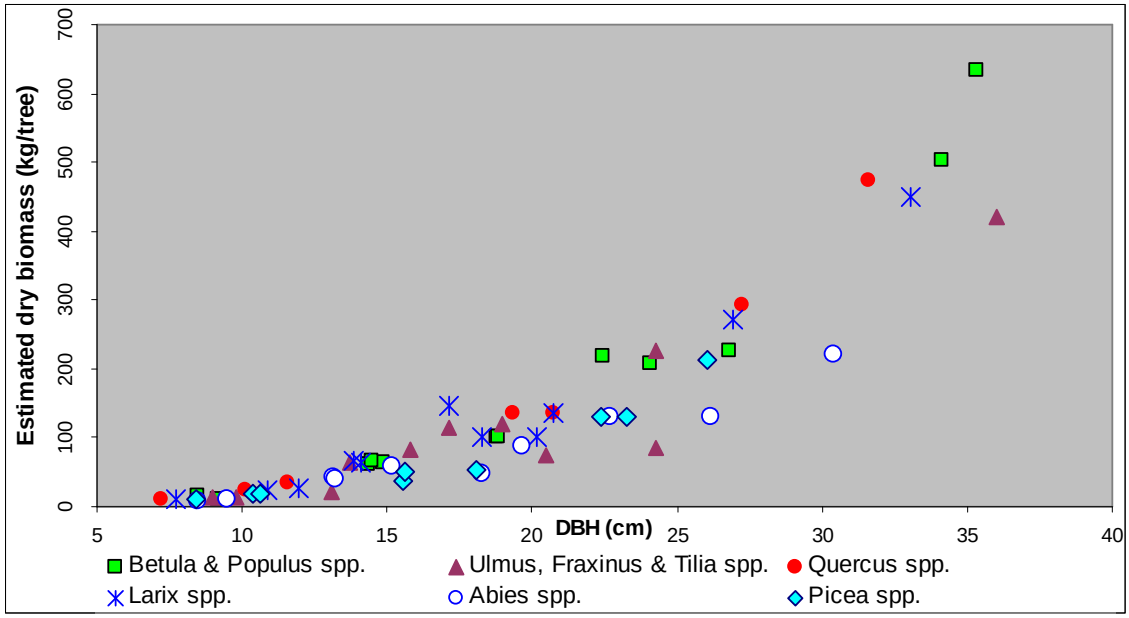

Figure 3.6 Scatter plot of dry biomass (kg) by species and similar species against dbh

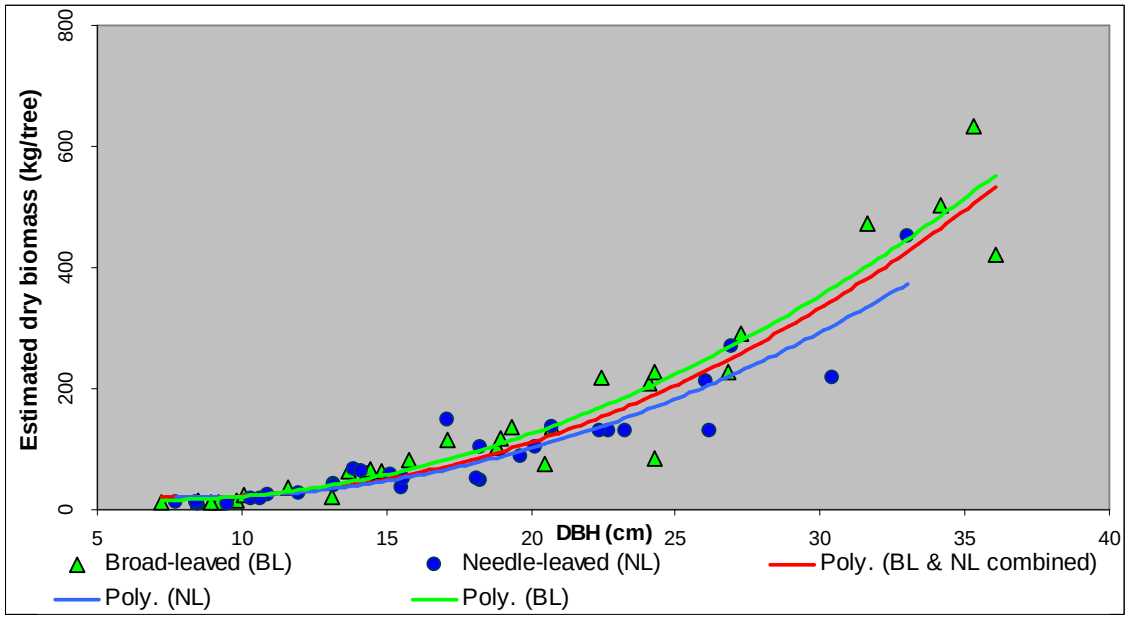

Figure 3.7 Third degree polynomial curves fitted to the broad-leaved, needle-leaved and all species together

The scatter plot of sample tree dry biomass[τ] against dbh (D) demonstrated a good least square fit by both the polynomial and power models (see Figure 3.8). However, the best fit, in terms of R^2 value (coefficient of determination), was observed from the combined variable model in the scatter plot of dry biomass against D^2H (dbh squared times total tree height). The R^2 value for the power model at the first look appeared higher than that of polynomial model. But the R^2 value from the power functions is biased because it is actually obtained from the log transformed linear model of the power function i.e. from the scatter plot of ln(biomass) against ln(dbh) (see Figure 3.8d). So, R^2 from the power fit could not be compared with that from the polynomial fitting. The models obtained from the ordinary least square fits in Figure 3.8 are given in the Table 3.4 below.

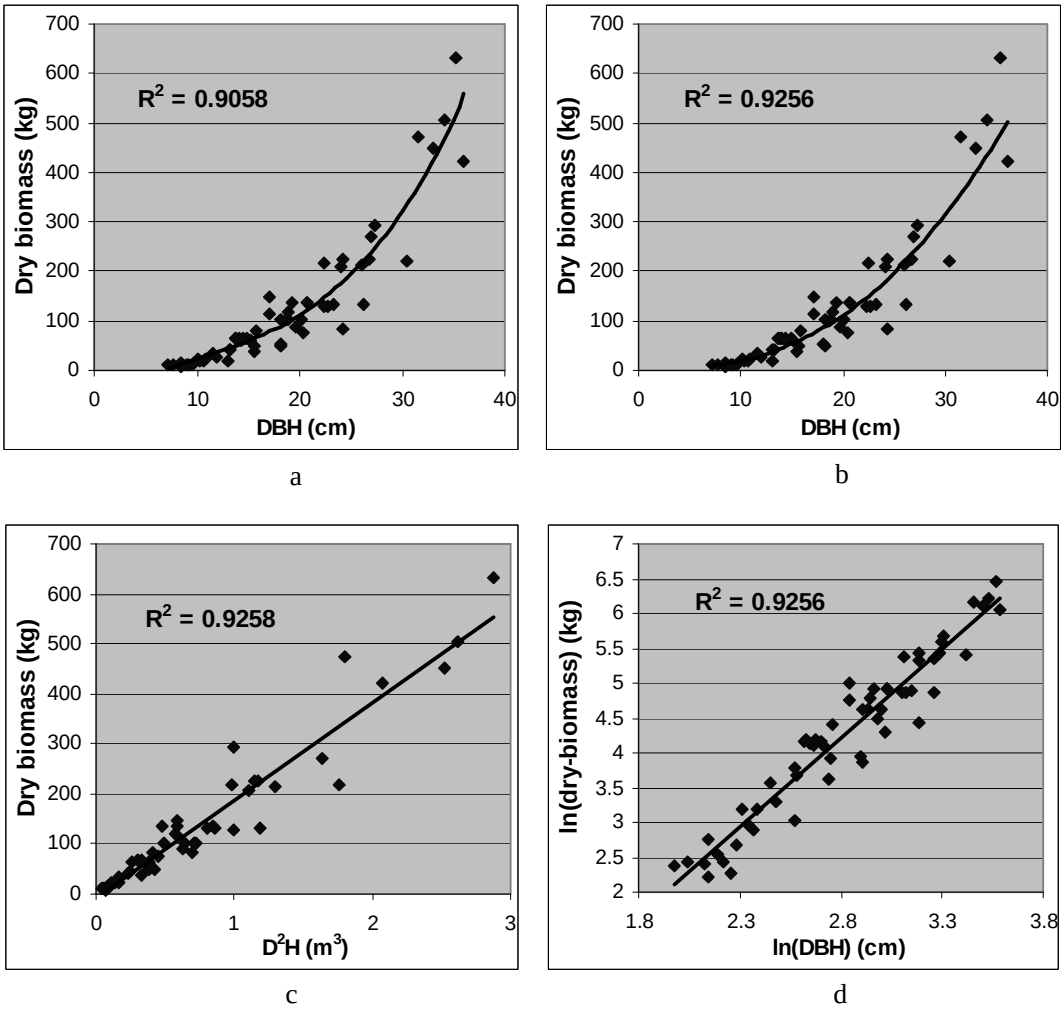

Figure 3.8 Fitting of (a) polynomial, (b) power, (c) combined variable and (d) log-transformed models to the sample tree dry biomass data

[τ] The graphs presented in the results and discussion chapters are only for the dry biomass data of the sample trees. The graphs for volume and fresh weight data are included in the Appendix 4.

Table 3.4 Biomass equations obtained from ordinary least square fit

Model	Equation
Polynomial	$DW = 2.0433\times10^{-2}D^3 - 6.2743\times10^{-1}D^2 + 13.4912D - 70.3641$
Power	$DW = 5.3157\times10^{-2}D^{2.5532}$
Combined variable	$DW = 1.9531\times10^{2}D^2H - 7.7030$
Log-transformed power	$lnDW = 2.5531\ lnD - 2.9345$
Where *DW* is dry weight of trees (in kg), *D* is dbh (in cm), *H* is total tree height (in m) and *ln* is natural logarithm; D^2H is in m^3	

The residuals of the polynomial and combined variable models showed heteroscedasticity as shown in Figure 3.9 below. So weighing was necessary for them. Weighted linear regression was performed in SPSS. The weights obtained for the polynomial and combined variable models were respectively $D^{4.88}$ and $(D^2H)^{2.3}$. So, just weight of D^5 was used for the polynomial and $(D^2H)^2$ was used for the combined variable model. The result of weighted linear regression is shown in Appendix 3. The backward elimination method of regression applied for the polynomial model resulted in only the D and D^3 terms to be significant i.e. removed the D^2 term. The power function did not require weighting because the residuals were not heteroscedastic; when power functions are linearized by log transformation, the resulting model has generally homoscedastic variance (Parresol, 1999).

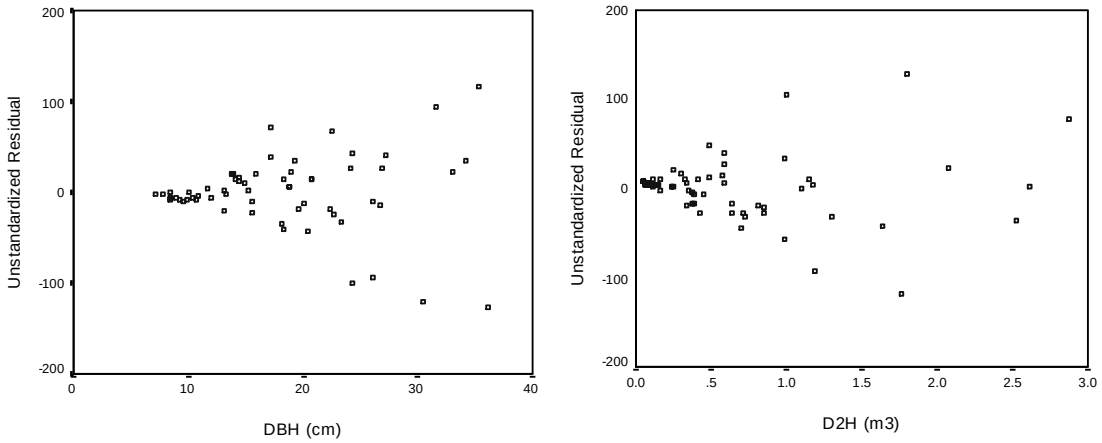

Figure 3.9 Heteroscedastic residuals in polynomial (left) and combined variable (right) models

The resulting polynomial equation for dry weight (*DW*) after weighted linear regression and backward elimination was

$DW = 8.9620\times10^{-3}D^3 + 3.4614D - 23.2628$

where *D* explained more than 89% of the variability (at $p<0.0001$) in the sample tree dry biomass.

The combined variable model for dry weight (*DW*) obtained after weighing was

$DW = 1.8144\times10^{2}D - 8.0423\times10^{-1}$

where D^2H explained more than 93% of the variability (at $p<0.0001$) of dry biomass which is higher than the un-weighted equation.

The heteroscedasticity in the residuals from the fitting of the reduced weighted polynomial and combined variable models was removed as can be observed from the Figure 3.10 below.

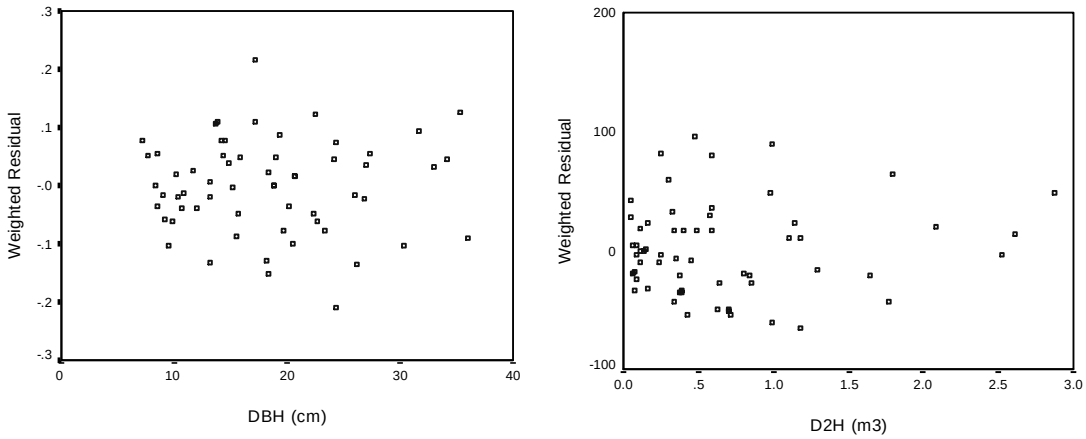

Figure 3.10 Homoscedastic residuals from weighted polynomial (left) and combined variable(right) models

Similarly, volume and fresh biomass equations were obtained. The scatter plots of volume and fresh biomass data fitted with polynomial, power and combined variable models are given in the Appendix 4. The volume and fresh biomass equations obtained in the three model forms after weighted linear regression of polynomial and combined variable models are as below:

Weighted volume equation in polynomial form, $V= 9.100\times10^{-6}D^3 +6.1236\times10^{-4}D^2 - 2.1180\times10^{-2}$
Volume equation in power form, $V =1.3400\times10^{-4}D^{2.5538}$
Weighted volume equation in combined variable form, $V = 4.4404\times10^{-1}D^2H - 1.044\times10^{-3}$
(Where V is volume in m^3; D is dbh in cm; H is total tree height in m and D^2H is in m^3)

Weighted fresh weight equation in polynomial form, $FW = 1.5370\times10^{-2}D^3 + 8.0613D - 54.6681$
Fresh weight equation in power form, $FW =1.1999\times10^{-1}D^{2.5091}$
Weighted fresh weight equation in combined variable form, $FW =3.4718\times10^{2}D^2H+2.8411\times10^{-1}$
(Where FW is fresh weight in kg; D is dbh in cm; H is total tree height in m and D^2H is in m^3)

3.4. Model comparison

After the models were determined, the next task was to identify the best fitting model. While all the models exhibited good fit to the biomass data, the combined variable model was the best because it gave the highest coefficient of determination. But the problem with the combined variable model is that it also requires the measurement of total tree height which is often erroneous and tedious for standing trees in forests with dense canopy. Comparison of the sample tree biomass estimates by using the polynomial and combined variable models showed that the estimates by the two models do not differ significantly (F_{stat}=0.016< F_{tab}=3.921, p=0.899, df=1,118) at 5% level of significance. So next attempt was made to decide which one is the best among polynomial and power models.

Since the common goodness of fit statistics of power function belongs to the log transformed linear model where log(biomass) is dependent variable, those statistics can not simply be compared with similar statistics obtained from polynomial (or combined variable) model where biomass is dependent variable. The usual fit statistics such as R^2 or RMSE was not enough to decide the best among the power or polynomial models. Another four statistics namely, coefficient of variation (CV), standard error of estimate (S_e), mean percent standard error (S%) and Furnival Index (FI) were calculated for each model. The fit statistics were calculated based on predicted and detransformed values as suggested by Parresol (1999) and Furnival (1961). The fit statistics are shown in the Table 3.5. As expected, combined model gave the best fit in terms of the values of RMSE, S_e, S% and CV, followed by the polynomial model. However, the FI was found to give misleading result. When the dependent variable is biomass, FI is simply equal to RMSE; but a lower value of FI means better fit which contradicts with all the other fit statistics of the combined and polynomial models that are better than the power model. It was concluded that the polynomial model fitted the data better than the power model.

Table 3.5 Fit statistics for the tree models

Model	RMSE (kg)	Se (kg)	CV %	S%	FI
Combined	37.72736	38.37232	31.15654	17.90655	37.72736
Polynomial	41.98332	43.07398	34.97406	24.55235	41.98332
Power	42.84172	43.57411	35.38015	24.88247	21.474

3.5. Comparisons of plot based biomass estimates with IPCC and local Chinese equations

Once it was found that the polynomial equation is better fitting than the power equation, the former equation was used to estimate the plots biomass. As the field plots were enumerated only for tree diameters at breast height, use of combined variable model to estimate the biomass was not applicable. Using the polynomial equation, biomass of each tree within the plots was calculated and summed to get the plots' biomass. Similarly, the existing local Chinese equation and the equations from the GPG of IPCC were also used to calculate the plots' biomass. Thus the biomass estimates of the plots using the three equations were compared to evaluate the effects on area based estimates while using different levels (i.e. from different geographical area) of equations. Considering the plot biomass estimates from the developed polynomial equation as standard (because it is based on field measurements, and therefore assumed to be the most accurate), the estimates from the existing Chinese and IPCC equations were compared in the scatter plot shown in the Figure 3.11 below.

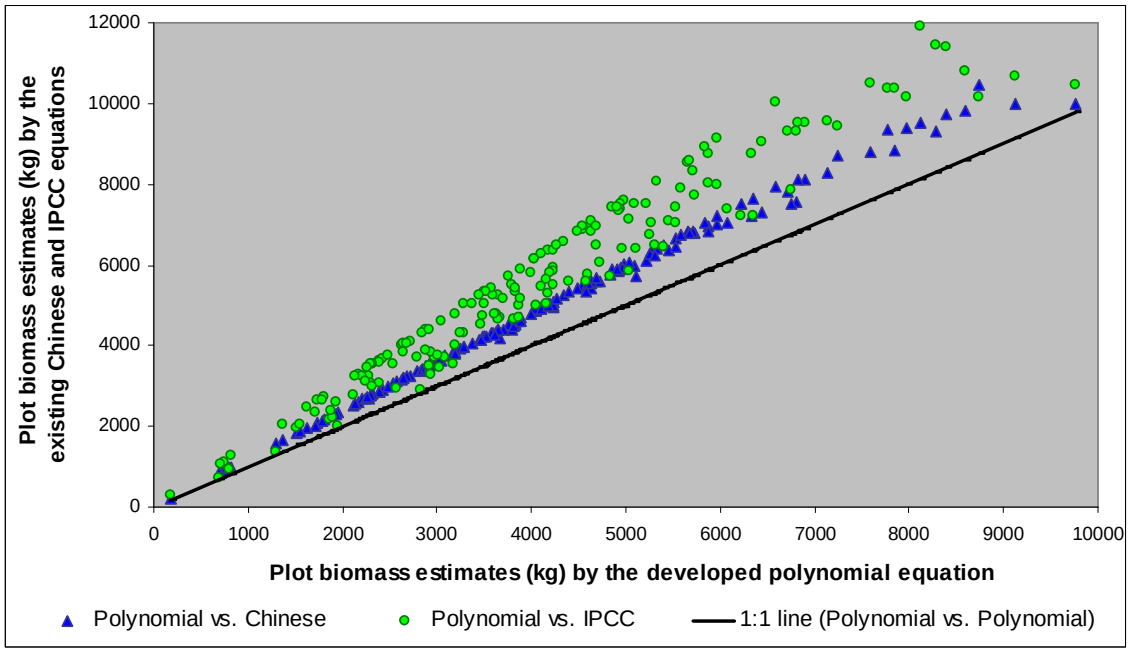

Figure 3.11 Comparisons of plot biomass estimates by the existing Chinese and IPCC equations versus the estimate by the developed polynomial equation of this study

From the Figure 3.11, it is clear that both the Chinese and IPCC equations are giving higher plot biomass estimates than the polynomial equation, although the Chinese estimates are closer to the polynomial estimates. Correlation analysis showed a higher correlation between the Polynomial and Chinese estimates (r=0.997) than between the Polynomial and IPCC (r=0.973), although both the coefficients are high. Simple linear regression between the plot biomass estimates by the polynomial and Chinese equations showed that Chinese equation estimated 1.178 (slope) times higher than the developed polynomial equation. Similarly, the linear regression between the polynomial and IPCC estimates showed that the estimate by the latter was 1.356 times higher. The individual sample plot biomass estimates by the Chinese equation were 2.41 to 21.79% higher while the estimates by IPCC equation were 3.01 to 53.20% higher than the corresponding estimates by the polynomial equation.

ANOVA test was performed to compare the plot biomass estimates by the three equations. It showed that the means of the plot level biomass estimates using the three equations differ significantly at 5% level of significance (F_{stat}=20.693> F_{crit}=3.013, p<0.0001, df=2,513). Paired sample *t*-test showed that the means by pair of the three estimates also differ significantly (t_{stat} was 32.75 for polynomial vs. Chinese, 25.12 for polynomial vs. IPCC and 16.57 for Chinese vs. IPCC whereas t_{crit} was 1.97 at 171 df and α=0.05). F-test calculated for each of the three pairs showed unequal variances among them.

The average of the plots' biomass obtained from the three levels of equations (i.e. locally developed polynomial of this study, existing local Chinese and global from IPCC) with their confidence intervals are given in the Table 3.6a below while the comparisons of medians and quartiles are shown in the box plot in the Figure 3.12.

Based on the estimated biomass of the plots, the average biomass on a per hectare basis (called biomass density) was calculates as 81.885, 97.113 and 112.122 metric tons respectively for the

polynomial, Chinese and IPCC equations with their 95% confidence limits as given in the Table 3.6b. The standard errors of the average biomass estimates per hectare were 2.852, 3.259 and 3.791 tons respectively for the polynomial, Chinese and IPCC equations. The lower confidence limits of the biomass estimates by both Chinese and IPCC equations are above the upper confidence limit of Polynomial equation which indicated over estimation by the former two equations.

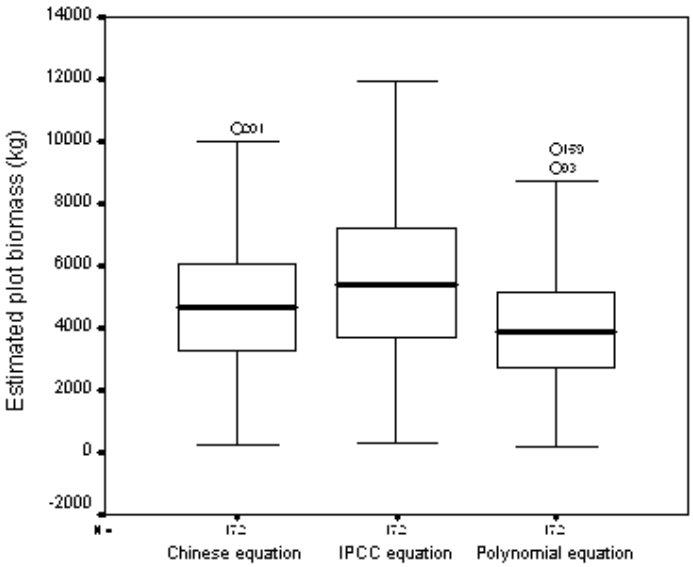

Figure 3.12 Box plot comparing medians and quartiles of estimated plots biomass (kg) using Polynomial, Chinese and IPCC equations

Table 3.6a Averages and confidence intervals of plot dry biomass estimates

Plots biomass estimated by	Average sample plot biomass (kg)	95% confidence limits for mean	
		Lower (kg)	Upper (kg)
Polynomial eq^{n}	4094.273	3812.762	4375.783
Local Chinese eq^{n}	4855.659	4534.002	5177.316
IPCC eq^{n}	5606.112	5231.869	5980.356

Table 3.6b Average per hectare dry biomass and confidence limits

Biomass density estimates by	Average per hectare biomass (tons)	95% confidence limits for mean	
		Lower (tons)	Upper (tons)
Polynomial eq^{n}	81.8854	76.2552	87.5156
Local Chinese eq^{n}	97.1131	90.6800	103.5463
IPCC eq^{n}	112.1222	104.6373	119.6071

As the area of the Wangqing forest was nearly 281478 ha (calculated from the classified Landsat TM image using GIS tool), the total estimated above-ground biomass in the forest using the polynomial equation was 23048938.62 ± 1584777.43 tons at 95 % confidence interval. Similarly, the biomass estimates using the Chinese and IPCC equations were respectively 27335201.16± 1810776.12 tons and 31559932.61±2106834.68 tons at 95 % confidence interval. The estimates by the Chinese and IPCC equations are respectively 18.6% and 36.9% higher than the polynomial-based estimate.

3.6. Assessment of annual wood increment and carbon sequestration

The study area has a distinct growing season for plants approximately from April till September. Most of the tree species, therefore, show annual growth rings. The rings were quite distinct in the needle-leaved species (viz. *Picea jezoensis*, *Larix olgensis*, *Abies holophylla*) and ring porous hardwoods (viz. *Quercus mongolica*, *Ulmus pumila*, *Tilia amurensis*, *Fraxinus mandshurica*), however, the rings

in the diffuse porous wood of *Betula platyphylla* and *Populus ussuriensis* were not conspicuous because of only minor color differentiation between late and early wood. The observations made on the outermost radial sections of the sample disks, collected from the breast height of the sample trees, showed that the trees do not have false rings (that develop due to the slowing of growth during ring formation, followed by resumption of growth) for the last ten years. This was expected because, in the study area, drought or severe early or late frosts did not occur in the last 10 years. The measurements on the widths of growth rings of the last five years as well as on the bark-thickness were made on the sample disks from 48 sample trees consisting of seven *Q. mongolica*, seven *U. pumila*, three *T. amurensis*, one *F. mandshurica*, nine *P. jezoensis*, eleven *L. olgensis* and ten *A. holophylla*. Two relations, one for annual under-bark diameter increment (calculated from the growth rings) and the other for annual bark thickness increments, both based on over-bark dbh of trees, were needed to get the relation for annual wood and carbon accumulation. The data of growth ring and bark thickness measurements are given in the Appendix 5.

The relationship between annual under-bark diameter increment (i_{dub}) and over-bark dbh (D_{ob}) was established from regression analysis and the scatter plot of the two variables, combining all species, as shown in Figure 3.13 below. Although the coefficient of determination was low (R^2=0.3335), a significant linear relationship was observed (F_{stat}=23> $F_{crit(1,46)}$=4.05, df=1,46, α=0.05); that meant larger diameters tend to correlate with larger increments. The linear relation was expected because the forests in the study area are nearly even aged, secondary and in growing stage. Further when the scatter plot (Figure 3.13) was fitted with third degree polynomial or power models similar R^2 values (0.3522 & 0.3463) were observed and backward elimination method of regression to the polynomial model again resulted in the linear relationship. The resulting linear relation was

$$i_{dub} = 1.2814\times10^{-2} D_{ob} + 9.0306\times10^{-2} \quad \text{.....(a)}$$

Where the under-bark diameter increment (i_{dub}) and over-bark dbh (D_{ob}) both are in cm.

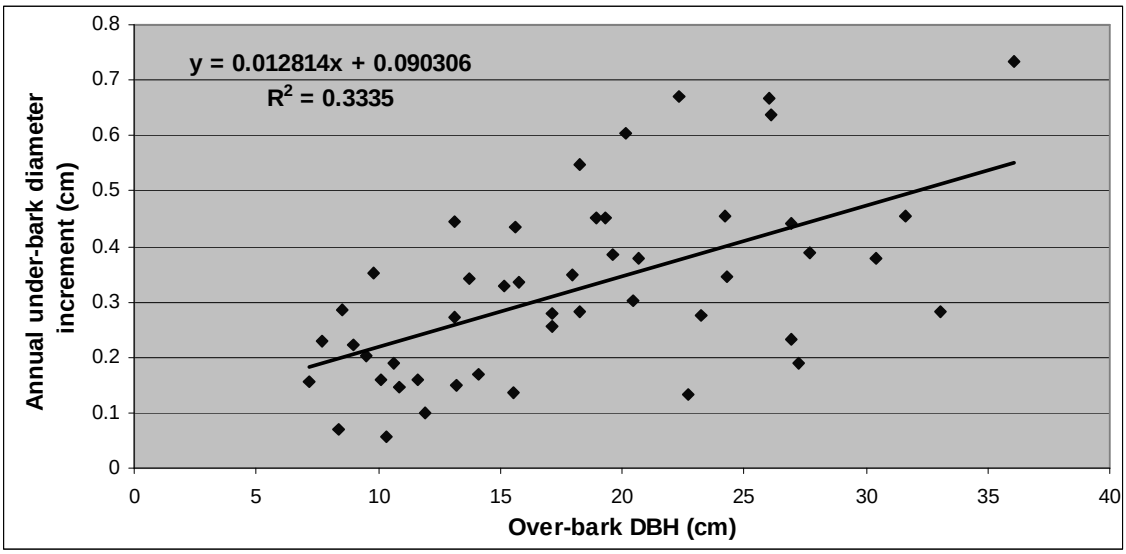

Figure 3.13 Relationship between annual under-bark diameter increment and overbark dbh

Similarly, a regression analysis was carried out, combining all species, relating double bark-thickness to over-bark dbh; double bark thickness was considered because the increment in double bark thickness supplements to the increment in over-bark dbh. A simple linear model proved satisfactory as shown in Figure 3.14. The resulting model was

$$T_{db} = 6.9871\times10^{-2} D_{ob} + 1.9755\times10^{-1} \quad \text{.....(b)}$$

Where the double-bark thickness (T_{db}) and over-bark dbh (D_{ob}) both are in cm.

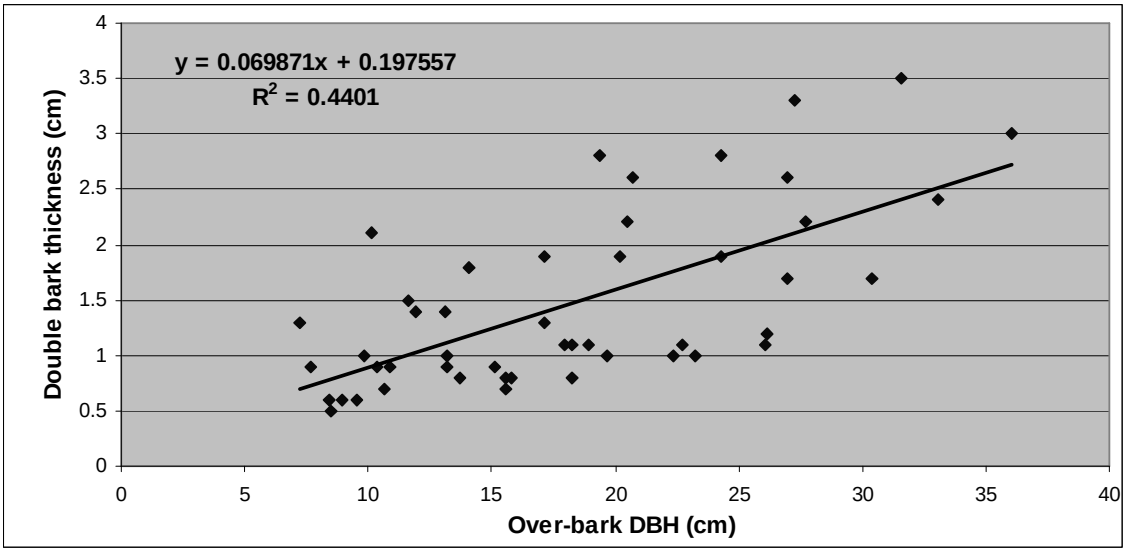

Figure 3.14 Relationship between double-bark thickness and over-bark dbh

Since $DW = 8.9620\times10^{-3} D_{ob}^3 + 3.4614 D_{ob} - 23.2628$ is the polynomial biomass equation derived in the section 3.3; using its first derivative with respect to (w.r.t.) D_{ob} in addition to the right hand side of the equation (a) and slope coefficient of equation (b) in the equation (6) derived in the section 2.4.3, the relation for annual wood accumulation on a per tree basis was obtained as below:

$$dDW = (3\times8.9620\times10^{-3} D_{ob}^2 + 3.4614)(1.2814\times10^{-2} D_{ob} + 9.0306\times10^{-2})/(1 - 6.9871\times10^{-2})$$

Or, $dDW = (2.6886\times10^{-2} D_{ob}^2 + 3.4614)(1.3776\times10^{-2} D_{ob} + 9.7089\times10^{-2})$ ……..…...…(c)

Where annual wood accumulation (dDW) is in kg and over-bark dbh (D_{ob}) is in cm.

Since roughly 50% of the dry wood constitutes carbon (IPCC, 2003), the annual carbon sequestration equation on per tree basis can be written as

$$C_{sequestration} = 0.5\times(2.6886\times10^{-2} D_{ob}^2 + 3.461438)(1.3776\times10^{-2} D_{ob} + 9.7089\times10^{-2}) \text{....} \quad \text{(d)}$$

Where $C_{sequestration}$ is in kg/ year and over-bark dbh (D_{ob}) is in cm.

Using the sample plot data on tree dbh in equation (d), annual carbon sequestration by each tree in the plots was calculated and summed to get plot level annual carbon sequestration. The average annual carbon sequestration by the forest was estimated to be 1.889576 tons/ ha with the 95% confidence interval from 1.764976 to 2.014175 tons/ ha (see Appendix 6). The total carbon sequestration estimated for the whole Wangqing forest (area 281478 ha) was 531874.07 ± 35072.15 ton per year at

the confidence interval of 95%. The average carbon density of the forest was calculated as 40.942 tons/ ha (half of the average biomass per hectare which was 81.885 tons).

3.7. VIs/ band ratio based biomass and carbon sequestration assessment

Having the plot biomass and annual carbon sequestration estimates, the next step was to relate these to the spectral signatures in corresponding plot pixels in the satellite image of the area. The spectral band values were extracted from the radiometrically and geometrically corrected TM imagery of 22 September 2006 and the VIs/ band ratios were calculated. Both linear and non-linear least square models were then fitted to the scatter plot of biomass (or carbon sequestrations) per plot as dependent variable versus VIs/ band ratios as independent variable. The usual goodness of fit statistics R^2 and RMSE were considered for determining the best fitting model and the likely VI that explain the variability of biomass most. The scatter plots in the Figure 3.15 below show the relationship between VIs/ band values and above-ground biomass of 142 plots together.

Although poor, a significant linear relationship was observed between biomass and a few VIs such as corrected-NDVI (NDVIc) and RSR and also TM band 5 reflectance. Third degree polynomials were also fitted to the scatter plots but in most of the cases the coefficients of X^3 and X^2 were found to be non-significant; the backward elimination method of regression in SPSS resulted in linear relationship. The best relation was observed with NDVIc (R^2=0.4175; F_{stat}=100.34> F_{crit}=3.91, $p<0.0001$, df= 1, 140) among the tested VIs/ band ratios. The significantly linear relation with NDVIc was Y = 12146.385630NDVIc + 1593.670823, where Y is pixel biomass in kg. The RMSE of this relation was 32.28% of the mean; the mean biomass of pixel size (30×30m) plots was estimated to be 7029.9 kg. From the Figure 3.15 (a), (b) and (c), it is clear that there is no saturation of VIs such as NDVIc and RSR with the increasing level of estimated plot biomass existing in the study area.

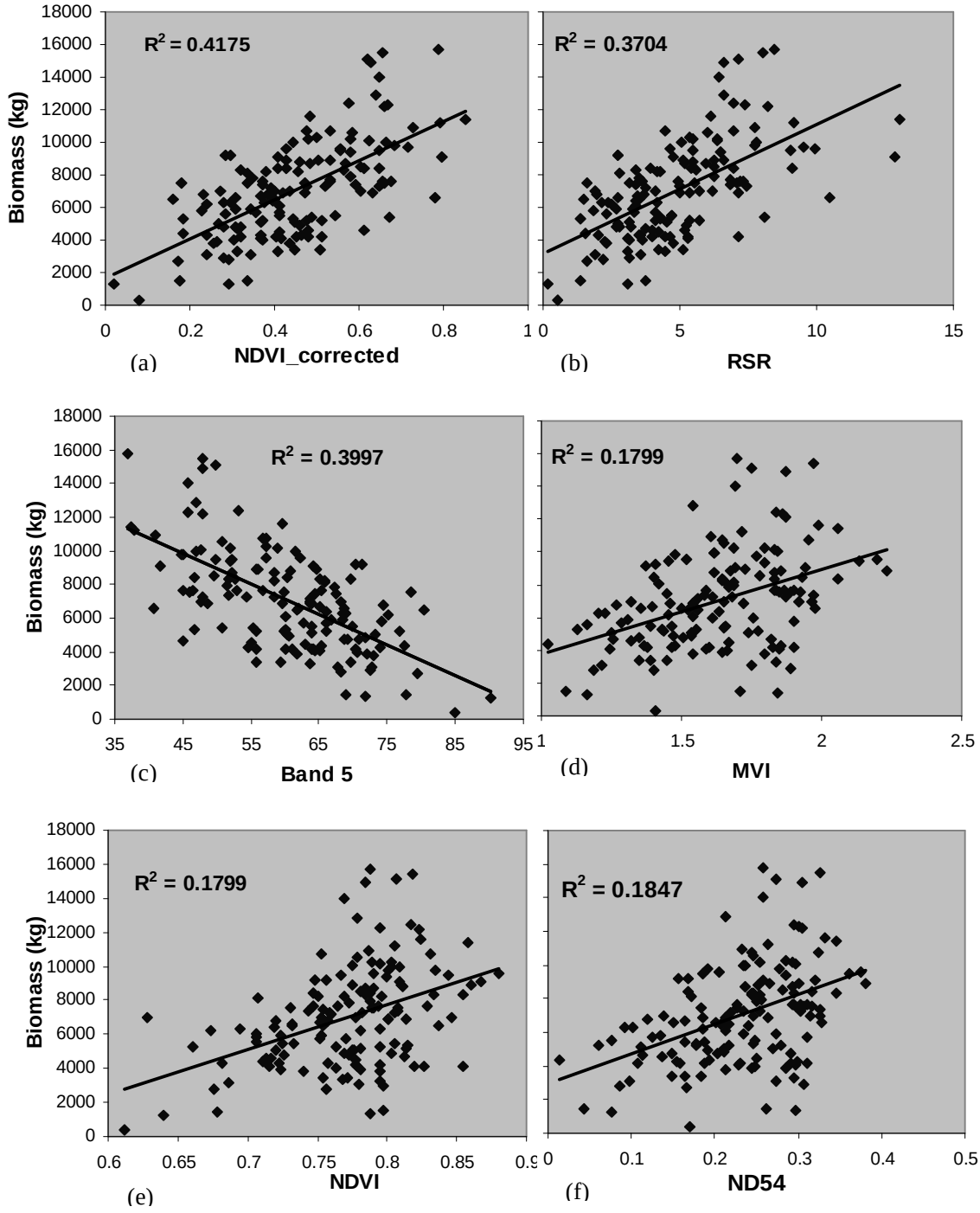

Figure 3.15 Scatter plots of biomass against vegetation indices/ band values

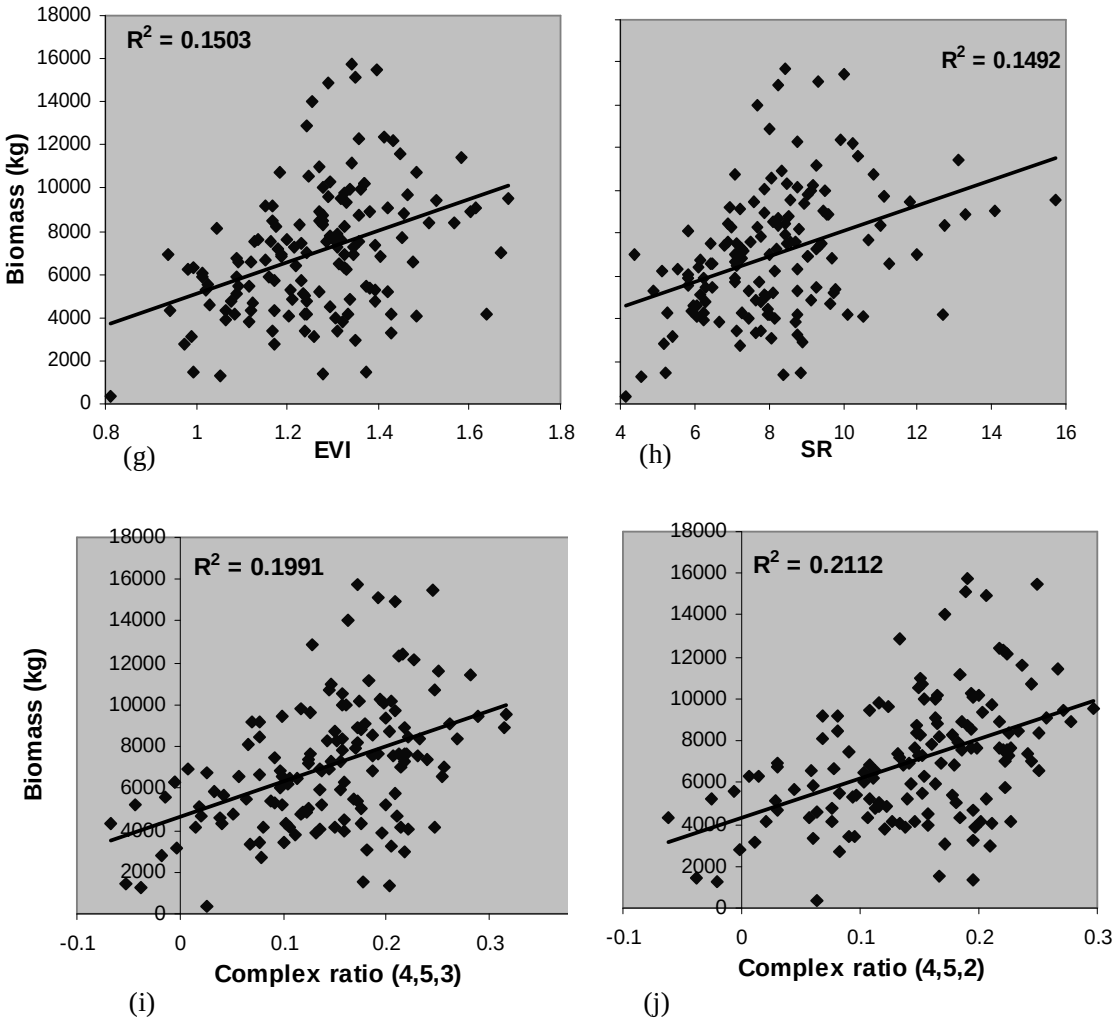

Figure 3.15 (……continued)

Although the above relations are not very strong, these were evaluated the best among the other alternatives tested. In search for better relation other options were tried. First the sample plot data were stratified into species dominance category based on composition and then relationship was analyzed. Next instead of extracting spectral signatures using point features of plot coordinates, a buffer of one and half pixel was used (as suggested by *Hall et al.*, 2006) around the points to extract the average spectral signatures for the plots in order to take account of the possible shift in plot positions due to GPS reading or error in geometric correction of the image. The results of fitting linear models to plot data after categorizing the plots into *Quercus*, *Betula*, needle-leaved and mixed needle-leaved broad-leaved forests (which are the major existing forest types in the area) are shown in the Table 3.7 below. From the R^2 values in Table 3.7, it is clear that biomass of needle-leaved forest is best related to the spectral values compared to the biomass of mixed and broad-leaved forests (*Betula* and *Quercus*). The poor relation between spectral values and the biomass of broad-leaved and mixed forests was constraint to go for biomass mapping by the forest classes. Still poor results were obtained when spectra were extracted using buffer of one and half pixel around the plot centres.

Table 3.7 R^2 values from linear regression between the plot biomass data by forest types against VIs/ band values (based on central pixel spectral signatures)

	Coefficients of determination (R^2) for the forest types			
VIs/ bands	Betula	Quercus	Needle-leaved	Mixed
NDVI	0.2292	0.1108	0.4717	0.2115
ND5,4	0.2262	0.0890	0.5260	0.2624
NDVIc	0.0656	0.4168	0.6641	0.3589
MVI	0.1989	0.0919	0.5198	0.2510
SR	0.1962	0.0838	0.4014	0.1918
RSR	0.0875	0.2987	0.5913	0.3534
EVI	0.1073	0.0912	0.4344	0.2374
Complex ratio 452	0.2089	0.1116	0.5554	0.2729
Complex ratio 435	0.2362	0.1153	0.5306	0.2703
TM Band 5	0.0488	0.4386	0.6357	0.3300

Note: the number of sample plots in the *Betula*, *Quercus*, needle-leaved and mixed forests was 12, 44, 19 and 67 respectively.

The best fitting model for carbon-sequestration was also related to NDVIc as the relation for carbon sequestration is a derivative of biomass equation. The significantly linear relation for carbon sequestration based on NDVIc was Y = 268.167295NDVIc + 42.436101 (R^2=0.4121; F_{stat}=98.15> F_{crit}=3.91, p<0.0001, df= 1, 140) where Y is annual carbon sequestration per pixel in kg. The RMSE of the model was 31.18 % of the mean; the mean annual carbon sequestration in the pixel size plots was estimated to be 162.4 kg.

Masking out the non-forest land cover types of the study area, maps for the distribution of above-ground biomass and annual carbon sequestration was produced using the above NDVIc dependent relations for them. The maps are shown in the Figures 3.16 and 3.17 below. The high biomass density areas can be seen in the forest at farther distance from the settlements.

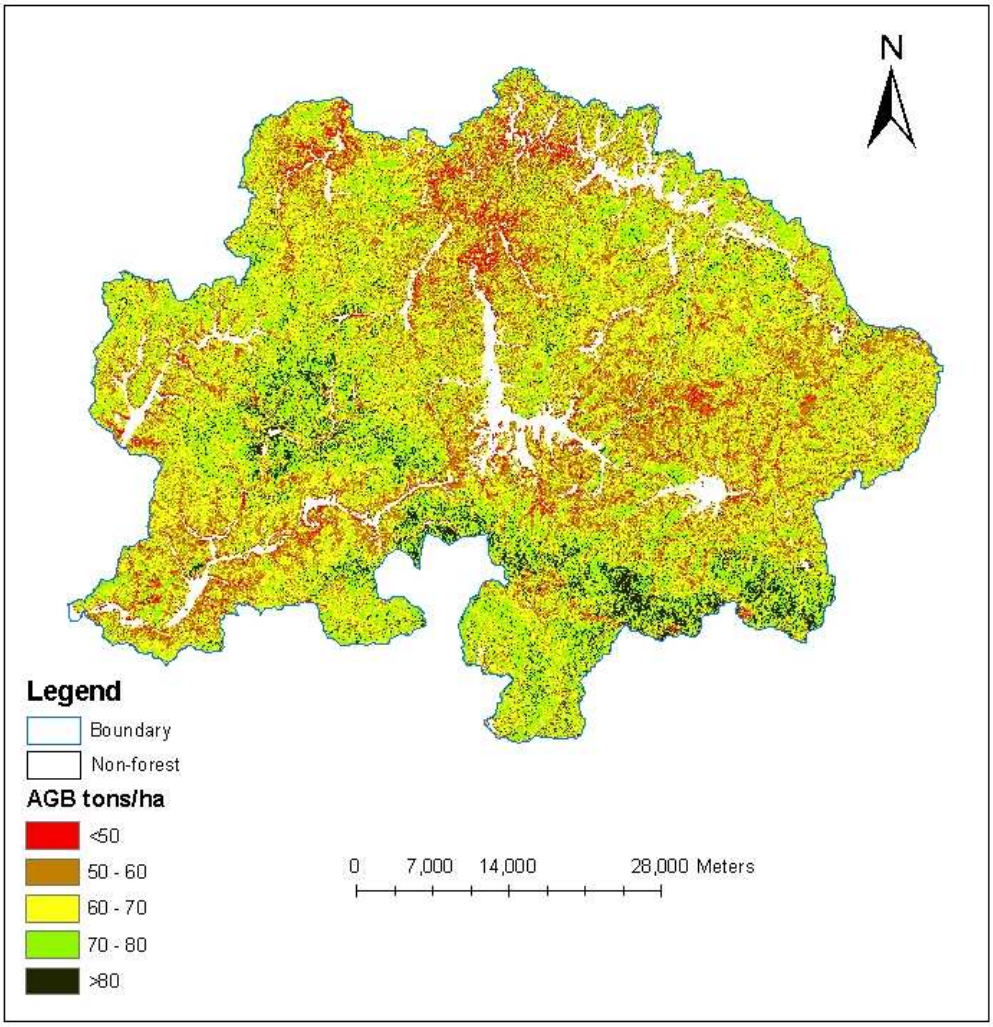

Figure 3.16 Distribution of Above Ground Biomass (AGB) density (tons/ ha) in Wangqing forest, North-east China

The average biomass density for the whole forest, estimated from the remote sensing based model dependent on NDVIc, was 65.36 tons/ ha. The total biomass of the forest was estimated to be 18400662.72 tons. Out of the total forest area of 281478 ha, only 18171 ha had biomass density above 80 ton/ ha while 18329 ha had lowest biomass density below 50 ton/ ha; the remaining forest areas had biomass in the range of 50-80 tons/ha. The high biomass density areas were mostly in mixed and needle-leaved forests. The mixed forests generally consisted of bigger sized trees of relatively fast growing species such as *Populus ussuriensis*, *Picea jezoensis*, *Abies holophylla*, *Betula platyphylla* and *Betula castata* compared to the slow growing smaller sized trees of *Quercus mongolica*, *Ulmus pumila*, etc in broad leaved forests. Needle leaved forest also had bigger trees mostly of *Abies holophylla*, *Picea jezoensis* and *Larix olgensis*. The biomass estimate by the NDVIc based model is lower than the estimate based on extrapolation of the sample plot data.

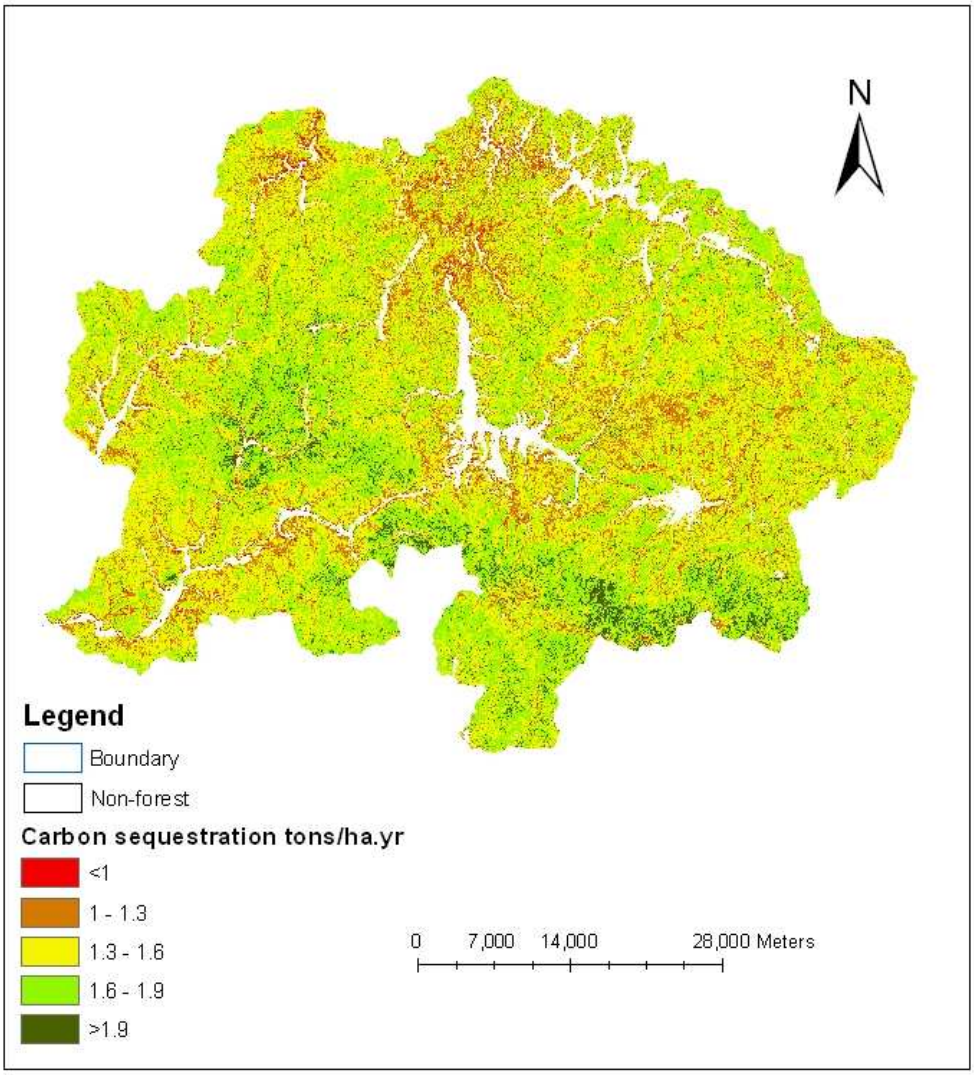

Figure 3.17 Distribution of carbon sequestration (tons/ ha.yr) in Wangqing forest, North-east China

The average carbon sequestration of the forest, estimated from the remote sensing based model (dependent of NDVIc), was 1.52 ton/ha.yr. The total carbon sequestration of the forest was estimated to be 428920.51 tons/yr. Out of the total forest area of 281478 ha, only 11865.51 ha had carbon sequestration above 1.9 ton/ha.yr while 3702.51 ha had the lowest carbon sequestration below 1 ton/ha.yr; the remaining forest areas had carbon sequestration in the range of 1-1.9 tons/ha.yr.

4. Discussion

4.1. Reliability of sub-sampling biomass estimates

Rather than putting efforts to validate existing equations, de Gier (1999) has advocated to establish original biomass equation for the population concerned. Tree sub-sampling method holds a good prospect for the purpose. Earlier studies have proved the cost-effectiveness of the sub-sampling method in terms of time usage and labour (Adel, 1993; De Gier, 1989; Kabore, 1991; Lemenih, 1995; Mabowe, 2006).

The method was easily implemented in the field just by two persons using an iPAQ based biomass assessment program and some common measurement tools such as caliper, measuring tape and weighing scale. The heaviest piece of equipment required in the process was the power saw. The method was also quicker for sample tree biomass estimation than the total weighing method. The method has the peculiarity of giving on-the-spot unbiased estimate of tree volume and fresh weight while tree dry weight is calculated after oven-drying the wood sub-samples.

The results from this study demonstrated very close relation of biomass estimates from sub-sampling method to the true weight of sample trees obtained by direct weighing in the field. The sub-sampling biomass estimates showed R^2 values of 0.9668 in the linear regression with true biomass (measured for 34 sample trees by direct weighing). The relation having non-significant intercept term was $Y=0.977353X+1.818551$ where Y is fresh biomass (kg) by total weighing and X is fresh biomass estimate (kg) by sub-sampling. This model shows that the true biomass increases by 0.977 kg for one kg increase is sub-sampling estimates. This led to the conclusion that sub-sampling estimates are close to the true AGB values of trees. Reliability of sub-sampling has also been validated by Mabowe (2006) in semi-arid woodlands and shrub-lands in Botswana. However, this is the first study that attempted to verify the reliability of sub-sampling estimates in the cool temperate forest characteristic of north-east China. The method is quick to implement in the field and overcomes the practical problem of laborious and time consuming total weighing approach generally used in the conventional method.

Tree biomass equations were developed in the study based on sub-sampling estimates, not on actually measured tree biomass. Although the sub-sampling estimates have inherent errors, this error component is automatically taken into account in the least square methods of regressions; the expected value of such error is zero as the sub-sampling estimates are unbiased. Parresol (1999) has mentioned that AGB can be estimated from a single path, but two or more paths are needed to compute the standard error of the estimate. Lemenih and de Gier (1999) calculated 110 sample trees and two sub-sampling measurements (i.e. two paths) per tree as optimum numbers to minimize the cost of sampling for a desired precision of tree biomass regression. However, measurements of only 60 sample trees and only one path per tree were limitations for this study because of practical reasons such as time constraint and permission for tree felling.

The method worked well for different tree species in the study area. The form (branching or crookedness) of trees was not found to have any influence on the sub-sampling biomass estimates as the difference in true biomass measured for some sample trees and their sub-sampling estimates did not have any relation with the number of nodes in the path of the trees.

4.2. Regression analysis of tree variables and biomass

Realizing that tree dbh and total tree height are the most commonly used variables to predict above ground biomass (de Gier, 2003; Husch *et al.*, 1982; Jenkins *et al.*, 2003; Parresol, 1999; Wang, 2006; Zianis and Mencuccini, 2004), three model forms namely polynomial, power and combined variables were used in regression analysis. All the three models show strong fit to the sub-sampling based AGB data. The combined variable model was found to have the best fit followed by the polynomial and power models, although the fit statistics were very close. The best fit with the combined model implies the need to consider tree height information in biomass assessment of the temperate forest. The observed goodness of fit of the models was in agreement with the previous works on the relationship between AGB and dbh or D^2H (Brown *et al.*, 1989; Brown, 1997; de Gier, 2003; Ketterings *et al.*, 2001, Wang, 2006; Cairns, 2003).

Zianis *et al.*, (2005), Zianis and Mencuccini (2004) and Jenkins *et al.*, (2003) have documented vast majority of biomass equations in the non-linear power form. The coefficients of power equations, however, are solved after linearizing it by logarithmic transformation. Several authors have warned that transformed models can not simply be retransformed to the non-linear form because this yields underestimates of up to 20% (Brown *et al.*, 1989). Parresol (1999) has reported that if $\hat{\mu}$ and $\hat{\sigma}^2$ are the mean and variance of a log transformed biomass data, then untransformed mean estimates would be $\exp\left(\hat{\mu}+\hat{\sigma}^2/2\right)$.

Many published biomass equations are found in combined variable form. For example, Zianis *et al*., (2005) in the review of biomass equations of European tree species found that out of 607 equations, 200 equations involved tree height as the second independent variable. Ketterings *et al.* (2001) and Wang (2006) observed that combined variable model gives a better prediction than only dbh based equation in power form. Among the several models tested by Cairns (2003), combined variable model produced highest coefficient of determination. Gregoire and Williams (1992) have also advocated for combined variable models in the development of volume equation. However, applications of combined variable model are often limited because of the practical problems in tree height measurement and cost factor. Nonetheless, new generation remote sensing techniques such as LiDAR and RADAR have demonstrated capability to measure tree heights accurately (Kasischke *et al.*, 2004; Roy *et al.*, 2003). Integrating tree height information from such remote sensing data with ground measurement of dbh can improve accuracy in biomass assessment.

Conventionally second degree polynomials are used for the development of biomass equations (Brown, 1989; de Gier, 2003). Brown *et al.* (1989) and Parresol (1999) have mentioned that weighted linear models, that may be polynomial or combined variable, can achieve as good fit as any non-linear

model. Third-degree polynomial was preferred in this study since second degree polynomials, sometime show strange behaviour (see Figure 4.1). For example, de Gier, (2003) observed that at smaller diameters the curve dips below the x-axis, resulting in negative biomass values, or the curve reaches a minimum above the minimum diameter, with the consequence that, below this point, biomass increases with decreasing diameter. The shortcoming of the second-degree polynomial can also be observed in the Figure 4.1 (left) where the second-degree polynomial curve is flat at lower diameters.

The assumption in ordinary regression analysis that variance of residuals are constant across the range of independent variables can also badly affect the precision of the model. In this study, the conditional variance of tree biomass was found to increase with tree size. De Gier (2003) has suggested that using a third-degree polynomial with backward elimination (to retain the significant coefficients) and combined with weighting can overcome the deficiency of second-degree polynomial and the problem of heteroscedastic residual variance (Figure 4.1, right). In order to obtain the weights, the variance of the residuals was computed by various classes of tree size and plotted; it was observed that the conditional variance was roughly proportional to D^5 and $(D^2H)^2$ which is in agreement with Brown *et al*., (1989) and de Gier (2003). Since the coefficients of polynomial and combined variable models were obtained by weighted linear (multiple) regression, the calculated coefficients and error statistics were unbiased.

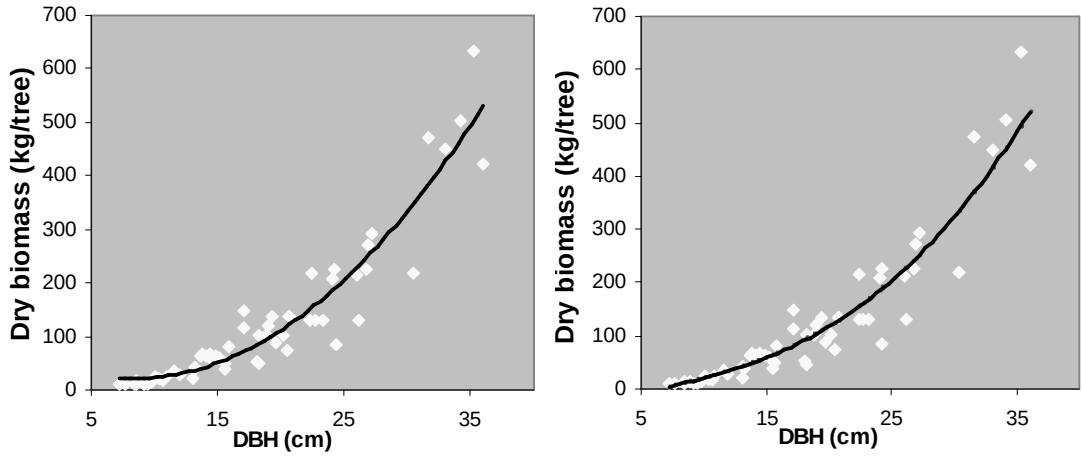

Figure 4.1 Unweighted second-degree polynomial (left) and weighted third-degree polynomial (right) for the same dry weight data of sample trees

Another interesting observation in the study was that species differences did not require the development of separate biomass equations. This observation is in line with de Gier (2003). Chojnacky (2003) also observed overlapping curves among many tree species of U.S.A. This finding is extremely important because one equation can serve for all tree species of the forest, and it can avoid another error, namely wrong species identification, a frequently encountered problem in many countries (de Gier, 2003).

The three scatter plots of sample tree biomass estimated by sub-sampling method against the predicted biomass by the three models are shown in the Figure 4.2. It is clear that all the estimates by the combined variable model are closer to the sub-sampling estimates.

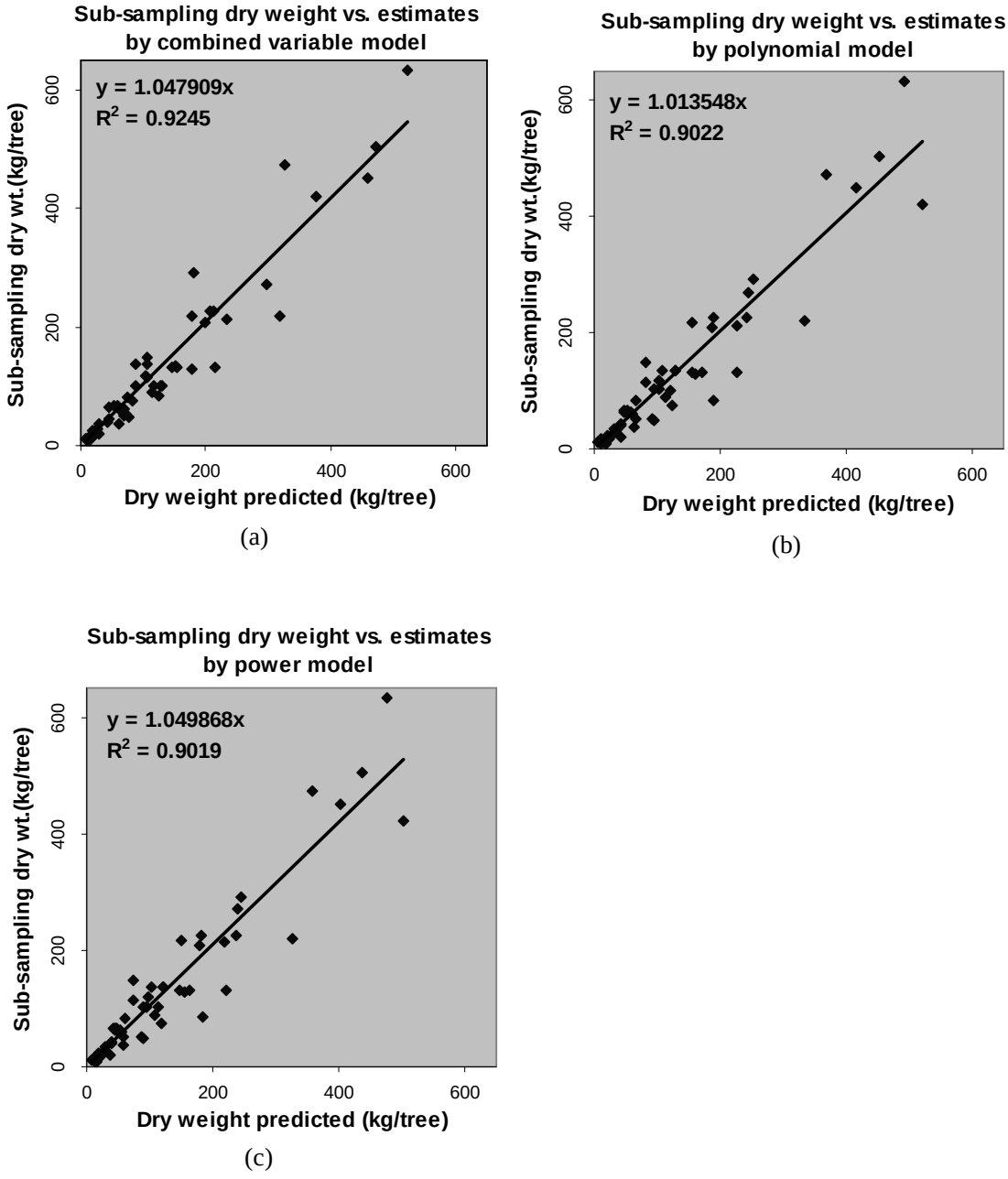

Figure 4.2 Dry weight estimates of the sample trees by sub-sampling method against the predicted values by (a) combined variable model, (b) polynomial model and (c) power function model

4.3. Comparision of biomass estimates with existing equations

Before existing tree based equations can be used in any biomass assessment program, one needs to verify whether they are indeed applicable to the area concerned. De Gier (2003) has observed large differences in biomass estimates while applying different equations from similar climatic zones but at the same time also found the estimates by equations from different climatic zones nearly overlapping. Jenkins *et al.,* (2003) has mentioned sources of errors in forest biomass assessment while using published equations.

The polynomial equation developed in this study was taken as reference for the biomass estimation of sample plots. The combined variable model could not be used because trees in the plots were not measured for height. The comparisons of tree dry biomass estimates obtained from the polynomial equation and the existing Chinese and IPCC equations is shown in the Figure 4.3 below. Four more curves are added in the graph showing how the dry biomass equations developed in other parts of the world compare to the polynomial equation of this study. The additional curves are based on equations developed for woodland and shrub-land tree species in The Netherlands, Tunisia, Ethiopia and Burkina Faso respectively by de Gier (2003), Adel (1993), Lemenih (1995) and Kabore (1991), all using the same sub-sampling method. All the equations are general (not species specific), except the IPCC equations which are separate for broadleaved and needle-leaved species.

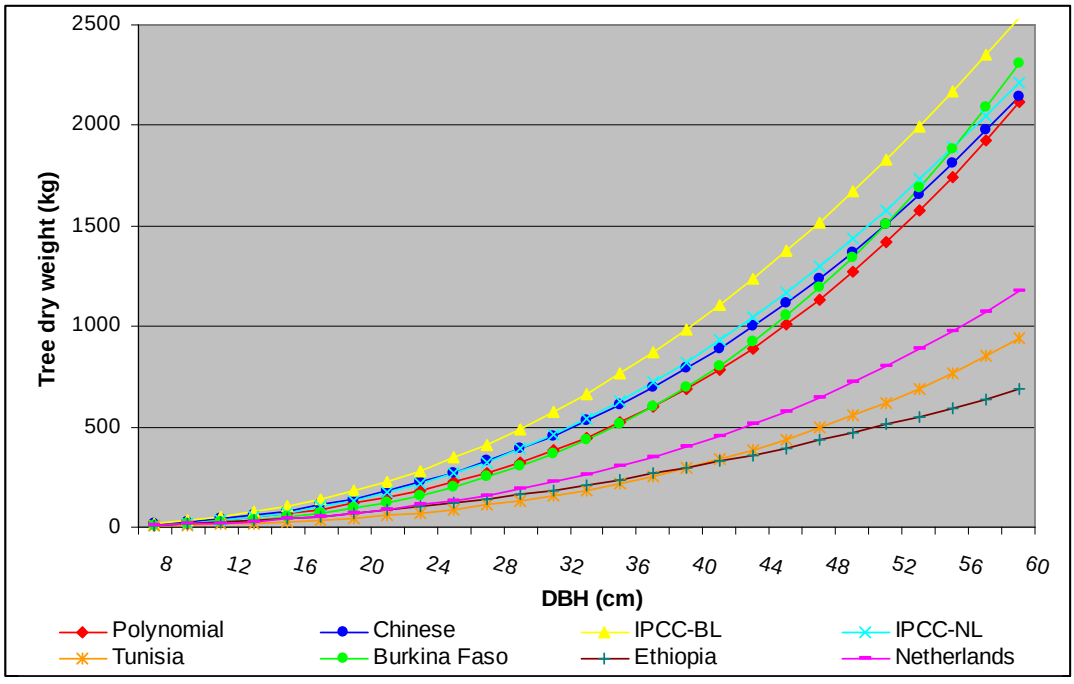

Figure 4.3. Comparison of biomass estimates by different equations

The Figure 4.3 clearly shows the anomaly in behaviour of the curves. The IPCC curve for broad-leaved (IPCC-BL) species is far from the polynomial curve of this study; however, the IPCC needle-leaved (IPCC-NL) curve is almost coinciding with the regional Chinese curve and is closer to the polynomial curve. Surprisingly, the curve from woodland of Burkina Faso, a semi-arid country, is overlapping with the polynomial curve of this study and is far away from the curve of Ethiopia- also a semi-arid country. The curves from The Netherlands (temperate country) and Tunisia (tropical

country) are closer, in contrast to the great difference between the polynomial curve of this study and the curve of The Netherlands (both from temperate zones). From this observation it can be concluded that biomass equations from one location can not simply be used in another location even when the areas are ecologically comparable. Also, the biomass equations developed for trees in dense forest can not be used for trees in woodlands or shrub-lands as different trend is evident in the above graph (woodland/ shrub-land curves are much below the forest curves except for Burkina Faso). One reason could be the branching pattern of trees (de Gier, 2003) i.e. even the same species of trees when growing inside forest have different branching pattern than when growing in open environment.

The biomass estimates by the developed polynomial are less than the estimates from the IPCC and the Chinese equations. This underestimation can be attributed to the difference in definitions of above-ground biomass. Both the Chinese and IPCC equations have defined above-ground biomass as the total weight of all the above-ground components including foliage and twigs while this study has considered only the above-ground woody components to the minimum branch diameter of 2.5 cm. Further the difference in the definition of oven-dry weight of wood is expected to cause the variation. The Chinese equation is based on oven drying of wood samples to a constant weight at 70^0C while all the other equations are based on oven drying of wood samples at 105^0C.

In brief, biomass equations show large differences among geographical areas and land cover types. Hence existing equations should not be used outside their area of origin without validation. This implies the need to develop a new equation based on sample trees taken from the area of interest.

4.4. Above ground biomass and carbon density

The average above ground biomass density calculated from the field inventory data of this study was 81.88 ton/ha; that means a carbon density of 40.94 ton/ha (50% of dry biomass). This figure of carbon density is in agreement with figures in literature for similar forests. The mean values of carbon density for Chinese forests range from 36-57.07 ton/ha (Zang *et al.,* 2007). Using the national forest inventory data of China from 1949 to 1998, Fang *et al.,* (2001) estimated the average carbon density of the north-east Chinese boreal forests to be approximately 50 tons/ha. Tan *et al.,* (2007) reported the average carbon density of nearly 55 ton/ha in Changbai mountain system that also covers the study area. Fang *et al.* (2006) reported that inventory-based forest carbon stock documented for major countries in the middle and high northern latitudes fall within a narrow range of 36-56 tons/ha with an overall area-weighted mean of 43.6 tons/ ha. The average vegetation carbon density for all forests of Europe, USA and Japan at similar latitudes are 32, 61 and 34.7 ton/ha respectively (Zhang *et al.,* 2007). Fang and Wang (2001) pointed out that forest carbon density in major temperate and boreal forest regions in the Northern Hemisphere has a narrow range from 29 to 50 ton/ha with a global mean of 36.9 ton/ha.

4.5. Annual wood accumulation and carbon sequestration

Annual production of above-ground biomass is key to carbon sequestration assessment. According to Brown (1999), estimations of net primary production (NPP) or carbon sequestration are generally based on the aboveground components only. Bouriaud *et al.,* (2005) observed high correlation between stem biomass increment and growth ring increment at breast height. Adopting the procedure suggested by de Gier, (1989), the annual production of woody biomass and carbon was estimated in this study from tree growth rings measurements and use of biomass equations. Husch *et al.* (1982) has mentioned that it is more convenient and more accurate to obtain growth ring measurements from the cut cross-sections. Since most biomass equations are dependent of dbh, cut disks from breast height were used to derive relation for carbon sequestration.

The relation for annual above-ground wood accumulation, dependent on over-bark (o.b.) dbh and annual increment of o.b. dbh, was obtained from the first derivative of biomass equation, namely polynomial equation. Since increment in o.b. dbh is the sum of increments in under-bark (u.b.) dbh and bark thickness, measurements for both growth rings and bark-thickness was necessary for the development of desired relation. A linear relationship was observed between u.b. dbh increment and o.b. dbh which is consistent with the relation obtained by de Gier (1989) for woodlands vegetation of the Netherlands. Morbes *et al.* (2003) has also observed positive correlation between diameter growth rate and dbh. This means that a large tree in developmental stage has higher growth rates (wider rings) than smaller trees. Also, a linear relation was observed between bark thickness and o.b. dbh. The linear relation between o.b. dbh and dbh increment was expected in the study because the forest is nearly even aged. The existing forest (secondary) is a result of protection measures by the Chinese government because forests in the area were destroyed by large-scale industrial logging since the turn of 20^{th} century (Wang, 2006).

The annual carbon sequestration in this study was assumed to be the half of annual wood (dry) accumulation according to literature (Brown, 1997; de Gier, 2003; IPCC, 2003). Although carbon sequestration rate of a forest is largely a function of growing conditions and age or stage of forest development (Brown, 1999), the results obtained in the study are consistent with the estimates of carbon sequestration made in similar forest types at other places. The average carbon sequestration value calculated in this study was 1.88 ton/ ha.yr. The range of NPP for all Chinese forests is 1.03 to 18.13 ton C/ha.yr (Ni, 2003). Fang (2007) obtained the carbon sequestration figures ranging from 1.33 to 3.55 ton/ ha.yr for Chinese temperate forests. For the similar forest types in eastern U.S.A., Brown and Schroeder (1999) estimated the average above-ground production of woody biomass for hardwood and softwood forests respectively as 5.2 and 4.9 ton/ ha.yr i.e. carbon sequestration of 2.6 and 2.9 ton/ ha.yr respectively.

Although comparable to the Chinese and U.S. figures, the rate of carbon sequestration obtained in this study may be an underestimation. One reason for that is the difference in definition of AGB. Some of the previous studies have considered the whole AGB including foliage and small branches in the assessment of carbon while other use national forest inventory data and expansion factors to calculate biomass increments that also accounts for the foliage and smaller branches (e.g. Brown and

Schroeder, 1999). This study, however, has defined AGB as the total mass of woody component to a minimum of 2.5 cm branch diameter.

Bouriaud *et al.,* (2005) has mentioned that despite numerous implications and reported evidence, the relationship between ring width measured at breast height and stem biomass increment has been quite poorly investigated. It means still little is known as to how the variations of growth at breast height reflect quantitative variations of stem biomass production at short time steps. Moreover, most of the previous studies are conducted for coniferous species. Further, Bouriaud *et al.,* (2005) has mentioned that computing annual biomass production from ring increment involves unverified assumptions. For example, the relative contribution of the variation in ring shape or annual fluctuations in wood density to the estimates of woody biomass increment is not assessed. Since this study combined the growth ring measurement data from all species together and does not consider the inter-annual variations in wood density or stem taper, the estimates of annual wood accumulation and carbon sequestration can only be taken as proxy. The accuracy needs to be verified by detailed study either by field measurements in permanent plots or intensive growth ring measurements considering the relative contribution of the variation in ring shape or annual fluctuations in wood density.

The Kyoto protocol clearly affirms the importance of increasing our understanding of forest carbon budgets and the role of forests in offsetting global carbon emission. This study has contributed in that direction. Forest managers interested in forest carbon management for stewardship purposes or to attain certification in sustainable forest management may benefit from these findings. It can also serve as basis for entry into CDM markets.

4.6. Remote sensing based biomass and carbon sequestration assessment

Previous studies using optical remote sensing data have had variable results for defining the most useful band or indices to map biomass, and have been inconclusive for suggesting a consistent relationship (Dong et al., 2003; Labrecque et al., 2006). Moreover, each application requires an assessment of the optical bands and indices for estimating biomass from spectral relationships (Foody *et al.*, 2003; Labrecque *et al.*, 2006). With all plot data pooled together, the best relationship of biomass and carbon sequestration in this study was observed with corrected-NDVI (NDVIc), followed by RSR and TM band-5 reflectance. Although the relationships are poor, better relation based on least square regression could not be established. Poor relation of biomass and spectral data have been observed in many studies (Foody *et al.*, 2003; Kasischke *et al.*, 2004; Labrecque *et al.*, 2006; Lu, 2006; Schlerf *et al.*, 2005). Most previous research on above-ground estimation is for coniferous forest because of its relatively simple structure (Lu, 2006; Zeng *et al.*, 2004) but for forest with complex structure and variety in species composition biomass estimation becomes difficult (Foody *et al.*, 2001). Shadows are likely to decrease the reflectance in all spectral bands as biomass increases (Muukkonen and Heiskanen, 2005). Kasischke *et al.* 2004 has mentioned the existence of relation between biomass and fraction of shadow in forest stand. The predominant topographic shadow in the study area due to the hilly terrain may be one cause for the poor relation.

The better prediction of biomass by NDVIc is in agreement with Zeng *et al.,* (2004) where they obtained strong relationship in a temperate forest ranging in biomass up to 220 ton/ha. NDVIc has the

capability to account for understory effects and is useful for secondary forests. The root mean square error with NDVIc was 32.28% of the mean which is comparatively lower than some other studies (Heiskanen, 2006; Labrecque *et al.*, 2006; Muukkonen and Heiskanen, 2005). NDVI was not found to be a good predictor of biomass which is also reported by Lu *et al.,* (2004) and Foody *et al.,* (2003).

Another better relation between biomass and RSR observed in this study can be related to Brown *et al.,* (2000) whereby they observed increased sensitivity of RSR in LAI retrieval. RSR has the advantages of reducing the effect of background reflectance and unifying deciduous and conifer species in forest parameters retrieval. Middle infrared (MIR) reflectance was also found to have good (but inverse) relation with biomass in this study. Inverse relation between MIR (TM band 5) reflectance and biomass has been observed in previous studies (Boyd *et al.*, 1999; Ingram *et al.*, 2005; Lu *et al.,* 2004; Steininger, 2000). Labrecque *et al.,* (2006) also found the band 5 to be the most correlated with biomass compared to other bands.

Kasischke *et al.,* (2004) has suggested using remote sensing to stratify forest types based on composition and structure and then use field sample plots to estimate the timber volume of each stratum. When the sample plot data were stratified by forest types, needle-leaved forest demonstrated good relation between biomass and spectral values. But the relation in case of broad-leaved and mixed forest was still poor. This finding is in agreement with Kasischke *et al.,* (2004) and Zheng *et al.,* (2004) where stronger relation between the attributes (LAI and biomass) of conifer forests and VIs have been explained. Even after stratifying the forest by species and cover types and using polynomial and multiple regressions based on VIs and band ratios, the maximum R^2 value obtained by Labrecque *et al.*, (2006) was 0.16 in a temperate forest with average biomass range of 88 to 125 tons/ ha.

Previous studies have shown significant variation in the form of regression between biomass and VIs due to the tendency of spectral indices to saturate at higher values of biomass (Kasischke *et al.*, 2004). No saturation of VI was observed in the study at the existing level of biomass density (average 81.88 ton/ha). This is in line with the result obtained by Steininger (2000) whereby saturation was observed at around 150 ton/ha. Rauste (2005) has reported that the saturation level depends on forest types, structure and understory conditions. The linear relationship obtained in this study is justifiable since saturation was absent.

When buffer was applied around the plot pixel to extract the average spectral signature of the pixel still poor relationship was observed between biomass and spectral data. The poor relation in this case may be explained on the ground that the average spectral signature can not be the representative of the biomass of the pixel concerned. When average value for a pixel is obtained, taking account of the surrounding pixels, the result is a form of smoothing which either increases or dampens the spectral value of the pixel concerned. The equal contribution of surrounding pixels that may be a non-forest, in such a case, can be a constraint in the relationship between biomass and spectral values.

One fundamental reason for poor prediction of biomass from optical remote sensing is that satellite sensors can only see the forest canopy and can not detect how much biomass is found under the canopy. In dense canopy forest, the stem biomass that is hidden from the sensor comprises majority of the above-ground biomass. Another reason mentioned in literature is the physiochemical properties of leaves such as structure, chlorophyll content and water content (Ingram *et al.,* 2004; Steininger, 2000).

Vegetation appears dark in TM band 3 due to chlorophyll absorption of red wavelengths and appears bright in band 4 due to high reflectance and multiple scattering of photons. Middle infrared bands (TM bands 5 and 7) are subject to absorption by water in leaf. Leaf senescence of deciduous species could have effect on spectral characteristics of the forest. As the imagery used was of 22 September, some deciduous species were already turning leaves to yellow. During the field visit in September, leaves of deciduous species in one part of the forest were still green while in the others part they were yellow.

It should be noted that out of the 172 plots for which plot biomass and carbon sequestration were calculated only 142 were taken for the development of relationship between the forest variables and VI. The reason was that some of the plot points, when overlaid on the image, were shifting from the actual position where it should have been. This was recognized when some of the peripheral plot points in the forest were noticed on agricultural fields or roads on the image.

5. Conclusions

Above ground biomass assessment is critical to understand the influential role of forest in global carbon cycle and climate change. Precise models, specific to local conditions, and good quality ground data are important for accurate biomass assessment. In addition to determining the best fitting biomass models, based on a reliable and unbiased method of sample tree measurements, the study has concluded the following:

How accurate is the estimate of tree biomass by sub-sampling method?
The sub-sampling method is promising for reliable and unbiased biomass estimation. The sub-sampling based biomass estimates explained more than 95 % of the variability of true biomass of the sample trees. Since the biomass estimates by the method are unbiased and statistically independent (i.e. the expected value of error is zero), the resulting equations from the least square regression are also accurate.

Which model out of polynomial, power and combined variable forms is appropriate for the estimation of AGB at a landscape scale while considering the accuracy and problems in tree variables measurement?
The combined variable model was found to be the best in describing the relationship of tree biomass and its variables dbh and height. While considering the practical problems in tree height measurement, the polynomial model was the next best alternative because its fit statistics differ little with the combined model compared to the power model. The weighting of third degree polynomial followed by backward elimination of non-significant coefficients was necessary to get rid of the heteroscedasticity and illogical behaviour of curve at lower dbh values.

How do the estimates from local Chinese and IPCC equations compare (w.r.t. precision) with the sub-sampling estimates and what would be their impact on assessing carbon reservoirs and sinks?
The geographical location of the existing tree-based equations was found to have significant effect in the area based estimates of biomass, although the estimate by Chinese equation was closer to the sub-sampling based estimates (i.e. from the polynomial equation). The estimates of biomass density using the Polynomial, Chinese and IPCC equations were found to be 81.885, 97.113 and 112.122 metric tons. The estimates by the Chinese and IPCC equations are respectively 18.6% and 36.9% higher than the polynomial estimate. The estimates by the tree equations differed significantly. Since the polynomial equation was based on field measurement by unbiased and reliable sub-sampling method, the estimate from it was assumed to be the most accurate.

How reliable is the estimate of carbon sequestration obtained from growth ring measurement?
The use of tree ring analysis is a valuable tool for the assessment of increment in woody biomass or carbon sequestration. The use of growth ring measurements for the assessment of annual carbon sequestration demonstrated agreement with the documented values in literature for the forests in

north-east China and the comparable forests elsewhere. Further investigation on the relationship between tree ring measurements and annual wood accumulation is required for improved understanding of the role of temperate forests as carbon sink and for sustainable management planning. The relation developed in the study needs to be verified by species and all species combined.

Which vegetation index or spectral bands best relate to AGB? And what is the biomass estimate of Wangqing forest?

Although poor, a significant relationship was observed between biomass (or annual carbon sequestration) and corrected-NDVI. The average biomass density of the forest was estimated to be 65.36 tons/ ha while the total biomass was 18400662.72 tons. The annual carbon sequestration was estimated at 1.52 ton/ha and the total annual carbon sequestration was 428920.51 tons.

Is there saturation problem of VI in the study area? If yes, at what level of biomass does VI start to saturate?

In general, saturation effect was not observed with VIs/ band ratios; however, because of the poor relationships detail evaluation could not be made for each of the tested VIs/ band ratios.

Finally, the equations developed in this study can be used for biomass and carbon inventories for ecological studies, for validating theoretical models and for planning the use of forest resources. The maps showing spatial distribution of biomass and annual carbon sequestration could serve as reference for the planners for sustainable management of the forest.

6. Recommendations

- Sub-sampling method can be used for reliable and cost effective biomass assessment. The reliability of the sub-sampling estimates should be consolidated by undertaking two path measurements per tree.
- Existing equations should not be used without validation. Original equation specific to the area under investigation is important.
- The equations developed in this study are valid only for the Wangqing forest for trees above 7.2 cm dbh and can be used to the maximum dbh of 40 cm. So the equations should be used with care for the locality and dbh limits. Application of the equation beyond the limits needs verification.
- Species specific relations for annual wood increment need to be developed for precise estimation of carbon sequestration because the diameter increment or the width of growth rings and hence the wood increment varies across species. The relation derived for carbon sequestration needs to be verified by the measurements of sample trees in permanent plots. Further research is required to see the effect of variations in wood density across the growth rings on tree biomass increment.
- Integrating the both diameter and height dimensions in the development of biomass equation could provide more accurate biomass estimation.
- Further research is required to establish better relation between biomass and spectral data. Additional data on forest types, canopy cover, height and age could be integrated to obtain better predictive model based on spectral data. The use of alternative imaging technology (e.g. RADAR, LiDAR, Hyper-spectral imagery, or high resolution imagery such as Quickbird or IKONOS) should be considered and methods to capture horizontal (e.g. canopy cover, basal area) and vertical (height) characteristics of the forest should be further studied.

References

Adel, S., 1993. Spot satellite response and tree sub-sampling approach for a cost-effective woody biomass estimation in Tunisia, ITC, Enschede, The Netherlands, 94+ pp.

Bouriaud, O., Breda, N., Dupouey, J.L. and Granier, A., 2005. Is ring width a reliable proxy for stem-biomass increment? A case study in European beech. Canadian Journal of Forest Research, 35(12): 2920-2933.

Boyd, D.S., Foody, G.M. and Curran, P.J., 1999. The relationship between the biomass of Cameroonian tropical forests and radiation reflected in middle infrared wavelengths. International Journal of Remote Sensing, 20(5): 1017-1023.

Boyd, D.S., Foody, G.M. and Ripple, W.J., 2002. Evaluation of approaches for forest cover estimation in the Pacific Northwest, USA, using remote sensing. Applied Geography, 22(4): 375-392.

Brown, L., Chen, J.M., Leblanc, S.G. and Cihlar, J., 2000. A shortwave infrared modification to the simple ratio for LAI retrieval in boreal forests: an image and model analysis. Remote Sensing of Environment, 71: 16-25.

Brown, S., 1997. Estimating biomass and biomass change of tropical forests: a primer. A forest resources assessment publication. FAO, Rome, 55 pp.

Brown, S., 2002. Measuring carbon in forests: current status and future challenges. Environmental Pollution, 116(3): 363-372.

Brown, S., Gillespie, A.J.R. and Lugo, A.E., 1989. Biomass estimation methods for tropical forests with applications to forest inventory data. Forest Science, 35(4): 881-902.

Cairns, M.A., Olmsted, I., Granados, J. and Argaez, J., 2003. Composition and aboveground tree biomass of a dry semi-evergreen forest on Mexico's Yucatan Peninsula. Forest Ecology and Management, 186(1-3): 125-132.

Chen, J.M., Thomas, S.C.,Yin, Y., Maclaren, V., Liu, G., Tian, Q., Zhu, Q., Pan, J.J., Shi, X., Xue, J. and Kang, E., 2007. Enhancing forest carbon sequestration in China: toward an integration of scientific and socio-economic perspectives. Journal of Environmental Management, 85(2007): 515-523.

Chojnacky, D.C., 2003. Allometric scaling theory applied to FIA biomass estimation. Forest Inventory Research, Enterprise Unit (USDA Forest Service; 1115-VMPR; 1400 Independence Avenue, Washington).

Cunia, T., 1986a. Error of forest inventory estimates: its main components. In: Wharton, E.H. and Cunia, T. (ed.), Estimating tree biomass regression and their error (Workshop proceeding; May 26-30, 1986, Syracuse): 1-13.

Cunia, T., 1986b. Construction of tree biomass tables by linear regression techniques. In: Wharton, E.H. and Cunia, T. (ed.), Estimating tree biomass regression and their error (Workshop proceeding; May 26-30, 1986, Syracuse): 27-36.

de Gier, A., 1989. Woody biomass for fuel- estimating the supply in natural woodlands and shrublands. (ITC Publication no. 9. ITC, Enschede, The Netherlands).

de Gier, A., 1999. Woody biomass assessment in woodlands and shrublands. (Proceedings of a workshop on off-forest tree resources of Africa, Arusha, Tanzania): 89-98.

de Gier, A., 2003. A new approach to woody biomass assessment in woodlands and shrublands. In: P. Roy (Ed), Geoinformatics for Tropical Ecosystems, Bishen Singh Mahendra Pal Sing, Dehra Dun, India: 161-198.

Dias, A.T.C., de Mattos, E.A., Vieira, S.A., Azeredo, J.V. and Scarano, F.R., 2006. Aboveground biomass stock of native woodland on a Brazilian sandy coastal plain: Estimates based on the dominant tree species. Forest Ecology and Management, 226(1-3): 364-367.

Dong, J., Kaufmann, R.K., Myneni, R.B., Tucker, C.J., Kauppi, P.E., Liski, J. Buermann, W., Alexeyev, V. and Hughes, M.K., 2003. Remote sensing estimation of boreal and temperate

forest woody biomass: carbon pools, sources and sinks. Remote Sensing of Environment, 84(2003): 393-410.

Fang, J., Chen, A., Peng, C., Zhao, S. and Ci, L., 2001. Changes in forest biomass carbon storage in China between 1949 and 1998. Science, 292.

Fang, J.Y., Liu, G.H., Zhu, B., Wang, X.K. and Liu, S.H., 2007. Carbon budgets of three temperate forest ecosystems in Dongling Mt., Beijing, China. SCIENCE IN CHINA SERIES D-EARTH SCIENCES, 50(1): 92-101.

FAO, 1981. Quantifying forest energy -Inventory methods to determine biomass. [Online] http://www.fao.org/docrep/p3350e/p3350e05.htm (Accessed on October 10, 2007).

FAO, 2004. National Forest Inventory -Field Manual, Working Paper 94/E. FAO Forest Resources Assessment Program, Rome.

FAO, 2005. Global Forest Resource Assessment 2005. FAO Forestry Paper 147. Food and Agriculture Organization of the United Nations, Rome.

Fehrmann, L. and Kleinn, C., 2006. General considerations about the use of allometric equations for biomass estimation on the example of Norway spruce in central Europe. Forest Ecology and Management, 236(2-3): 412-421.

Foody, G.M., Boyd, D.S. and Cutler, M.E.J., 2003. Predictive relations of tropical forest biomass from Landsat TM data and their transferability between regions. Remote Sensing of Environment, 85(4): 463-474.

Foody, G.M. et al., 2001. Mapping the biomass of Bornean tropical rain forest from remotely sensed data. Global Ecology and Biogeography, 10(4): 379-387.

Furnival, G.M., 1961. An index for comparing equations used in constructing volume tables. Forest Science, 7(4): 337-341.

Gower, S.T., Kucharik, C.J. and Norman, J.M., 1999. Direct and indirect estimation of leaf area index, fAPAR and net primary production of terrestrial ecosystems. Remote Sensing of Environment, 70(1999): 29-51.

Green, C., Tobin, B., O'Shea, M., Farrell, E.P. and Byrne, K.A., 2005. Above-and belowground biomass measurements in an unthinned stand of Sitka spruce (*Picea sitchensis* (Bong) Carr.). Eur J Forest Res(DOI 10.10007/s10342-005-0093).

Gregoire, T.G. and Williams, M., 1992. Identifying and evaluating the components of non-measurement error in the application of standard volume equations. The Statistician, 41: 509-518.

Hall, R.J., Skakun, R.S., Arsenault, E.J. and Case, B.S., 2006. Modeling forest stand structure attributes using Landsat ETM+ data: Application to mapping of aboveground biomass and stand volume. Forest Ecology and Management, 225(1-3): 378-390.

Heath, S., 2000. Carbon sequestration in live trees: methods analysis of dendrometry in Harvard Forest. [Online] http://harvardforest.fas.harvard.edu/publications/symposium/stusym00.html (Accessed on October 15, 2007).

Heiskanen, J., 2006. Estimating aboveground tree biomass and leaf area index in a mountain birch forest using ASTER satellite data. International Journal of Remote Sensing, 27(6): 1135-1158.

Huete, A. et al., 2002. Overview of the radiometric and biophysical performance of the MODIS vegetation indices. Remote Sensing of Environment, 83(2002): 195-213.

Hurcom, S.J. and Harrison, A.R., 1998. The NDVI and spectral decomposition for semi-arid vegetation abundance estimation. International Journal of Remote Sensing, 19(16): 3109-3125.

Husch, B., Miller, C.I. and Beers, T.W., 1982. Forest Mensuration. John Wiley & Sons, New York, 402 pp.

Ingram, J.C., Dawson, T.P., and Whittaker, R.J., 2005. Mapping tropical forest structure in southern Madagascar using remote sensing and artificial neural networks. Remote Sensing of Environment, 94(2005): 491-507.

IPCC, 2003. Good Practice Guidance for land use, land-use change and forestry. IPCC National Greenhouse Gas Inventories Program; Penman, J., Gytarsky, M., Hiraishi, T., Krug, T.,

Kruger, D., Pipatti, R., Buendia, L., Miwa, K., Ngara, T., Tanabe, K. and Wagner, F. (eds); Published by the Institute for Global Environmental Strategies (IGES), Japan.

IPCC, 2006. 2006 IPCC Guidelines for National Greenhouse Gas Inventories (Volume 4, AFOLU). National Greenhouse Gas Inventories Program; Eggleston, H.S., Buendia, L., Miwa, K., Ngara, T. and Tanabe, K. (eds); Published: IGES, Japan.

IPCC, 2007. Summary for Policymakers. In: S. Solomon et al. (Editors), Climate Change 2007: The Physical Science Basis. Contribution of Working Group I to the Fourth Assessment Report of the Intergovernmental Panel on Climate Change. Cambridge University Press, Cambridge, United Kingdom and New York, NY, USA.

Jenkins, J.C., Chojnacky, D.C., Heath, L.S. and Birdsey, R.A., 2003. National-Scale Biomass Estimators for United States Tree Species. Forest Science, 49: 12-35.

Kabore, C., 1991. A methodological approach to woody biomass assessment for fuelwood production using a tree sub-sampling procedure and NOAA/AVHRR data, ITC, Enschede, The Netherlands, 78+ pp.

Kasischke, E.S. et al., 2004. Remote sensing for natural resource management and environmental monitoring. Manual of remote sensing, 4. John Wiley & Sons, Inc.

Ketterings, Q.M., Coe, R., van Noordwijk, M., Ambagau, Y. and Palm, C.A., 2001. Reducing uncertainty in the use of allometric biomass equations for predicting above-ground tree biomass in mixed secondary forests. Forest Ecology and Management, 146(1-3): 199-209.

Labrecque, S., Fournier, R.A., Luther, J.E. and Piercey, D., 2006. A comparison of four methods to map biomass from Landsat-TM and inventory data in western Newfoundland. Forest Ecology and Management, 226(2006): 129-144.

Leeds, I.S.S., 2007. Advanced modelling technique: weighted linear regression. [Online] http://www.leeds.ac.uk/iss/documentation/tut/tut116/tut116-4.html (Accessed on December 25, 2007).

Lemenih, M., 1995. Woody biomass assessment of trees and shrubs for fuelwood in Ziway region woodland, Ethiopia, ITC, Enschede, The Netherlands, 78+ pp.

Lemenih, M. and de Gier, A., 1999. Optimizing tree sub-sampling and regression analysis for woody biomass assessment. Proceedings of a workshop on off-forest tree resources of Africa, Arusha, Tanzania: 99-106.

Lu, D., 2006. The potential and challenge of remote sensing-based biomass estimation. International Journal of Remote Sensing, 27(7-10): 1297-1328.

Lu, D., Mausel, P., Brondizio, E. and Moran, E., 2004. Relationships between forest stand parameters and Landsat TM spectral responses in the Brazilian Amazon Basin. Forest Ecology and Management, 198(2004): 149-167.

Mabowe, B.R., 2006. Aboveground woody biomass assessment in Serowe woodlands, Botswana, ITC, Enschede, 82 pp.

Maynard, C.L., Lawrence, R.L., Nielsen, G.A. and Decker, G., 2007. Modeling vegetation amount using bandwise regression and ecological site descriptions as an alternative to vegetation indices. GIScience and Remote Sensing, 44(1): 68-81.

Meng, Q., Cieszewski, C.J., Madden, M. and Borders, B., 2007. A linear mixed-effects model of biomass and volume of trees using Landsat ETM+ images. Forest Ecology and Management, 244(1-3): 93-101.

Mutanga, O., 2004. Hyperspectral remote sensing of tropical grass quality and quantity. Ph.D. Thesis, Wageningen University.

Muukkonen, P. and Heiskanen, J., 2005. Estimating biomass for boreal forests using ASTER satellite data combined with standwise forest inventory data. Remote Sensing of Environment, 99(4): 434-447.

Ni, J., 2003. Net primary productivity in forests of China: scaling-up of national inventory data and comparison with model predictions. Forest Ecology and Management, 176(2003): 485-495.

Parresol, B.R., 1999. Assessing tree and stand biomass: a review with examples and critical comparisons. Forest Science, 45(4): 573-593.

Rauste, Y., 2005. Multi-temporal JERS SAR data in boreal forest biomass mapping. Remote Sensing of Environment, 97: 263-275.

Roy, P.S., Joshi, P.K. and Lohani, B., 2003. LiDAR remote sensing for forest ecosystem studies. In: P. Roy (Ed), Geoinformatics for Tropical Ecosystems, India(309-334).

Samalca, I., 2007. Estimation of forest biomass and its error : a case in Kalimantan, Indonesia, ITC, Enschede, 74 pp.

Schlerf, M., Alzberger, C. and Hill, J., 2005. Remote sensing of forest biophysical variables using HyMap imaging spectrometer data. Remote Sensing of Environment, 95(2005): 177-194.

Schroeder, P., Brown, S., Mo, J., Birdsey, R. and Cieszewski, C., 1997. Biomass estimation for temperate broadleaf forests of the United States using inventory data. Forest Science, 43(3): 424-434.

Somogyi, Z. et al., 2006. Indirect methods of large-scale forest biomass estimation. Eur J Forest Res(DOI 10.1007/s10342-006-0125-7).

Steininger, M.K., 2000. Satellite estimation of tropical secondary forest above-ground biomass: data from Brazil and Bolivia. International Journal of Remote Sensing, 21(6-7): 1139-1157.

Tan, K., Piao, S., Peng, C. and Fang, J., 2007. Satellite-based estimation of biomass carbon stocks for northeast China's forests between 1982 and 1999. Forest Ecology and Management, 240(1-3): 114-121.

Tenkabail, P.S., Smith, R.B. and Pauw, E.D., 2000. Hyperspectral vegetation indices and their relationships with agricultural crop characteristics. Remote Sensing of Environment, 75: 158-182.

Ter-Mikaelian, M.T. and Korzukhin, M.D., 1997. Biomass equations for sixty-five North American tree species. Forest Ecology and Management, 97(1): 1-24.

UNEP, 2007. Climate change fact sheets. United Nations Environment Programme. [Online] http://www.unep.org/themes/climatechange/Fact_Sheets/index.asp (Accessed on February 7, 2008).

UNFCCC, 2007. UN breakthrough on climate change reached in Bali (press release 15 Dec 2007). United Nations Framework Convention on Climate Change. [Online] http://unfccc.int/files/press/news_room/press_releases_and_advisories/application/pdf/20071215_bali_final_press_release.pdf (Accessed on December 25, 2007).

Valentine, H.T., Tritton, L.M. and Furnival, G.M., 1984. Sub-sampling trees for biomass, volume or mineral content. Forest Science, 30(33): 673-681.

Wang, C., 2006. Biomass allometric equations for 10 co-occurring tree species in Chinese temperate forests. Forest Ecology and Management, 222(1-3): 9-16.

Wang, X., Fang, J., Tang, Z. and Zhu, B., 2006. Climatic control of primary forest structure and DBH-height allometry in Northeast China. Forest Ecology and Management, 234(2006): 264-274.

West, G.B., Brown, J.H. and Enquist, B.J., 1997. A general model for the origin of allometric scaling laws in biology. Science, 276: 122-126.

Xing, Y., 2007b. Estimating Aboveground Forest Biomass Using Spaceborne Lidar Waveforms in the Cool-temperate Forest of Northeastern China. Ph.D. Research Document, ITC, The Netherlands.

Zhao, M. and Zhou, G.-S., 2005. Estimation of biomass and net primary productivity of major planted forests in China based on forest inventory data. Forest Ecology and Management, 207(3): 295-313.

Zheng, D., Rademacher, J., Chen, J., Crow, T., Bresee, M., Le Moine, J., and Ryu, S., 2004. Estimating aboveground biomass using Landsat 7 ETM+ data across a managed landscape in northern Wisconsin, USA. Remote Sensing of Environment, 93(3): 402-411.

Zianis, D. and Mencuccini, M., 2004. On simplifying allometric analyses of forest biomass. Forest Ecology and Management, 187(2-3): 311-332.

Zianis, D., Muukkonen, P., Makipaa, R. and Mencuccini, M., 2005. Biomass and stem volume equations for tree species in Europe. Silva Fennica (Monographs 4): 1-63.

Appendices

Appendix 1: Sample tree measurements

Tree #	dbh (cm)	ht (m)	Species	FWS	FWT	FWC	VS	DWS
1	26.8	16.4	*B. platyphylla*	365		392.4	0.5096	225.77
2	9.2	8.7	*B. platyphylla*	19.6	22.6		0.0375	11.31
3	22.5	19.5	*B. platyphylla*	388.6		457.5	0.4595	217.29
4	18.8	20.4	*B. platyphylla*	184.2		262.7	0.3178	101.74
5	14.4	18.7	*B. platyphylla*	113.4	108		0.149	61.44
6	15.8	16.3	*U. pumila*	175.3	163		0.1729	81.70
7	9.8	8.6	*U. pumila*	30.5	34		0.0311	14.44
8	19	16	*U. pumila*	246.6			0.2441	118.61
9	13.7	13.6	*U. pumila*	134.9	100		0.1144	64.16
10	36.1	16	*U. pumila*	785.3			0.9827	420.56
11	17.1	20.2	*F. mandshurica*	201.2		245.3	0.2687	114.85
12	18.3	12.7	*A. holophylla*	137.3	131		0.1909	47.70
13	19.4	12.9	*Q. mongolica*	219.8	204		0.2474	135.96
14	20.7	13.8	*Q. mongolica*	226.8		255.7	0.2732	135.95
15	19.7	16.4	*A. holophylla*	207.8	197		0.2535	88.94
16	8.5	8.6	*A. holophylla*	22.9	23		0.0278	9.13
17	13.2	14.4	*A. holophylla*	115.7	109		0.1213	43.63
18	13.2	13.6	*A. holophylla*	90	83		0.1055	40.01
19	26.2	17.3	*A. holophylla*	345.4		290.8	0.3938	131.41
20	10.4	10.5	*P. jezoensis*	44.8	42		0.0516	19.36
21	26.1	19.1	*P. jezoensis*	460.8			0.6005	212.86
22	18.3	19.3	*L. olgensis*	251.9		171.4	0.2695	101.72
23	13.9	17.1	*L. olgensis*	108.9	108		0.1365	66.05
24	27	22.6	*L. olgensis*	463.5		419.4	0.6556	270.48
25	33.1	23.2	*L. olgensis*	786.1		726.2	0.9729	450.00
26	22.7	19.2	*A. holophylla*	318.7		316.2	0.4012	129.09
27	20.5	10.8	*T. amurensis*	144.1	152		0.198	74.28
28	24.3	11.8	*T. amurensis*	174			0.2559	84.36
29	14.9	15.2	*B. platyphylla*	114.6	117		0.1472	63.96
30	24.1	19	*B. platyphylla*	363.9		438.7	0.545	207.88
31	35.3	23.1	*B. platyphylla*	1141			1.2874	632.47
32	8.5	12.9	*B. platyphylla*	29.2	32		0.0375	15.86
33	8.95	10.6	*U. pumila*	26.8	23		0.0308	12.85
34	24.3	19.5	*U. pumila*	485.1			0.6346	225.83
35	34.2	22.4	*B. platyphylla*	948			1.1832	504.09
36	14.5	14.2	*P. ussuriensis*	117.3	121		0.1636	66.49

Appendix 1: …continued

37	18.9	19.9	*P. ussuriensis*	214.1		257.0	0.335	102.02
38	18.1	12	*P. jezoensis*	114.6	129		0.1825	52.10
39	9.5	7.8	*A. holophylla*	27.5	24.5		0.0329	9.58
40	10.1	11.1	*Q. mongolica*	37.7	41.7		0.052	24.12
41	11.6	12.5	*Q. mongolica*	54.4	61		0.0691	35.11
42	7.2	9.2	*Q. mongolica*	17.8	18		0.0215	10.82
43	27.3	13.4	*Q. mongolica*	473.5			0.5806	291.78
44	31.6	18	*Q. mongolica*	786.2			1.1097	472.51
45	12	10.8	*L. olgensis*	51.4	50		0.0704	27.35
46	30.4	19.1	*A. holophylla*	530.9		551.2	0.7495	219.62
47	15.2	15.3	*A. holophylla*	142.1		115.9	0.1548	59.05
48	15.6	13.8	*P. jezoensis*	83	103		0.1017	37.51
49	15.6	15.6	*P. jezoensis*	156.8	149		0.1659	50.17
50	8.4	7.8	*P. jezoensis*	22.4	22		0.028	11.19
51	23.3	15.8	*P. jezoensis*	218.5			0.3724	131.69
52	17.1	20.2	*L. olgensis*	243.2	222.5		0.266	147.57
53	7.7	11.1	*L. olgensis*	23	23		0.0253	11.42
54	10.7	10.2	*P. jezoensis*	36	42		0.0528	18.01
55	10.9	11.5	*L. olgensis*	48.7	51		0.0594	23.97
56	14.1	19	*L. olgensis*	112.6	123		0.1476	62.91
57	20.7	19.7	*L. olgensis*	246	288		0.3041	135.75
58	13.1	9.3	*T. amurensis*	42.3	43		0.066	20.87
59	22.4	16.2	*P. jezoensis*	262.4		214.0	0.3694	130.61
60	20.2	12.1	*L. olgensis*	209.8			0.2424	101.62

FWS: Fresh weight (kg) estimate by sub-sampling; FWT: Fresh weight (kg) by total weighing; FWC: Fresh weight (kg) estimate by combined approach of volume calculation and weighing; VS: Volume (m^3) estimate by sub-sampling; DWS: Estimated dry weight (kg) by sub-sampling

Appendix 2

2-A: ANOVA test for the comparison of dry biomass estimates of tree in the dbh range of 10-40 cm and at 2 cm class interval by broad-leaved (BL), needle-leaved (NL) and combined species equations obtained from fittings to sub-sampling dry biomass data

SUMMARY				
Groups	*Count*	*Sum*	*Average*	*Variance*
Polynomial estimates for NL sps	16	4199.184	262.449	61625.19
Polynomial estimates for BL sps	16	4456.176	278.511	50542.13
Polynomial estimates for combined sps	16	4324.112	270.257	55092.71

ANOVA						
Source of Variation	*SS*	*df*	*MS*	*F*	*P-value*	*F crit*
Between Groups	2064.433	2	1032.217	0.018514	0.981664	3.204317
Within Groups	2508900	45	55753.34			
Total	2510965	47				

2-B: *t*-test (paired two sample for means) to compare the significance of difference of means of dry biomass estimates by polynomial equations respectively for BL, NL and all species combined for trees in the dbh range 10-40 cm at class interval of 2 cm

	Pair 1		Pair 2		Pair 3	
	Estimates for NL	*Estimates for BL*	Estimates for BL	Estimates for combined	Estimates for NL	Estimates for Combined
Mean	262.449	278.511	278.511	270.257	262.449	270.257
Variance	61625.187	50542.125	50542.125	55092.705	61625.187	55092.705
Observations	16	16	16	16	16	16
Pearson Correlation	0.985		0.996		0.997	
Hypothesized Mean Difference	0		0		0	
df	15		15		15	
t Stat	-1.363		1.425		-1.301	
P(T<=t) one-tail	0.096		0.087		0.106	
t Critical one-tail	1.753		1.753		1.753	
P(T<=t) two-tail	0.193		0.175		0.213	
t Critical two-tail	2.131		2.131		2.131	

Appendix 3

3-A: Results of weighted linear regression by backward elimination method applied to the polynomial model based on dry biomass data of the sample trees

Model Summary

Model	R	R Square	Adjusted R Square	Std. Error of the Estimate
1	.944(a)	.891	.885	.08250491
2	.944(b)	.891	.887	.08177814

a Predictors: (Constant), D^3, D, D^2

b Predictors: (Constant), D^3, D

ANOVA (c,d)

Model		Sum of Squares	df	Mean Square	F	Sig.
1	Regression	3.125	3	1.042	153.019	<0.001(a)
	Residual	.381	56	.007		
	Total	3.506	59			
2	Regression	3.125	2	1.562	233.627	<0.001(b)
	Residual	.381	57	.007		
	Total	3.506	59			

a Predictors: (Constant), D^3, D, D^2; b Predictors: (Constant), D^3, D

c Dependent Variable: Dry-biomass; d Weighted Least Squares Regression - Weighted by D^5

Coefficients (a,b)

Model		Un-standardized Coefficients		Standardized Coefficients	t	Sig.
		B	Std. Error	Beta		
1	(Constant)	-23.766	34.887		-.681	.499
	D	3.569	7.241	.330	.493	.624
	D^2	-.007	.452	-.018	-.015	.988
	D^3	.009	.009	.658	1.064	.292
2	(Constant)	-23.263	9.156		-2.541	.014
	D	3.461	1.034	.320	3.348	.001
	D^3	.009	.001	.648	6.791	<0.001

a Dependent Variable: Dry-biomass

b Weighted Least Squares Regression - Weighted by D^5

Excluded Variables (b,c)

Model		Beta In	t	Sig.	Partial Correlation	Collinearity Statistics
						Tolerance
2	D2	-.018(a)	-.015	.988	-.002	.001

a Predictors in the Model: (Constant), D^3, D

b Dependent Variable: Dry-biomass

c Weighted Least Squares Regression - Weighted by D^5

3-B: Results of weighted linear regression applied to combined variable model based on dry biomass data of the sample trees

Model Summary

Model	R	R Square	Adjusted R Square	Std. Error of the Estimate
1	.967(a)	.935	.934	38.844

a Predictors: (Constant), D^2H

ANOVA(b,c)

Model		Sum of Squares	df	Mean Square	F	Sig.
1	Regression	1262787.072	1	1262787.072	836.900	<0.001(a)
	Residual	87515.462	58	1508.887		
	Total	1350302.535	59			

a Predictors: (Constant), D^2H

b Dependent Variable: Dry-biomass

c Weighted Least Squares Regression - Weighted by $(D^2H)^2$

Coefficients(a,b)

Model		Un-standardized Coefficients		Standardized Coefficients	t	Sig.
		B	Std. Error	Beta		
1	(Constant)	-.804	1.087		-.740	.462
	D^2H	181.438	6.272	.967	28.929	<0.001

a Dependent Variable: Dry-biomass

b Weighted Least Squares Regression - Weighted by $(D^2H)^2$

Appendix 4: Curves fitting to the sample tree volume and fresh biomass data

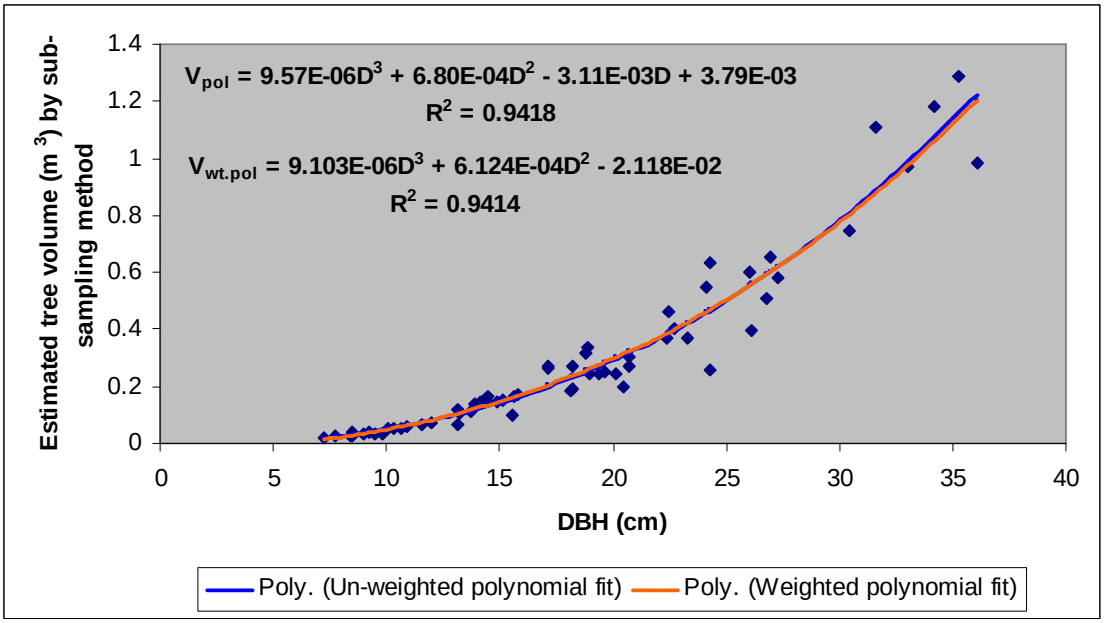

Figure 4A: scatter plot of volume data (obtained from sub-sampling method) against DBH fitted with un-weighted and weighted third degree polynomial models. V_{pol} is volume estimate by un-weighted polynomial; $V_{wt.pol}$ is volume estimate by weighted polynomial; and D is dbh.

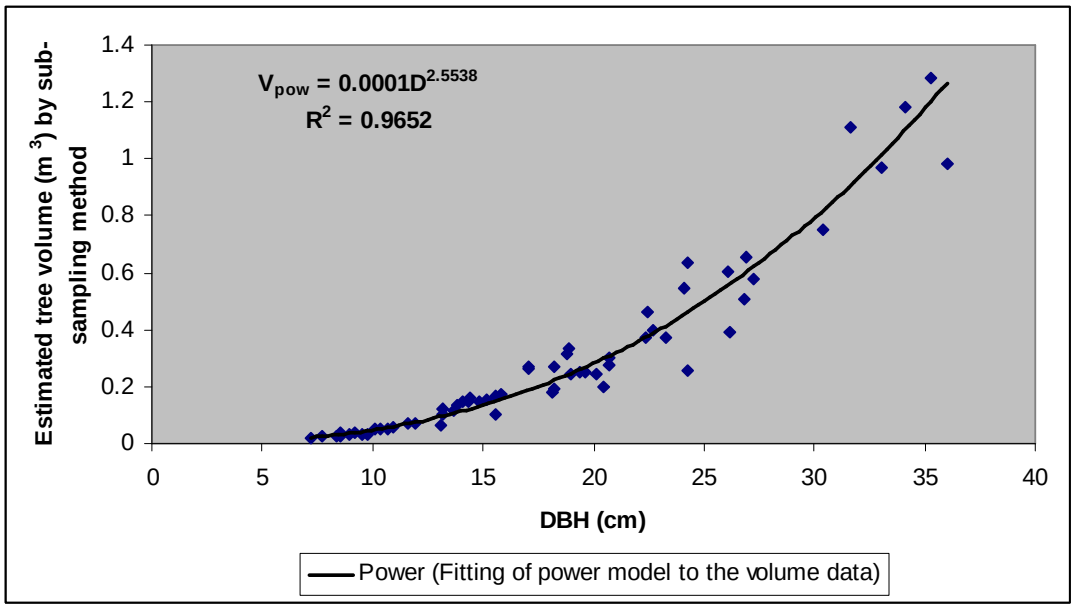

Figure 4B: scatter plot of volume data against DBH fitted with power model

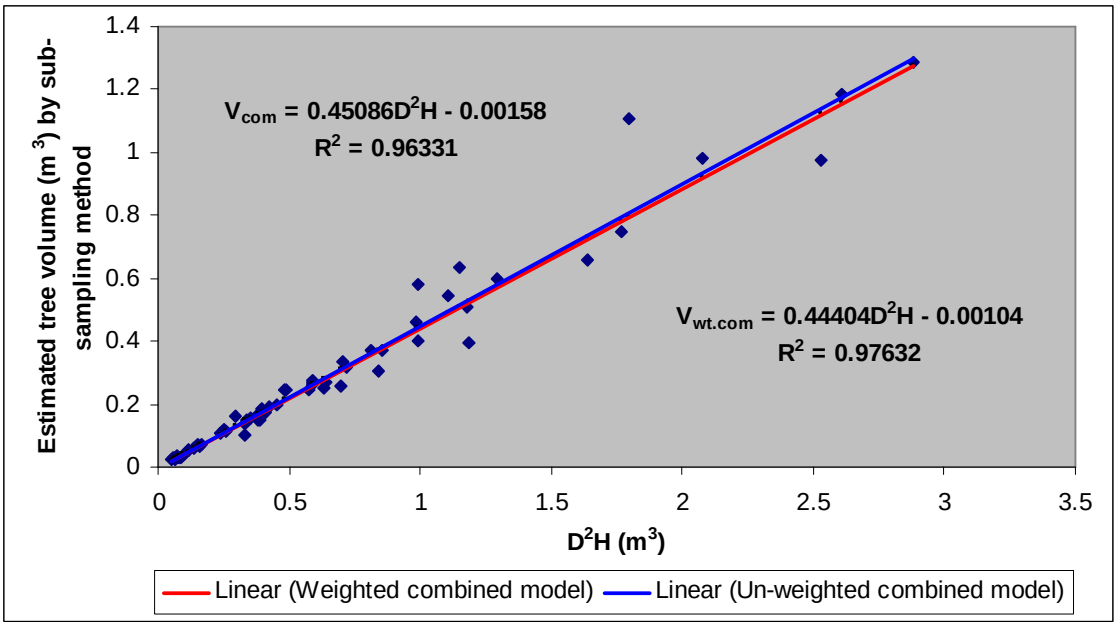

Figure 4C: scatter plot of volume data (obtained from sub-sampling method) against D^2H fitted with un-weighted and weighted combined variable models. V_{com} is volume estimate by un-weighted combined variable model; $V_{wt.com}$ is volume estimate by weighted combined variable model; and D is dbh.

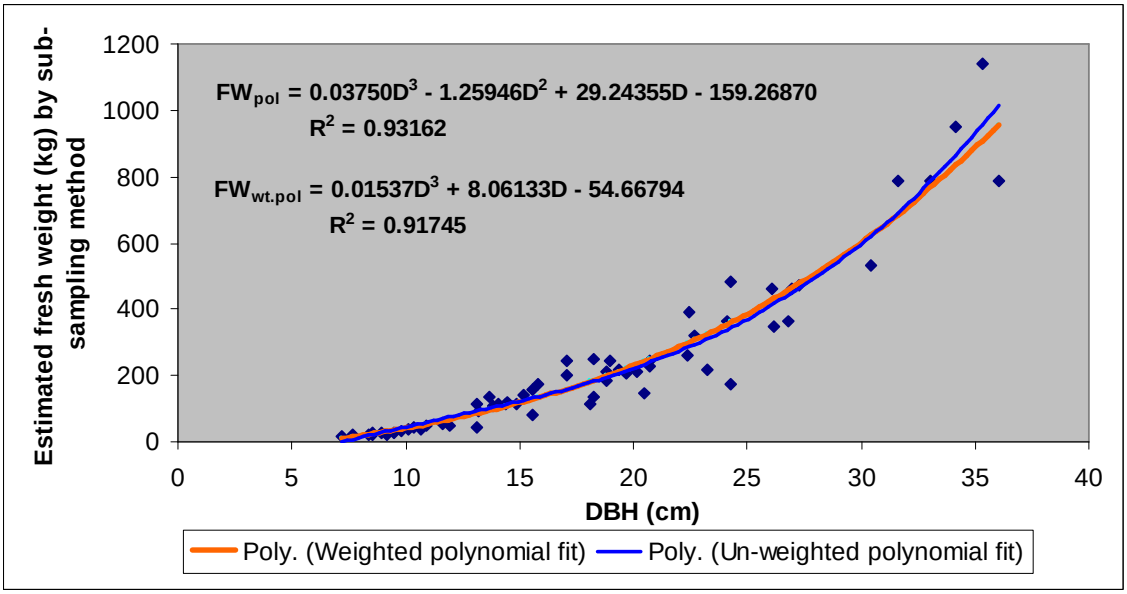

Figure 4D: scatter plot of fresh weight data against DBH fitted with un-weighted and weighted third degree polynomial models. FW_{pol} is fresh weight estimate by un-weighted polynomial; $FW_{wt.pol}$ is fresh weight estimate by weighted polynomial; and D is dbh.

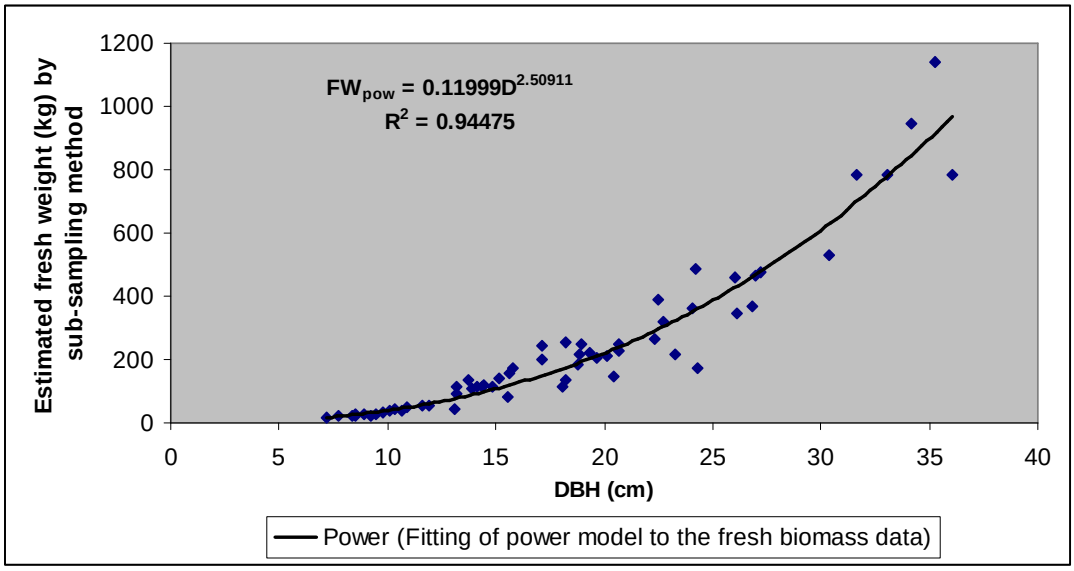

Figure 4E: scatter plot of fresh biomass data of sample trees against DBH fitted with power model

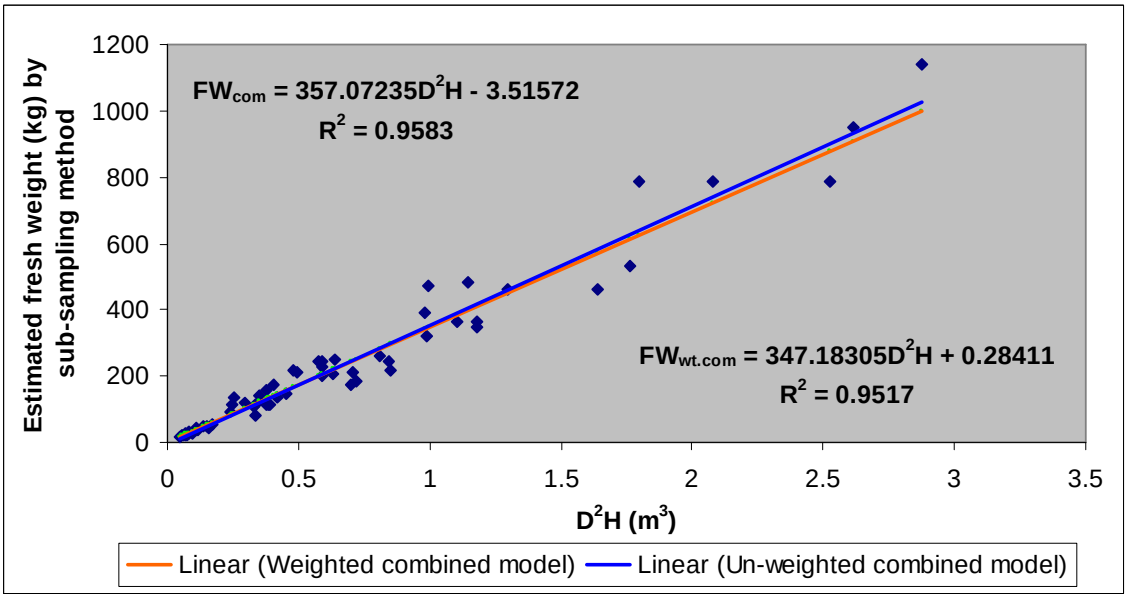

Figure 4F: scatter plot of fresh biomass data against D^2H fitted with un-weighted and weighted combined variable models. FW_{com} is fresh weight estimate by un-weighted combined variable model; $FW_{wt.com}$ is fresh weight estimate by weighted combined variable model; and D is dbh.

Appendix 5: Measurements for the growth rings and bark-thickness made on 48 sample disks

Tree #	Species	Over-bark DBH (cm.)	Av. width (cm) of the rings of last five years	Av. annual under-bark diameter increment (cm)	Av. bark thickness (cm)	Double-bark thickness (cm)
1	*Ulmus pumila*	9.8	0.88	0.352	0.50	1
2	*Ulmus pumila*	15.8	0.84	0.334	0.40	0.8
3	*Ulmus pumila*	8.95	0.56	0.222	0.30	0.6
4	*Ulmus pumila*	36.05	1.84	0.734	1.50	3
5	*Ulmus pumila*	13.7	0.86	0.342	0.40	0.8
6	*Ulmus pumila*	18.95	1.13	0.450	0.55	1.1
7	*Ulmus pumila*	24.25	1.14	0.454	1.40	2.8
8	*Fraxinus spp.*	17.1	0.64	0.254	0.97	1.9
9	*Quercus mongolica*	7.2	0.39	0.156	0.67	1.3
10	*Quercus mongolica*	10.1	0.40	0.158	1.07	2.1
11	*Quercus mongolica*	11.6	0.40	0.160	0.75	1.5
12	*Quercus mongolica*	27.25	0.47	0.189	1.67	3.3
13	*Quercus mongolica*	19.35	1.13	0.450	1.40	2.8
14	*Quercus mongolica*	20.7	0.94	0.377	1.30	2.6
15	*Quercus mongolica*	31.6	1.14	0.455	1.73	3.5
16	*Abies holophylla*	18.25	0.71	0.282	0.40	0.8
17	*Abies holophylla*	9.5	0.51	0.204	0.30	0.6
18	*Abies holophylla*	30.4	0.95	0.380	0.83	1.7
19	*Abies holophylla*	26.15	1.60	0.639	0.60	1.2
20	*Abies holophylla*	15.15	0.82	0.328	0.45	0.9
21	*Abies holophylla*	19.65	0.96	0.385	0.50	1
22	*Abies holophylla*	13.15	0.68	0.271	0.50	1
23	*Abies holophylla*	13.2	0.38	0.151	0.45	0.9
24	*Abies holophylla*	8.5	0.72	0.287	0.25	0.5
25	*Abies holophylla*	22.7	0.33	0.132	0.53	1.1
26	*Picea jezoensis*	17.95	0.87	0.348	0.55	1.1
27	*Picea jezoensis*	26.05	1.67	0.668	0.55	1.1
28	*Picea jezoensis*	23.25	0.69	0.276	0.50	1
29	*Picea jezoensis*	15.6	1.09	0.434	0.35	0.7
30	*Picea jezoensis*	15.55	0.34	0.137	0.40	0.8
31	*Picea jezoensis*	10.65	0.47	0.189	0.35	0.7
32	*Picea jezoensis*	10.35	0.15	0.058	0.45	0.9
33	*Picea jezoensis*	8.4	0.18	0.070	0.30	0.6
34	*Picea jezoensis*	22.35	1.67	0.669	0.50	1
35	*Larix olgensis*	11.95	0.25	0.098	0.70	1.4
36	*Larix olgensis*	26.95	1.11	0.443	1.30	2.6

Appendix 5: …continued

37	*Larix olgensis*	27.7	0.97	0.389	1.10	2.2
38	*Larix olgensis*	33.05	0.70	0.281	1.20	2.4
39	*Larix olgensis*	17.1	0.69	0.277	0.67	1.3
40	*Larix olgensis*	26.95	0.58	0.232	0.85	1.7
41	*Larix olgensis*	14.1	0.43	0.171	0.90	1.8
42	*Larix olgensis*	18.25	1.37	0.547	0.55	1.1
43	*Larix olgensis*	10.9	0.37	0.147	0.43	0.9
44	*Larix olgensis*	7.7	0.58	0.231	0.45	0.9
45	*Larix olgensis*	20.15	1.51	0.603	0.95	1.9
46	*Tilia amurensis*	13.1	1.11	0.444	0.70	1.4
47	*Tilia amurensis*	20.45	0.76	0.303	1.10	2.2
48	*Tilia amurensis*	24.3	0.87	0.347	0.95	1.9

Appendix 6: Location of sample plots along with the calculated quantity of biomass, annual wood increment and carbon sequestration in them

Plot ID	Plot coordinates		Plot biomass (kg) estimate from poly. equation	Annual wood accumulation (dM) per plot (kg)	Carbon sequestration per plot (kg)	Carbon sequestration scaled up to per ha (tons)
	X	Y				
1RA	617261	4809276	1371.34	78.15	39.08	0.78
2RA	617488	4809052	747.43	44.63	22.32	0.45
3RA	617072	4808604	3170.24	152.14	76.07	1.52
4RA	616372	4811341	3089.98	137.02	68.51	1.37
5RA	616094	4810874	2387.64	116.62	58.31	1.17
7RA	616263	4811167	2165.92	105.47	52.73	1.05
8RA	616116	4811914	1522.94	75.40	37.70	0.75
9RA	615817	4812460	2793.06	136.60	68.30	1.37
10RA	614867	4811362	3375.49	157.98	78.99	1.58
11RA	614886	4811254	4178.92	207.25	103.62	2.07
12RA	614849	4810957	3652.09	176.91	88.46	1.77
13RA	618919	4795537	2422.68	123.33	61.67	1.23
14RA	617320	4793180	4234.22	195.88	97.94	1.96
15RA	617316	4793016	8588.93	380.50	190.25	3.81
16RA	617615	4794363	4114.32	194.01	97.01	1.94
17RA	617537	4794473	4035.71	189.12	94.56	1.89
18RA	619431	4791536	4541.40	215.88	107.94	2.16
20RA	619340	4790570	4641.24	207.88	103.94	2.08
21RA	619509	4789615	4043.85	189.13	94.56	1.89
22RA	619174	4790038	4688.92	215.29	107.64	2.15
23RA	621894	4800602	1855.75	81.90	40.95	0.82
24RA	620055	4802986	3197.45	142.70	71.35	1.43
25RA	621566	4800236	4973.29	234.02	117.01	2.34
26RA	620186	4788157	7143.70	322.42	161.21	3.22
28RA	620151	4788801	4230.38	205.30	102.65	2.05
29RA	620041	4789242	3592.33	182.11	91.06	1.82
30RA	620175	4789631	4040.90	182.95	91.47	1.83
31RA	619700	4788102	7777.05	348.79	174.39	3.49
32RA	619512	4787888	8737.47	414.97	207.49	4.15
33RA	619829	4788219	5963.04	275.85	137.93	2.76
34RA	636144	4819632	3865.38	178.74	89.37	1.79
35RA	636042	4819604	1739.21	81.84	40.92	0.82
37RA	635929	4819402	4343.30	199.03	99.52	1.99
38RA	635906	4819854	3476.31	158.51	79.25	1.59
39RA	635839	4820081	3759.89	171.40	85.70	1.71

Appendix 6: …continued

40RA	635460	4820249	5117.33	227.96	113.98	2.28
41RA	634187	4814496	2983.42	133.99	67.00	1.34
42RA	634070	4814587	3676.39	171.91	85.95	1.72
43RA	633952	4814607	7586.30	340.96	170.48	3.41
44RA	634267	4816289	1899.28	84.90	42.45	0.85
46RA	635631	4817351	4839.53	221.62	110.81	2.22
48RA	637545	4822770	3500.72	166.93	83.46	1.67
49RA	637762	4822190	2288.86	103.08	51.54	1.03
50RA	638742	4821928	2919.97	130.08	65.04	1.30
51RA	638490	4820263	5881.09	264.18	132.09	2.64
52RA	634241	4814071	1951.41	104.67	52.34	1.05
53RA	634241	4813480	2933.87	140.08	70.04	1.40
54RA	633299	4811699	4936.72	236.95	118.47	2.37
55RA	632865	4810322	6355.95	295.79	147.90	2.96
56RA	633022	4810237	4193.15	213.54	106.77	2.14
57RA	641554	4817662	2936.45	141.89	70.94	1.42
58RA	641354	4817484	718.76	36.24	18.12	0.36
59RA	641279	4817757	5408.38	241.13	120.56	2.41
60RA	642116	4818439	2821.39	152.43	76.22	1.52
61RA	617860	4800986	3504.01	170.39	85.20	1.70
4D	617919	4801835	701.15	41.06	20.53	0.41
6D	617811	4802522	829.17	45.86	22.93	0.46
9D	616694	4809387	1627.64	95.80	47.90	0.96
10D	616659	4809568	4162.29	195.70	97.85	1.96
11D	616646	4809733	2716.47	128.27	64.13	1.28
13D	616382	4811277	3701.60	169.19	84.60	1.69
14D	616418	4811113	2544.03	122.01	61.00	1.22
15D	616440	4811935	2307.37	105.95	52.97	1.06
16D	616468	4810771	2621.17	129.06	64.53	1.29
17D	616498	4810592	6710.62	310.95	155.48	3.11
18D	616524	4810431	189.45	11.13	5.56	0.11
20D	616576	4810071	807.12	36.47	18.23	0.36
22D	616076	4813173	2654.47	138.20	69.10	1.38
23D	616109	4813004	2204.62	103.55	51.77	1.04
24D	616131	4812832	3287.79	151.29	75.65	1.51
25D	616162	4812660	3249.38	159.81	79.90	1.60
26D	616187	4812486	5723.11	264.00	132.00	2.64
27D	616228	4812316	1807.94	90.61	45.30	0.91
28D	616280	4811970	2111.93	100.51	50.26	1.01
29D	616299	4811805	3828.74	178.19	89.10	1.78
31D	618978	4795322	4943.12	223.14	111.57	2.23

Appendix 6: …continued

32D	619011	4795155	3289.55	155.61	77.80	1.56
33D	619035	4794979	4238.19	193.31	96.65	1.93
34D	619066	4794806	3192.42	146.28	73.14	1.46
35D	619100	4794644	5716.80	263.15	131.58	2.63
36D	619127	4794454	4928.69	230.19	115.09	2.30
37D	619179	4794115	6804.92	308.35	154.18	3.08
38D	619211	4793939	4858.26	222.12	111.06	2.22
39D	619238	4793777	3577.94	173.41	86.71	1.73
43D	619596	4791552	3894.39	183.42	91.71	1.83
44D	619621	4791368	6437.58	291.58	145.79	2.92
45D	619648	4791191	6595.23	304.52	152.26	3.05
46D	619683	4791023	5965.31	275.21	137.61	2.75
47D	619701	4790859	2882.79	133.66	66.83	1.34
48D	619738	4790675	8288.08	369.11	184.56	3.69
49D	620152	4788115	4003.00	181.71	90.85	1.82
50D	620123	4788276	2383.19	113.62	56.81	1.14
51D	620096	4788454	9126.98	408.07	204.03	4.08
54D	620013	4788971	7980.95	357.04	178.52	3.57
55D	619959	4789172	4970.44	228.63	114.32	2.29
56D	619961	4789310	4227.34	206.12	103.06	2.06
57D	619930	4789475	5212.98	235.86	117.93	2.36
58D	619907	4789652	5651.92	258.91	129.46	2.59
59D	620177	4787928	7253.22	326.13	163.06	3.26
61D	620239	4787596	5272.18	237.70	118.85	2.38
62D	620272	4787424	5448.37	246.20	123.10	2.46
63D	620300	4787244	2577.68	120.87	60.43	1.21
64D	620328	4787072	6218.60	282.39	141.20	2.82
65D	636716	4819417	2839.03	137.24	68.62	1.37
66D	636693	4819248	2887.31	130.16	65.08	1.30
68D	636651	4818903	2392.67	110.80	55.40	1.11
69D	636633	4818730	3792.74	174.61	87.30	1.75
70D	636614	4818554	2323.49	103.89	51.95	1.04
71D	636590	4818385	1888.56	85.66	42.83	0.86
72D	636563	4818218	3637.82	162.66	81.33	1.63
73D	636556	4818038	3017.61	133.48	66.74	1.33
74D	636534	4817871	1548.56	68.58	34.29	0.69
77D	636764	4819761	4265.47	198.31	99.16	1.98
78D	636784	4819930	6327.68	286.99	143.49	2.87
79D	636808	4820107	4910.75	221.11	110.56	2.21
80D	636830	4820276	2691.22	120.93	60.47	1.21
81D	636857	4820446	2320.52	112.63	56.31	1.13

Appendix 6: …continued

82D	636873	4820618	2312.68	105.73	52.87	1.06
83D	636894	4820792	2307.57	105.06	52.53	1.05
84D	636918	4820968	2914.97	135.28	67.64	1.35
85D	636945	4821137	4629.39	205.16	102.58	2.05
86D	636960	4821304	3523.33	158.38	79.19	1.58
87D	636984	4821479	2484.61	110.72	55.36	1.11
88D	637008	4821659	2127.10	100.37	50.18	1.00
89D	637089	4822344	5328.57	240.34	120.17	2.40
90D	637102	4822518	3823.09	169.32	84.66	1.69
91D	637137	4822692	1928.84	87.94	43.97	0.88
92D	637157	4822857	3811.42	177.94	88.97	1.78
93D	637182	4823034	5671.58	249.97	124.98	2.50
95D	637224	4823388	5536.47	248.03	124.02	2.48
96D	637245	4823550	3043.83	133.90	66.95	1.34
97D	637261	4823724	5043.05	225.39	112.70	2.25
98D	637283	4823900	3439.91	153.51	76.75	1.54
99D	632371	4784583	4161.65	190.94	95.47	1.91
100D	632334	4784240	3641.95	170.37	85.18	1.70
101D	632312	4784073	4734.85	217.75	108.88	2.18
102D	632416	4784929	3870.25	174.57	87.28	1.75
103D	632476	4785456	4105.06	189.66	94.83	1.90
2YQ	618582	4803904	4642.25	210.06	105.03	2.10
3YQ	618610	4803731	2648.59	123.53	61.77	1.24
9YQ	617641	4805735	2242.37	105.24	52.62	1.05
10YQ	617615	4805915	5537.11	242.47	121.23	2.42
12YQ	617562	4806256	1783.16	85.98	42.99	0.86
13YQ	617538	4806423	2265.01	108.30	54.15	1.08
14YQ	617508	4806595	1709.18	78.19	39.09	0.78
15YQ	617479	4806776	4687.88	214.75	107.37	2.15
18YQ	617333	4807618	4551.56	210.72	105.36	2.11
23YQ	620008	4795154	5083.64	224.73	112.36	2.25
27YQ	620123	4794470	5839.73	267.76	133.88	2.68
30YQ	620202	4793957	8117.23	361.52	180.76	3.62
33YQ	620291	4793445	4496.23	208.81	104.40	2.09
38YQ	620560	4788073	4180.59	200.07	100.03	2.00
39YQ	620587	4787902	8396.59	378.19	189.09	3.78
42YQ	620668	4787385	1304.72	66.21	33.10	0.66
43YQ	620695	4787215	3031.21	143.39	71.70	1.43
48YQ	620363	4789267	3883.05	180.67	90.34	1.81
73YQ	633406	4784567	4600.69	207.82	103.91	2.08
77YQ	633296	4783706	4582.97	205.48	102.74	2.05

Appendix 6: …continued

78YQ	633274	4783533	9765.13	440.85	220.43	4.41
79YQ	633254	4783362	5253.25	243.86	121.93	2.44
80YQ	633221	4783189	5038.65	233.87	116.94	2.34
81YQ	633211	4783018	3468.47	165.29	82.65	1.65
82YQ	633189	4782847	3617.54	166.75	83.38	1.67
84YQ	632072	4783839	6893.48	310.63	155.32	3.11
85YQ	632051	4783669	6759.78	299.52	149.76	3.00
86YQ	632030	4783496	5305.83	239.71	119.86	2.40
87YQ	632009	4783323	7844.52	348.53	174.27	3.49
88YQ	631988	4783153	5869.70	269.87	134.93	2.70
91YQ	631924	4782638	6083.27	270.92	135.46	2.71
97YQ	632177	4784699	4393.66	212.49	106.25	2.12
99YQ	632220	4785043	6826.66	310.34	155.17	3.10
100YQ	632243	4785215	5586.57	254.45	127.22	2.54